THE UNIVERSITY OF
SYDNEY

THE UNIVERSITY OF SYDNEY

# POLYMER CROSSLINKING: A NEW STRATEGY TO ENHANCE MECHANICAL PROPERTIES AND STRUCTURAL STABILITY OF BIOACTIVE GLASSES

**BY**

ALI NEGAHI SHIRAZI

A DISSERTATION SUBMITTED IN FULFILMENT OF THE REQUIREMENTS FOR THE DEGREE OF DOCTOR OF PHILOSOPHY

In

The School of Chemical and Biomolecular Engineering

The University of Sydney

March 2015

# Declaration

I hereby declare that this submission is my own work and that, to the best of my knowledge and belief, it contains no material previously published or written by another person nor material which to a substantial extent has been accepted for the award of any other degree or diploma of the University or other institute of higher learning, except where due acknowledgment has been made in the text.

Ali Negahi Shirazi

March 2015

# Ethical Approval for Animal Studies

An *in vivo* subcutaneous mice implantation studies was conducted under approved protocols by Animal Welfare Committee of NSW Local Health District, the protocol number of 2013/019A. A copy of this ethical approval is attached in the appendix at the end of this document.

# List of Publications

## Book chapter and Journal paper

1. **Ali Negahi Shirazi1**, W. Chrzanowski, A. Khademhosseini and F. Dehghani, "Anterior Cruciate Ligament: Structure, Injuries and Treatments", Submitted in Engineering Mineralized and Load Bearing Tissues, Luiz Bertassoni Ed., in Advances in Experimental Medicine and Biology Series, Springer Publishing.
2. A. Fathi, S. Lee, A. Breen, **Ali Negahi Shirazi**, P. Valtchev and F. Dehghani, "Enhancing the Mechanical Properties and Physical Stability of Biomimetic Polymer Hydrogels for Micro-patterning and Tissue Engineering Applications", *European Polymer Journal*, **2014**; 59: 161-170 (IF 3.067).
3. **Ali Negahi Shirazi**, A. Fathi, Y. Wong and F. Dehghani, "Photocrosslinking of Organic-Inorganic Hybrid, a Solution for Enhancing their Physicochemical and Mechanical Properties", Ready to submit.

## Conferences

1. A. Fathi, A. Breen, **Ali Negahi Shirazi**, P. Valtchev and F. Dehghani, "Stable Micropatterned Hydrogels from Gelatin", 5th ISSIB/ASBTE, 7-10 April **2015**, Sydney, Australia.
2. **Ali Negahi Shirazi**, A. Fathi and F. Dehghani, "The Effect of Cellulose Nanofibres on Mechanical Properties and Bioactivity of Natural Polymers", *MRS Proceedings*, **2013**; 1498: 242.
3. **Ali Negahi Shirazi,** R. Watson, A. Fathi and F. Dehghani, "Improving the Mechanical Properties of Natural Hydrogels Using Bio-Based Microfibers", EMBS Micro and Nanotechnology in Medicine Conference, 3-7 December **2012**, Hawaii, USA.
4. A. Fathi, S. Lee, M. Bash, W. Chrzanowski, **Ali Negahi Shirazi**, R. Ravarian and F. Dehghani**, "**Fabrication of Bioactive Composite Poly(Lactic Ethylene Oxide Fumarate)/Gelatin Scaffolds for Bone Tissue Engineering Applications", 9th World Biomaterials Congress, 1-5 June **2012**, Chengdu, China.

# Acknowledgments

I would like to thank my supervisor, Professor Fariba Dehghani for her continued encouragements and supports. She always takes time out for sharing her intellectual ideas and providing stimulating discussions. She changed the direction of my life and been there for me throughout my studies at the University of Sydney. I learnt a lot from Fariba, but most importantly, I learnt how to seize the opportunities around me and to never give up. These are all lifetime lessons that I would always appreciate.

I would like to acknowledge the financial support from Australian Government for my Australian Postgraduate Research Award scholarship. This project involved learning a diverse range of techniques, and I am grateful to a number of people for their assistance and help. I would like to start with Dr Yiwei Wang in the Concord Hospital for *in vivo* animal studies. Thanks to Mr Alex Faragó for all his supports and friendly's attitude for designing the proper moulds. I also, appreciate the supports of Dr Wojciech Chrzanowski from the Faculty of Pharmacy and Dr Kim-Yen Phan-Thien from Faculty of Agriculture and Environment for giving me access to their facilities. I would also acknowledge the assistance of Mr Ehsan Pourazadi for the thermal gravimetric analyses and Dr Jeffrey Shi in the Safety Committee.

I would also acknowledge the facilities, the scientific and technical assistance of the Australian Microscopy & Microanalysis Research Facility at the Australian Centre for Microscopy & Microanalysis at the University of Sydney. My appreciation goes to Ms Naveena Gokoolparsadh for her friendly attitudes and problem-solving even with short notices. I also grateful to Ms. Ellie Kable, Dr Pamela Young and Dr Yingying Su for their patience during the confocal microscopy training; Mr Steven Moody, Dr Matthew Floy and Dr Hongwei Liu for instructing me to use SEM and TEM microscopies. I also appreciate Mr Toshi Arakawa for his efforts on maintenance and troubleshooting of TEM microscopy.

I am grateful to my good friends Dr Ali Fathi and Mr Ali Zafaranloo whom their friendships and supports are endless, thanks for the fun, laughter and all your supports. I would like to appreciate my past and present colleagues in the Bioengineering research lab Dr Peter Valtchev, Dr Sherry Lee, Dr Aydin Berenjian, Dr Roya Ravarian, Mr Iman Manavi, Mrs Bahareh Bahramian, Mr Mohd Fareed Sairi, and Dr Negar Talaei Zanjani thank you all for your endless supports. Ms Elizabeth Dobrinsky, thank you for your technical supports, I truly enjoyed your company in the past four years. I would appreciate Dr Tahereh Noeiaghaei, Mr Nordin Mohamad Kalis and Mr Rasha Watson from School of Chemical Engineering.

Most of all, I would like to appreciate the people whom their friendships made the earth so spacious. I would like to thank Mr Saman Nikkhah, Mr Bardia Konh and Mrs Najme Mohammadpour and most importantly my family for all their sacrifices, constant strong positive encouragement and moral supports, yet I cannot find a word to represent my complete gratitude.

# Abstract

The organic-inorganic hybrids fabricated by the sol-gel method are intrinsic bioactive materials with extensive applications in bone tissue engineering. The brittleness and limited water uptake capacity of these monoliths, however, restrict their applications for engineering the soft tissues and their interfaces with bone. To address these challenges, a unique class of organic-inorganic hybrid was developed in which polymer crosslinking ceased the over-condensation of a bioactive glass component and eradicated the formation of brittle structure.

In this study, an organosilane-functionalized gelatin methacrylate (GelMA) was covalently bonded to a bioactive glass during the sol-gel process, and the condensation of silica networks was controlled by photocrosslinking of GelMA. The physicochemical properties and mechanical strength of these hybrid hydrogels were then tuned by the incorporation of secondary crosslinking agents such as poly(ethylene glycol diacrylate) (PEGDA). The resulting bioresorbable hydrogels displayed elastic properties with ultimate elastic compression strain above 0.2 (mm/mm) and tuneable compressive modulus in the range of 42-530 kPa. The swelling ratio of these hybrids, however, was suitable for tissue engineering applications. In addition to remarkable enhancement in the mechanical properties of gelatin-based hydrogels, their structural integrity was significantly increased. As an example, these hybrid hydrogels kept their structures for more than 28 days, and only 30% of gelatin was released during this period in simulated body fluid. The presence of homogeneously distributed bioactive glass in these hydrogels, moreover, promoted the precipitation of calcium phosphate particles as the main inorganic compositions of the bone extracellular matrix. The continuous increase of alkaline phosphatase activity of bone progenitor cells for at least 28 days post-culture confirmed the osteoconductive properties of these hybrid hydrogels. The *in vivo* mice-subcutaneous implantation, moreover, confirmed the biocompatibility and bio-resorption of these hydrogels. A bioactive hydrogel with a gradient of

mineralisation was also fabricated to confirm the feasible application of these hybrid hydrogels in interface tissue engineering.

In summary, an organic-inorganic hybrid was developed that has favourable swelling properties and higher mechanical strength compared to ceramic based scaffolds. These hybrids were also bioactive, cytocompatible and bioresorbable. These gelatin-bioactive glass hydrogels can be used for regeneration of bone defects. It can also be used for the fabrication of gradient bioactive hydrogels for enhancing the integration of soft to hard tissue interfaces such as ligament and tendon.

# Table of Schemes, Tables, and Figures

# Table of Contents

# Chapter 1. Introduction

Bone is a dynamic tissue with a unique capacity to heal and regenerate without leaving a scar [1]. In addition to these remarkable properties, bone mobilises the stored minerals on the metabolic demands, supports muscular contraction resulting in motion, withstands load bearing, and protects internal organs [2]. The significant alterations in the bone structure, therefore, can dramatically alter the body equilibrium and quality of life. The severe post-operation complications of current reconstructive surgeries include donor site morbidity, disease infection, and deficient supply [3, 4]. These restrictions induce the total economic burden of hundred millions of dollars on public health per annum. It is critical to developing a new approach to addressing these issues and minimising the risk of failure of current bone repair operations. This strategy promotes the proliferation of progenitor cells specifically in their interface with soft tissues. The potential of this approach has not yet been exploited, and this is the focus of this project.

Bioactive glass is a class of ceramics, which regulates the metabolism of soft and hard tissues through stimulating the osteogenic differentiation [5-7], enhancing the pro-angiogenesis of endothelial cells [8-10], and modulating the intercellular interactions [11-14]. Despite their particular biological behaviour, the intrinsic brittleness of bioactive glasses restricts their direct application in bone regeneration. Different compositions of bioactive glass and polymers with enhanced mechanical properties have been developed to mimic the structure of bone [15-17].

The sol-gel method is superior to melt-quenching process for the preparation of polymer-bioactive glass hybrids. The intriguing benefits of the sol-gel method include the low reaction temperature [18], controllable kinetic of reaction [19], and convenience in modification of composition [20]. This technique composed of two main steps of hydrolysis and condensation followed by ageing and drying processes. In particular, the collagen-inorganic composite has been used for musculoskeletal tissue engineering, as these components comprise the chemical structure of bone [21, 22]. However, the limited mechanical properties of these composites may evoke severe clinical complications [23]. Gelatin is a disintegrated

derivative of collagen and possesses the intrinsic capacity to form a hydrogel through distinct methods. The formation of gelatin-bioactive glass composites is deemed to be a more favourable alternative for mimicking the bone structure [24, 25].

The heterogeneity of dissimilar phases, however, is the main associated drawback of these organic-inorganic composites [26]. The uniform distribution of bioactive glass within polymer phase is the main advantage of chemically modified organic-inorganic hybrids with enhanced bioactivity and physicochemical properties [27, 28]. In addition to their synergetic nature of hybridisation, cost-effectiveness and tuneable mechanical properties of these materials introduce them as proper candidates for bone regeneration. The complete condensation of the inorganic compound in these hybrids, however, carries out through drying and ageing steps and yields brittle structures [29]. The fabrications of two-dimensional monoliths with very limited water uptake capacity are their main drawbacks for hard-to-soft interface tissue engineering [30].

The aim of this study was to develop a unique structure for reconstruction of bone structure and its interface with soft tissues. It was hypothesised that the fabrication of an organic-inorganic hybrid with enhanced mechanical performance and high swelling ratio might promote the proliferation of bone progenitor cells. To achieve this objective, a covalently bonded hybrid of gelatin-bioactive glass was fabricated by a sol-gel process. It was hypothesised that the crosslinking of the organic component might control the condensation of the inorganic phase, prevent the formation of the brittle structure, and tune the physicochemical and mechanical properties of hybrid.

This dissertation is comprised of 7 chapters. In ***Chapter 2,*** a review of the bone tissue engineering is provided. Different methods of polymer crosslinking, and the fabricated organic-inorganic hybrids for bone tissue engineering are also discussed in detail. The hypotheses of this project arose from the shortfalls of current bone tissue engineering are also explained. In ***Chapter 3,*** different methods for fabrication of organic-inorganic hybrid

hydrogels are presented. Various methods to assess the biological and physicochemical properties and mechanical performance of these hybrid hydrogels are also described. In ***Chapter 4,*** the effects of external stimuli and polymer-crosslinking on the physical status and brittleness of interpenetrated hybrids are presented. In ***Chapter 5,*** the impacts of organosilation and formation of covalently bonded gelatin-hybrid on the physicochemical properties of hydrogels are assessed. The effect of incubation media on the degradation profile of hybrid hydrogels is also investigated. In ***Chapter 6***, the secondary polymer-crosslinking approach is used to form a bioconjugated hybrid hydrogel. The mechanical performance and degradation profiles of these hybrid hydrogels are discussed. The *in vitro* bioactivity and biocompatibility are also conducted to examine the proliferation of bone progenitor cells in these constructs. Finally, the biocompatibility and the biological properties of this class of hydrogels were evaluated by conducting *in vivo* mice implantation performed under an ethically approved protocol (2013/019A). The potential of these hybrid hydrogels for interface tissue engineering is also investigated. In ***Chapter 7,*** the overall conclusions and recommendations for the continuation of this project are presented.

# Chapter 2. An Overview to Bone Tissue Engineering

## 2.1 Introduction

Bone is a dynamic, highly vascularised tissue with a unique capacity to heal and regenerate without leaving a scar [1]. In addition to these remarkable properties, bone mobilises the stored minerals on the metabolic demands, supports muscular contraction resulting in motion, withstands load bearing, and protects internal organs [2]. The significant alterations in the bone structure, therefore, can dramatically alter the body equilibrium and quality of life. Musculoskeletal defects due to congenital anomalies, skeletal diseases, sport and life-related traumas impose an economic burden of approximately one billion dollars per annum on the Australian economy, with 70% of the expenditure on long recovery period and hospitalisation services [31].

The current treatment of bone fractures is replacement of the damaged tissue with different biological grafts from the patient (autograft) [4, 32] or cadaver (allograft) [33], and synthetic grafts [34]. Despite the intrinsic osteoconductivity and osteoinductivity of biological grafts, concern issues are associated with the risk of disease transfer, donor site morbidity, chronic pain, infection and increase of operative time and cost [3, 4]. Tissue engineering is considered as a new approach, which might remedy these shortfalls. In this chapter, the bone structure and current methods for substituting the bone fracture are reviewed. Moreover, the ongoing research on the development of bone tissue engineering is discussed in detail.

## 2.2 Current Treatment Approaches for Bone Regeneration

Bone possesses an intrinsic capacity for regeneration as a part of the repair process in response to injury, as well as during skeletal development or continuous remodelling throughout adult life [35]. Bone regeneration is comprised of a well-orchestrated series of biological events of bone induction and conduction, involving a number of cell types and intracellular and extracellular molecular signalling pathways [36, 37]. Prior to introducing the current treatment approaches for bone regeneration, it is of great importance to understand the chemical composition and cellular constitution of bone structure.

### 2.2.1 The Bone Structure

Bone is constructed from cells and an extracellular matrix (ECM). The cellular architecture of bone is predominantly comprised of osteoblasts [38], osteocytes, osteoclasts [39], and mesenchymal stem cells (MSC) [40] that differentiate into committed progenitors of osteoblasts, osteoclasts and other cells [41]. Osteoblast cells are found at the active sites of bone formation and synthesise the non-mineralised organic matrix called osteoid. The osteoid is comprised of collagen, glycoproteins, glycosaminoglycans, and bone morphogenetic proteins (BMP) to participate in the mineralisation process. Osteocytes are the most abundant cell population on the bone that are terminally differentiated osteoblasts [42]. Osteocytes have significant impacts on the bone performance by regulating the ECM maintenance and calcium homoeostasis and initiating of the remodelling cascade [43]. Finally, osteoclasts are the bone resorbing cells, which keep bone healthy and new through remodelling and renewal processes [44].

The bone extracellular matrix is particularly mineralised. Inorganic compounds such as calcium phosphates comprise 65% of ECM, and the rest is fabricated from organic components. Collagen is the main organic component that combines to other glycoproteins and glycosaminoglycans to construct the osteoid and ECM and modulate the cellular activity and intercellular signalling [45]. The inorganic compounds, moreover, are found within and between the length of collagen fibres to improve their mechanical performances towards bending and compressive loads. Hydroxyapatite (HAp) is the most abundant calcium phosphate in bone structure that can combine with other materials such as carbonates, citrates, magnesium, fluorides and strontium [45]. The presences of these organic and inorganic components have significant impacts on the cellular constitution of bone. Magnesium has an important impact on the calcification process, bone fragility, and mineral metabolism [46]. While the presence of strontium promotes the bone growth and formation [47], zinc fosters the proliferation and differentiation of osteoblasts [48]. Potassium [49], sodium [50], and chlorine [51], moreover, possess a versatile nature in

the regulation of bone remodelling process. The significant alterations in the cellular constitution or chemical composition of bone, therefore, can dramatically alter the body equilibrium and quality of life. The severe bone fracture cannot regenerate through bone remodelling process. The surgical treatment, therefore, is the only clinical treatment to remedy these shortfalls.

### 2.2.2 Clinical Treatments for Bone Repair

Different biological grafts including autografts and allografts have been transplanted to repair the injured or damaged bone. The intrinsic biocompatibility and non-immunogenicity of autologous grafts promote their applications as the gold standard for bone grafts [52]. Despite the promising osteoinductivity, osteogenesis, and osteoconductivity of autografts, they are associated with some issues and complications. Donor side morbidity, chronic pain, possible immunogenicity, and an increase of operative time and cost are some examples of these complications [53]. The size limitation, moreover, restricts the application of autografts while the defect site requires a larger volume of bone [54].

Allografts represent the second most common bone-grafting technique by transplanting donor bone tissue, often from a cadaver [55, 56]. Allogeneic bone is a cytocompatible tissue, which is available in various sizes depending on the host-site requirements [57, 58]. The high risk of immunogenicity and transmission of infections, the reduced osteoconductivity, and the substantial cost issues, however, are limiting factors on clinical application of allografts [59, 60]. Despite the significant impacts of current transplantation methods on bone regeneration, they suffered from some intrinsic complications including low osteoinductive and angiogenic potencies, limited availability, and a high donor side morbidity. Tissue engineering is considered as a new approach, which might remedy these shortfalls.

## 2.3 Bone Tissue Engineering

Tissue engineering integrates osteoprogenitor cells, biological and mechanical stimulations, and scaffolds to regenerate the bone structure [61-

64]. The scaffold is a temporary structure and logistic template for tissue engineering. It serves as “informational templates” to the cells, by patterning implementation, binding ligands and sustained releasing of cytokines [65]. The ideal scaffold has three dimensional (3D) structure composed of biocompatible materials with a controllable degradation profile. The degradation rate needs to be commensurate with neotissue formation while still maintaining the mechanical properties over the degradation period and tissue regeneration. The presence of interconnected pores with an average diameter with the range of 50 to 200 μm is critical for bone repair [66]. This interconnectivity acquires sufficient mass transfer feature for nutrients and waste, which provides an appropriate environment for cell adhesion, proliferation, and differentiation [67-69].

The selection of a proper material to fabricate a scaffold is the most important factor towards the engineering the bone. While the ceramics represent intrinsic osteoinductive and osteoconductive behaviours, their limited degradation profiles restrict their applications in bone tissue engineering. The application of natural and synthetic polymers with controllable degradation profiles, moreover, is limited due to their lack of bioactive characteristics. The modified bioactive polymers [70-72], biodegradable ceramics [73-76], and their organic-inorganic complexes [77, 78], therefore, have been assessed to design a biomimetic scaffold for bone regeneration. Hydrogels, for instance, mimic the chemical composition of ECM due to their intrinsic biocompatibility and desirable physicochemical characteristics [79]. The shortfalls of hydrogels including low mechanical properties and fast degradation profiles must be overcome prior to their applications for bone tissue engineering [80]. In this session, an overview of biomaterials that have been used for bone regeneration was presented.

### 2.3.1 Polymer-based Scaffold for Bone Tissue Engineering

Collagen is the most abundant organic component in the bone structure [45]. The lack of osteoinductive and osteoconductive behaviour restricts the application of pure collagen for bone tissue engineering. The combination of bioactive compounds such as inorganic materials [81-83] or biological

motifs [84-86] to collagen-based scaffolds, for instance, is an attempt to mimic the bone structure. These scaffolds, however, possess insufficient mechanical properties due to difficult reproducing of collagen spatial conformation in osteon sites [45]. In addition to extensive application of collagen [87], other natural-based polymers including alginate [88-90], chitosan [91-93], gelatin [94-97], Gellan gum [98, 99], and silk [100-102] have been used to fabricate a biocompatible complex for bone tissue engineering.

Synthetic polymers such as aliphatic polyesters and their copolymers were extensively used to fabricate a biodegradable scaffold incorporated with bioactive compounds for bone tissue engineering [103, 104]. Several attempts have been approached on the fabrication of 3D scaffolds from poly(lactic acid) (PLA) [105, 106], poly(lactic-co-glycolic acid) (PLGA) [6, 107, 108], poly (ε-caprolactone) (PCL) [109-112], poly anhydrides [113], and poly(phosphazenes) [114]. The incorporation of osteoconductive components in these polymers promoted their application in bone tissue engineering. Hydrogels fabricated from synthetic, or natural polymers possess superior impacts on tissue engineering. The biodegradable hydrogels mimic the chemical composition of ECM due to their intrinsic biocompatibility and desirable physicochemical characteristics, which guide the spatially complex multicellular processes of tissue regeneration [115].

The intermolecular interactions between polymer chains have a significant effect on their physicochemical and mechanical properties. These interactions, as well as chemical stimulus, can form a 3D network by crosslinking of polymer chains. The physicochemical associations including ionic interactions [116-120], crystallisation [121-124], and self-assembly [125-133] induce gelation of polymers upon hydrogen bonding, and van der Waals and π- π intermolecular interactions. The limiting factors of these physically crosslinked hydrogels are their weak mechanical properties, fast dissociation in the physiological condition, and the lack of interconnected porosity within their structures [134]. The formation of a covalent bond between polymer chains, however, leads to the hydrogels with superior

mechanical strength and enhanced degradation profile. In the next session, different chemical and photocrosslinking methods to fabricate a hydrogel are discussed, briefly

### 2.3.2 Hydrogel Fabrication *via* Chemical Crosslinking

Chemical stimulus induces gelation of the polymeric solution by forming chemical changes in the molecular structure of precursors or by the fabrication of covalent bonds in their polymeric systems [135]. These covalent interactions include Michael addition, Schiff and click reactions, redox-polymerisation, disulphide formation, and enzymatic- or photocrosslinking. The schematic of these chemical reactions is shown in Scheme 2-1.

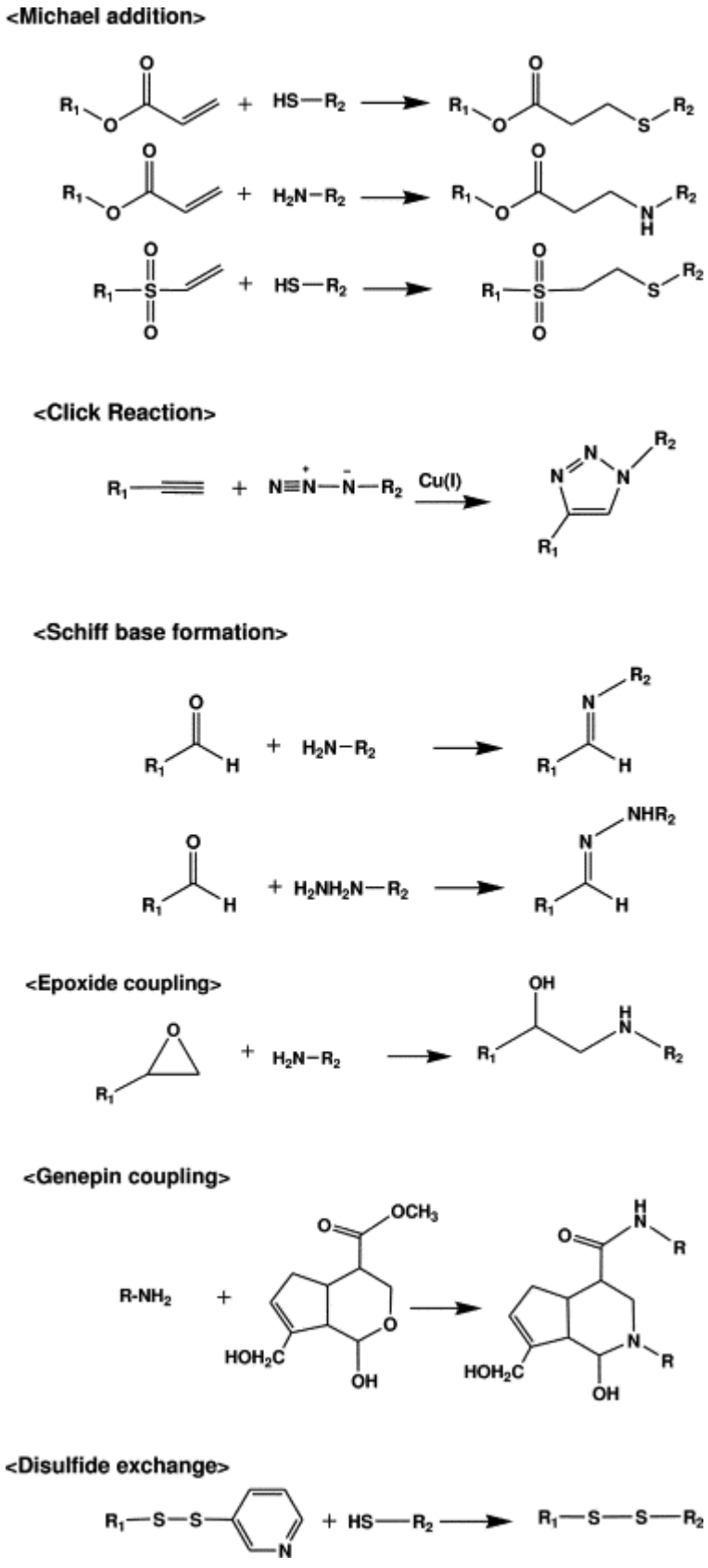


**Scheme 2-1 Scheme of chemical reactions used for covalent crosslinking of polymers [136].**

**Michael Addition**

Michael addition is the 1, 4- addition of nucleophiles to α,β-unsaturated electrophiles. The nucleophile components comprised from thiol- and amine-functionalised macromeres, whereas ketones or esters with vinyl sulfone-, acrylate-, methacrylate-, or methacrylamide functional groups have been used as electrophiles [136]. The high efficacy of this gelation scheme under aqueous physiological conditions without the formation of any side products favours this method for biomedical applications. The nucleophilic derivatives of natural polymers including dextran [137], gelatin [138-140], hyaluronic acid [141-144] and collagen [145], and synthetic polymer such as poly(ethylene glycol) (PEG) [146-148] have been used to form a biocompatible hydrogel for tissue engineering or drug delivery applications. The thiolated gelatin, for instance, formed a hydrogel in the presence of acrylate-derivative of PEG as a crosslinking agent [140]. The encapsulation of fibroblasts within these hydrogels enhanced their cytoplasmic spreading and proliferation. The nucleophilic derivatives PEG were also used to fabricate biocompatible hydrogels for encapsulation of biological active agents [149, 150] and chondrocyte cells [151]. Despite the fast hydrogel formation using Michael addition, the complex mechanism of synthesis using toxic components, and the insufficient mechanical properties and degradation profile of resulting hydrogels limited their applications for bone tissue engineering.

**Schiff's Base Reaction**

A Schiff's base crosslinking is a condensation of an amine functional group by an aldehyde group without the use of any catalysts. Glutaraldehyde, for instance, has extensively used to crosslink different natural and synthetic polymers. Collagen [152, 153], chitosan [154, 155], and gelatin [156], for instance, have been crosslinked by glutaraldehyde to form a hydrogel for engineering different tissues. The associated problems with a high concentration of glutaraldehyde such as heterogeneous crosslinking and the intrinsic cytotoxicity have been overcome at low concentration [157]. The

chemical modification of polysaccharides with oxidative agents such as sodium periodate ($NaIO_4$) to create aldehyde groups is another approach to forming a hydrogel with amine-functionalised polymers. The oxidisation of dextran [158, 159], alginate [160], and hyaluronic acid [161] formed an *in situ* hydrogel with amine groups of gelatin and chitosan. The external stimuli including pH and ionic strength of the solution, and degree of oxidisation had a significant impact on gelation rate of these hydrogels [162]. Despite the high gelation efficiency of Schiff base in physiological condition [163], the *in vivo* performances of these hydrogels may be altered due to the inflammation and calcification of surrounded tissue upon the reaction with aldehyde functional groups [164].

Genipin is a natural-based crosslinking agent showing 10,000 times less cytotoxic than glutaraldehyde [165]. The mechanism of protein-crosslinking with genipin is not entirely understood [166]. However, it is known that the free amine groups of the peptide such as Arg-Gly-Asp (RGD) interact with genipin to form a heterocyclic structure [167]. The genipin-crosslinking, moreover, is a pH-dependant mechanism that undergoes ring-opening polymerisation under basic conditions [168]. At acidic or neutral conditions, however, genipin directly reacts with the primary amine functional groups. Different natural polymers such as chitosan [169, 170], collagen [171, 172] and gelatin [173, 174] have been crosslinked by genipin for tissue engineering application.

**Disulphide Formation**

An *in situ* hydrogel forms upon the formation of disulphide bonds between intermolecular chains of polymers with thiol functional groups [175]. The crosslinking proceeds through the oxidation of thiol groups at pH above 5 in the presence of oxidising agent [176]. The reversible hydrogel of thiolated hyaluronic acid, for instance, was fabricated through disulphide crosslinking approach in physiological condition [177, 178]. The physicochemical properties of hydrogels fabricated through this scheme are highly dependent upon the nature of the polymer backbone [179], the degree of oxidisation

[180] and the chemistry of oxidising agent [181]. Despite the controllable degradation profile of these hydrogels, the complex mechanism of crosslinking and the presence of oxidising agent restrict the practical application of these hydrogels.

**Click Reaction**

A click reaction is the cycloaddition of azide and alkyne to form a triazole ring in the presence of Cu(I) as a catalyst. This approach has a vast range of application in biomedical engineering due to its rapid proceeding and high conversion rate without side products in physiological condition [182, 183]. The orthogonal nature of this strategy, moreover, ensures the absence of cross-reactions with other functional groups [134, 184]. Different synthetic and natural polymers such as poly(vinyl alcohol) [185], PEG [186-188], polypeptide [189], hyaluronic acid [190], and gelatin [191] were converted to their azide or acetylene derivatives to form a hydrogel via click reaction. The toxicity of the catalyst renders such reactions undesirable for *in situ* cell encapsulation. The residual Cu (I) trapped in the gels during the synthesis needs to be extracted thoroughly before the gels can be used for cell culture. A copper-free click reaction, therefore, has been developed using cyclooctyne derivatives [192]. In this approach, azide and cyclooctyne derivatives undergo rapid cycloaddition reactions under physiological conditions in the absence of auxiliary reagents [193-195]. A hydrogel with enhanced physicochemical and mechanical properties and tuneable gelation was fabricated from the functionalised chitosan-PEG complex using copper-free click chemistry. Despite the possible application of these hydrogels as injectable biomaterials [196], the copper-free click chemistry is infancy, and further research is required to understand the biological effects of this method at the insertion site.

**Redox-polymerisation**

The release of free radicals from redox reactions in an aqueous solution can trigger the crosslinking of polymers with acrylate or methacrylate functional groups. This approach is initiated by the addition of ammonium persulphate

(APS) to tetramethylethylenediamine (TMEDA) [197] or ascorbic acid (AA) solutions [198]. The redox-polymerisation has been used to fabricate biocompatible hydrogels with enhanced mechanical properties and degradation profiles. For instance, synthetic polymers such as poly(propylene fumarate-*co*-ethylene glycol) [199], oligo(poly(ethylene glycol)fumarate) [200] and poly(lactic-ethylene oxide fumarate) [201], and acrylate-derivatives of natural polymers including dextran [202] and chitosan [203] formed biodegradable hydrogels for different biomedical applications. Moreover, the encapsulation of cytocompatible moieties such as growth factors [204], drugs [205], and cells [206] within their 3D structures extensively enhanced their biomedical application. Despite the biologically benign process of redox-polymerisation, the residue of free radical ions is an issue for biomedical applications.

**Enzymatic-crosslinking**

The selective cleavage or ligation of enzymes to a particular bond promotes their application as a crosslinking agent without interfering with other chemical moieties of the polymer. Different enzymatic reactions including horseradish peroxidase [207], transglutaminase [208], phosphatase [209], tyrosinase [210], themolysin [211], α-galactosidase [212], and esterase [213] have been used to form a hydrogel. Horseradish peroxidase (HRP) is extensively used to prepare an enzymatic hydrogel. A solution of HRP in $H_2O_2$ is added to an aqueous solution of polymers containing tyrosine or $_L$-3,4-dihydroxyphenylalanine (DOPA) to catalyse their oxidative coupling reactions. The peptide-functionalised derivatives of PEG [214], chitosan [215], dextran [207], gelatin [216], heparin [217], and hyaluronic acid [218] were used for the substrate of HRP. The incorporation of HRP/$H_2O_2$ to these solutions rapidly formed a hydrogel by oxidative coupling of their peptides. A tyrosine-modified solution of hyaluronic acid, for instance, was subcutaneously injected into the rats to form an enzymatically crosslinked hydrogel in less than 20 s [219]. The concentration of hydrogen peroxide and enzyme have significant impacts on the gelation time and physicochemical and mechanical properties of these hydrogels [220].

Transglutaminase (TG) is another enzyme that catalyses a calcium-dependent acyl transfer reaction between amines and ɣ-glutaminyl functional groups. The presence of polypeptides containing lysine and polymers with glutamine groups is vital for these reactions [221]. A glutamine-modified PEG, for instance, was enzymatically crosslinked with poly(lysine-*co*-phenylalanine) in an aqueous solution of TG [222]. Gelatin is a biopolymer with a sequence of lysine residues and glutamine functional groups. A cell-encapsulated hydrogel, therefore, was fabricated by enzymatic crosslinking of gelatin in the presence of TG [223]. Despite the high selectivity of this crosslinking method, the presence of unreacted enzymes acts as an impurity and has adverse impacts on biocompatibility of the system through denaturing of hydrogel as well as the encapsulated compound [136].

**Photocrosslinking**

Photocrosslinking provides some economic advantages over other chemical crosslinking methods including fast hydrogel formation in physiological condition, organic-solvent free formulation as well as the low cost [224]. Typically, an aqueous solution of macromer goes through short exposure of visible light [225, 226], ultraviolet (UV) [227, 228], or laser [229, 230] in the presence of a light-sensitive component called as photoinitiator. The efficiency of this approach is dependent upon the nature of photoinitiator, beam wavelength, and the macromer. The chemistry of photoinitiator determined the specific parameters of the reaction such as the rate, spectral sensitivity, light resistance, and the stability of materials under storage conditions [224]. Two types of photoinitiators exist to crosslink the macromer. The first type of photoinitiators generates the active radicals with the capacity of initiating the radical polymerisation. The α-hydroxyalkylphenones derivatives such as 4-(2-hydroxyethylethoxy)-phenyl–(2-hydroxy-2-methyl propyl) ketone (Irgacure® 2959) are extremely reactive and form benzoyl and alkyl radicals upon UV-irradiation. The second type of photoinitiators, however, requires a tertiary amine molecule as a co-initiator to abstract the hydrogen. Eosin, for instance, reacts with

triethanolamine as a co-initiator to form intermediary species. The photo-initiation continues with an electron and hydrogen transfer resulting in the radical formation [231].

Different natural and synthetic polymers have been converted to their acrylate-derivatives to form a photocrosslinkable hydrogel. Natural polymers such as alginate [232], chitosan [233], chondroitin sulphate [234], gelatin [235], heparin [236], hyaluronic acid [237], starch [238], and tropoelastin [239, 240] were widely used to fabricate a photocrosslinkable hydrogel. Methacrylated hyaluronic acid, for instance, forms a photocrosslinkable hydrogel under laser [229] or UV irradiation [237]. The laser crosslinking process was initiated in the presence of eosin/triethanolamine using an argon laser at 514 nm. Upon laser exposure, eosin is excited to the triplet state, and triethanolamine donates an electron to generate a radical anion of eosin and a radical cation of ethanolamine. These free radicals polymerise an aqueous solution of functionalised-hyaluronic acid [229].

The bioprintable hydrogel, on the other hand, was designed by UV-irradiation of methacrylate-derivatives of gelatin and hyaluronic acid in the presence of acetophenone as a photoinitiator [237]. The various cell-laden structures for engineering the different tissues were fabricated from the methacrylated gelatin (GelMA) [241-243]. The free amine groups of gelatin were converted to their methacrylate derivatives to form a hydrogel in the presence of Irgacure as a photoinitiator [244-246]. Despite the promising biological behaviour of these naturally derived hydrogels, their compressive modulus was inferior and varied in the range of 0.5 kPa to 100 kPa [230, 234, 247].

PEG-based polymers were also modified to their acrylate derivatives to form a photocrosslinkable hydrogel. Despite the favourable physicochemical and mechanical properties of these hydrogels [248-250], the lack of cell motifs in these hydrogels restricts their biomedical applications. This drawback was addressed by incorporation of polypeptides such as RGD [251, 252], growth factors [253], and naturally derived

polymers [254-257]. A cell-laden hydrogel, for instance, was fabricated by photocrosslinking of an MSC-suspended solution of hyaluronic acid and PEG diacrylate (PEGDA) in the presence of transforming growth factor (TGF-β3) [253]. After subcutaneous injection of the suspension into mice, their skin was exposed to UV radiation to facilitate *in situ* hydrogel formation. The stem cells were chondrogenically differentiated and expressed cartilage-specific genes over 3-weeks of implantation. A micro-patterned hydrogel, moreover, was fabricated upon the photocrosslinking of an aqueous solution of PLEOF-PEGDA incorporated with GelMA [254]. While the physical stability and mechanical properties of hydrogels relied on the synthetic polymers, the presence of GelMA promoted the proliferation of encapsulated osteoblasts. Despite the extensive advantageous of photocrosslinking for hydrogel formation and micro-patterning, UV-induced polymerisation might have negative impacts on the encapsulated cells, drugs or growth factors [258]. The proper selection of photoinitiator and beam wavelength could minimise these drawbacks.

## 2.4 Ceramic Scaffolds for Bone Tissue Engineering

Bioceramic is a solid compound comprised of inorganic and non-metallic elements formed by the application of heat and pressure [259]. The intrinsic osteoconductive behaviours and high mechanical strength of these class of materials introduce them as a proper candidate for tissue engineering [260]. The slow degradability of these materials and their osteoinductivity, however, must be modified prior to their application as a bone scaffold. The fabrication of porous structures with interconnected pores [261] or the incorporation of polymers into bioceramic structure [262], for instance, are some attempts to enhance their degradation profile. The osteoinductivity of bioceramics, moreover, is modified using calcium phosphate ceramics. These bioceramics demonstrate unique biological interactions towards their physiological environment upon inducing of calcification and promoting the osteoinductivity [54].

### 2.4.1 Calcium Phosphate Ceramics

Calcium phosphate ceramics (CPCs) is extensively used in the forms of tricalcium phosphate (β-TCP, $Ca_3[PO_4]_2$) and hydroxyapatite (HAp, $Ca_{10}[PO_4]_6[OH]_2$) [263]. Despite the similar elemental composition of HAp and β-TCP, their physicochemical properties are significantly different. β-TCP, for instance, exhibits an adversely high dissolution rate with an immunologic response [264]. On the other hand, HAp possesses a crystalline structure with limited *in vivo* degradation profile [265]. This variation is a result of dissimilarity in the density and crystalline structure of HAp and β-TCP due to their different fabrication process.

The sintering process of CPCs carries out in the range of 800°C to 1500°C and the partial pressure of water in this atmosphere has a significant impact on the formation of final ceramics. While the β-TCP is fabricated upon thermal decomposition, the presence of water promotes the rate of phase transition of β-TCP to HAp [266, 267]. The wet fabrication process such as precipitation, hydrothermal and hydrolysis of other CPCs are used to fabricate HAp [268]. Despite the attractive feature of these materials, their clinical applications were limited to non-load bearing applications due to their intrinsic brittleness [269]. Different approaches including the ionic-substitution [270], and the formation of polymer-ceramic composites [17, 271] have been attempted to overcome these shortfalls.

The mineral component of bone is similar to HAp but contains other ions in the composition that play a significant role in the biological behaviour of bone. The ionic incorporation into the structure of β-TCP and HAp, therefore, can regulate their lattice structure, microstructure, crystallinity, and dissolution rate of CaPs [272, 273]. The ionic incorporation of fluoride [274], magnesium [275], manganese [276], silver [277], strontium [278], and zinc [279], within CPCs had significant impacts on the biological behaviour of these bioceramics. The incorporation of silicon into nano-calcium phosphates, for instance, facilitate the adhesion, spreading, growth and proliferation of osteoblasts on these ceramic-based scaffolds [280].

### 2.4.2 Bioactive glass

Bioactive glass (BG) is a class of ceramics, which regulates tissue metabolism through stimulating the osteogenic differentiation [5-7], enhancing the pro-angiogenesis of endothelial cells [8-10], and modulating the intracellular interactions [11-14]. Silicon as the essential component of BG attributes to the collagen formation [281] and calcification of bone tissue [282]. The incorporation of other ionic components such as calcium [283, 284], phosphorous [20, 285], strontium [286, 287], and borate [288, 289] enhances the therapeutic properties of BG towards a particular biological response [290].

Bioactive glass is fabricated through the melt-quenching process [291-294] or sol-gel method [295-298]. In the melt-quenching process, the melted mixture of alkali or alkali earth salts in a predetermined composition is quenched to form a glass with a disordered structure [299]. This structure is further milled to produce a BG with desired particle size [300]. Despite the basic nature of the melt-quenching process, the high processing temperature, difficult shaping process, and the high risk of contamination may have adverse impacts on the composition and bioactivity of BG. These issues could overcome by the sol-gel method, which comprised from hydrolysis and condensation reactions. The mechanism of the sol-gel method would be discussed at the end of this chapter.

### 2.4.3 Modification of Ceramic Structure by Polymers

The incorporation of polymeric components in the structure of bioceramics can enhance their mechanical properties and degradation profile. Several attempts such as foam replica method [301, 302] and polymer-ceramic composite formation [303-305] have been attempted to design a scaffold for bone tissue engineering.

Foam replica method is based on the impregnation of an aqueous suspension of bioceramic in porous polymeric foam. After totally filling the pores, the excess suspension is removed from the impregnated foam upon passing through a roller or centrifuging [306]. The foam is then carefully heated at

temperatures between 300ºC and 800ºC for slow decomposition and diffusion into polymeric template [307]. The porous scaffold is then densified upon sintering at temperatures ranging from 1100ºC to 1700ºC to produce macro-porous structures with an interconnected pores [308, 309]. The mechanical strength of these structures, however, can be degraded by the formation of cracked struts during the decomposition of the foam [301].

Nanocomposite hydrogels are defined as an organic-inorganic composites crosslinked in the presence of nanoparticles [310-314]. The presence of the inorganic compound in theses hydrogels enhance their physicochemical and biological behaviours [315]. An injectable nanocomposite hydrogel, for instance, was fabricated from PEG and nano-HAp [316]. This composite possessed elastic mechanical properties with promoted biological behaviour. Despite the extensive application of polymer-ceramic composites, the heterogeneous distribution of ceramic nanoparticles within the polymer network may have a negative impact on their *in vivo* bone tissue engineering application. Fabrication of organic-inorganic hybrid could enhance the homogeneous distribution of mineralised phases within the polymeric scaffold.

## 2.5 Organic-Inorganic Hybrids

The first classification of organic-inorganic hybrid materials dates back to the beginning of the 1990s when Novak introduced them in five distinct types [317]. The chemical structure of the organic component (*i.e.,* polymer or monomer) and the chemical interaction between organic and inorganic phases are their main distinctive criteria. The first class of organic-inorganic hybrid comprises from embedding a polymer within an inorganic precursor. In these hybrids, an interpenetrated network of organic-inorganic compounds is formed via intermolecular forces such as van der Waals, whereas, in type II, a polymeric is covalently bonded to the inorganic network structure.

The second class of hybrids is fabricated from the simultaneous interpenetration of organic monomers within the inorganic precursors. The

presence of covalent bond between these two phases converts type III materials to type IV hybrid [318-324]. The last type of hybrids, also known as a non-shrinking material, is fabricated through mutual polymerisation of organic-inorganic precursors in the presence of polymerisable catalysts and solvents [325, 326]. The presence of the catalyst, organic solvents, and monomers for these simultaneously formed hybrids are their major burdens for their biomedical applications.

The organic-inorganic hybrids possess broad biomedical applications. Scaffold fabrication [259, 327], coating the surface of implants [328-330], constructing the optical biosensor [331, 332], and encapsulation of biological components [333-338] are few examples of their applications in biomedical engineering. These biomaterials are commonly fabricated from type I or II hybrids through the sol-gel method. The presence of covalent bond between components has a significant effect on their properties. The applications of these hybrids (type I and II) in bone tissue engineering are discussed in the following sections. In addition, the mechanism of the sol-gel method would be discussed at the end of this chapter.

### 2.5.1 The Interpenetration of Polymer within Inorganic Network

Type I hybrid is generated from the interpenetration of a polymer within an inorganic network using the sol-gel method. These dissimilar phases fabricate macroscopically uniform materials while their nanostructures are entirely separated [339]. It is crucial to optimise the conditions of the fabrication process to prevent the polymer phase separation during gel formation and drying processes. The selection of a suitable solvent for dissolving both polymer and inorganic phase is a crucial in the formation of hybrids to eradicate phase separation and insufficient mechanical integrity [340].

Solvents such as water, alcohols, hydrochloric acid, and formic acid are used to prepare organic-inorganic hybrids. The presence of liberated methanol or ethanol during the gel formation, however, can modify the solvent properties. A polymer that is initially soluble in the solvent may

precipitate at later stages of gel formation due to the bulk conversion of solvent from polar aprotic to polar protic [317]. Poly(vinyl pyrrolidone) (PVP), for instance, formed a homogenous solution with formic acid and tetraethyl orthosilicate (TEOS) mixture. The irreversible polymer precipitation, however, occurred upon release of ethanol into the reaction prior to the condensation of the silica network [317]. The homogenous hybrid of PVP-TEOS, on the other hand, was formed in the presence of isopropyl alcohol [341] as a solvent. The chemical structure of the polymer and its feasible interaction with alcohols, therefore, is critical.

The chemical structure of the organic phase is a critical factor in the formation of the type I hybrids. The presence of basic functional groups, such as amine and pyridine, makes the organic phase soluble in the acidic catalysed solution of silica during the condensation and drying processes [342]. On the other hand, the presence of hydrogen bond acceptor groups in the backbone of the polymer enhances the formation of van der Waals interactions between polymer and inorganic phase [343]. Different natural and synthetic polymers were incorporated into bioactive glass (BG) precursors to form a hybrid are discussed in detail.

**Interpenetration of Natural Polymers within the Inorganic Network**

The first application of the interpenetrated network of organic-inorganic compounds in tissue engineering dated back to the end of the 1990s. An ethanol-catalysed silica solution was added to an acidic solution of chitosan to form an artificial skin [344]. The presence of the silica network had significant effects on oxygen permeation and also a proliferation of L929 fibroblasts on these membranes [345]. These outcomes encouraged researchers to develop a protein-silica complex for tissue engineering applications. For instance, an interpenetrated network of silica and collagen was prepared for bone tissue engineering [346-348]. The interpenetrated hybrid with 60 wt% collagen, for instance, displayed a splitting tensile strength of 20 MPa. These monoliths, however, demonstrated brittle structures and broke at 6% compression strain [348]. Gelatin as a

disintegrated derivative of collagen is extensively used for fabricating of organic-inorganic complex [24, 25]. The gelatin-silica microgels, for instance, was fabricated to protect the encapsulated cardiac side population cells within their structure [349]. The silica hybridisation significantly enhanced cell proliferation. These complexes with a young modulus of 1.87 kPa, however, were not suitable for hard tissue engineering.

**Interpenetration of Synthetic Polymers within the Inorganic Network**

Synthetic polymers are the favourite class of materials due to their tuneable and predictable physicochemical and mechanical properties upon the modification of their functional groups [350]. The presence of siloxane functional group in the backbone of poly(dimethylsiloxane) (PDMS), for instance, made this biocompatible polymer as a first candidate for fabrication of a bioactive organic-inorganic hybrid [351-353]. Despite the promising bioactivity and mechanical performances of these interpenetrated networks [354, 355], their slow degradation profiles restrict their applications in tissue engineering. More recently, a porous and crack-free monolith was fabricated from PDMS-TEOS hybrids incorporated with PCL pellets for bone repair applications [356]. The mechanical properties and degradation profile of these monoliths, however, were not evaluated.

Poly(ε-caprolactone) is a biocompatible and biodegradable aliphatic polyester with an extensive range of applications in the biomedical application [357-362]. The incorporation of metal oxide precursors including titanium oxide [363], zirconium oxide [364], and silica [365] within PCL solutions formed bioactive interpenetrated networks for tissue engineering [366] and drug delivery systems [367]. The hydrolysis of these metal oxide precursors yielded to the formation of hydroxyl groups. Further formation of hydrogen bonds between these hydroxyl groups with carbonyl functional groups of PCL enhanced the compressive modulus of hybrids up to 310 MPa [368] and improved their angiogenesis and osteogenesis properties [369]. These brittle monoliths, however, tolerated a very limited

range of compression, and they lost their physical integrities under 10.8 % compressive strain [370].

Poly(vinyl alcohol) (PVA) is a water-soluble poly(hydroxylate) with thermoplastic features [371-373]. The presence of hydroxyl groups in the structure of this polymer facilitates the formation of interpenetrated network with inorganic compounds [374]. A solution of BG, for instance, was incorporated within a PVA solution to form a cytocompatible construct with a compressive modulus of 5.9 MPa [375]. This hybrid, however, demonstrated a fast dissolution profile, and brittle structure with an ultimate compressive strain of 5 %. These shortfalls were overcome by chemical crosslinking of the organic phase [376]. The presence of glutaraldehyde as a crosslinking agent enhanced their ultimate compressive strain 3-fold [377]. The degradation profile of these cytocompatible hybrids was also modified to surface erosion upon chemical crosslinking [378].

Despite the significant enhancement of physicochemical and mechanical properties of the hybrids, these interpenetrated networks are formed through hydrogen bond formation between the residual hydroxyls of silica and polymer molecules. These interactions, however, are weak and unstable in aqueous media [29]. These drawbacks could be addressed by covalent bond formation between the polymer and the inorganic components. In the next session, the application of covalently bonded organic-inorganic hybrids in tissue engineering is reviewed.

### 2.5.2 The Fabrication of Covalently Bonded Organic-Inorganic Hybrids

The second type of hybrids is formed through the covalent bonding of a polymer into an inorganic compound. Prior to hybridisation, the preformed polymer is converted to its alkoxysilyl derivative (*i.e.,* R`-C-Si-$(OR)_3$) to form a covalent bridge with a metal oxide component. The fabricated alkyl carbon-silicon is an inert bond toward the hydrolysis and does not change the rate of alkoxides hydrolysis from the silicon centre. The pendant silyl group, therefore, is incorporated into the inorganic structure to form a

covalently bonded organic-inorganic hybrid. The alkoxysilylation of polymer carries out in two different approaches. In the first approach, the hydrosilation reaction takes place through the terminal alkene functional groups of the polymer in the presence of platinum as a catalyst [379, 380]. The presence of toxic organic solvents and the complicated nature of this approach restrict the application of these polycarbosilanes in tissue engineering.

In the second approach for the fabrication of organic-inorganic hybrids, an organosilane coupling agent makes a covalent bridge between a polymer and an inorganic network [75, 381]. The organosilane coupling agent is a heterobifunctional compound that forms a covalent bond with a polymer through its functional organic terminal. The other silane terminal, however, goes through hydrolysis and condensation reactions with the inorganic phase [382]. The chemical interaction of cellulose acetate and 3-(isocyanatopropyl)-trimethoxysilane as a coupling agent, for instance, forms cellulose urethane with pendant alkoxysilane groups. The hydrolysis and further condensation of these pendant groups with hydrolysed TEOS solution turn to a covalently bonded cellulose-silica hybrid with enhanced mechanical performances [383-385].

Different natural and synthetic polymers were converted to their organosilane derivatives to form a covalently bonded hybrid for biomedical application [386]. A polyelectrolyte complex, for instance, was fabricated by the combination of organosilane derivative of alginate and tetramethyl orthosilicate (TMOS). A modified derivative of alginate by 3-(aminopropyl)-trimethoxysilane (APTMS) formed a hydrogel in the presence of calcium chloride as a crosslinking agent. The resulting microbeads were then immersed into an *n*-hexane solution of TMOS to covalently coat with silica [386]. The encapsulation of pancreas islets of Langerhans into these microbeads followed by *in vivo* transplantation into mice confirmed their feasible application as an artificial pancreas [387]. The presence of metal oxide in organic-inorganic hybrid displays an intrinsic bioactivity that is preferable for bone tissue engineering applications. To

this end, different natural and synthetic polymers were covalently bonded to the silica precursors. The physicochemical properties and mechanical performance of these hybrids are presented in Table 2-1.

**Table 2-1 The physicochemical and mechanical properties of covalently bonded hybrids for bone tissue engineering**

| Organic Phase | Hybrid Formation[*;†;‡] | Physicochemical and Mechanical Properties[þ] | Ref |
|---|---|---|---|
| **Chitosan** | **I;-;A&B** | **ESR**= 0.50 mg/mg; **E**= 4.5 MPa; **σ**= 20 MPa; **ε**= 5% | [388-391] |
| **Collagen** | **I&II;-;C&D** | - | [392, 393] |
| **Gelatin** | **I;-;A&B&E** | **ESR**= 7.38 mg/mg; **E**=1.94MPa; **ε**= 17.34% | [394-396] |
| | **I;1&2;A&B** | - | [397-399] |
| | **I;2;F** | **E**= 331-1270 kPa; **ε**= 5.2-8.88 % | [400, 401] |
| | **I;3;B** | **σ**= 4.3 MPa, **ESR**= 0.15 mg/mg | [402] |
| | **I;4;F** | | [403] |
| **PCL** | **III;2;G** | - | [404] |
| **PDMEMA** | **IV;5;B&F** | **H**= 527 MPa | [405-407] |
| **PGA** | **I;6;F&H** | **H**= 520 MPa; **E**= 30-40 MPa; **σ**= 3-10 MPa; **ε**= 15-32% | [408-411] |
| **PLLA** | **II;3&7;B&F** | - | [412, 413] |
| **PMMA** | **IV;2;I** | **H**= 3.14 MPa; **E**= 6 MPa; **ε**= 14% | [414] |

[*]Organosilane coupling agent: **I**: *(3-Glycidoxypropyl) trimethoxysilane*; **II**: *(3-Aminopropyl) triethoxysilane*; **III**: *(3-Isocyanatopropyl) triethoxysilane*; **IV**: *(3-Methacryloxypropyl) trimethoxysilane*.

[†]Inorganic Precursor: **1.** *Calcium nitrate*; **2.** *Tetraethyl orthosilicate*; **3.** *Tetraethyl orthosilicate-Hydroxyapatite*; **4.** *Tetramethyl orthosilicate*; **5.** *Zirconium peroxide*; **6.** *Tetraethyl orthosilicate-Calcium nitrate*; **7.** *Calcium carbonate*.

[‡]Biological evaluations: **A**: *MG63*; **B**: *MC3T3-E1*; **C**. *L-929;* **D**: *C2C12*; **E**: *Neonatal olfactory bulb ensheathing cell;* **F**: *Mesenchymal stem cell*; **G:** *in vitro Mesenchymal stem cell and in vivo study in Rabbit*; **H**: *Saos-2*; **I**: *in vitro primary osteoblast and in vivo study in Mice*.

[þ]**ESR**: *Equilibrium swelling ratio*; **H**: *Hardness*; **E**: *Young modulus*; **σ**: *Ultimate stress*; **ε**: *Ultimate strain*.

Materials: **PCL**: *Poly(ε-caprolactone)*; **PDMEMA**: *Poly((dimethylamino) ethylmethacrylate)*; **PGA**: *Poly(ɣ-glutamic acid)*; **PLLA**: *Poly($_L$-lactic acid)*; **PMMA**: *Poly(methyl methacrylate)*.

## Formation of Covalent Bonding between Natural Polymers and Inorganic Precursors

The natural bone comprises from a homogeneous hybrid of collagen and hydroxyapatite [415, 416]. The formation of collagen-inorganic complex, therefore, is fascinating to mimic the bone structure [22, 417]. Despite the extensive applications of collagen-hydroxyapatite composites [418-421], the collagen-inorganic hybrids were limited to the organosilation of collagen in the absence of inorganic precursors [392, 393]. The hydrogel formation

from a chemical modified collagen with (3-aminopropyl) triethoxysilane (APTES), for instance, displayed a 60-fold enhancement in their rheological properties [392]. The organosilation with (3-glycidoxypropyl) trimethoxysilane (GPTMS), moreover, enhanced the adhesion and proliferation of osteoblast cells on the surface of alkoxysilyl derivatives of collagen [393]. Chitosan is another biopolymer that chemically modified by GPTMS to form a hybrid [391]. This organosilation process yielded to the fabrication of porous structures with enhanced cytocompatibility towards the osteoblast progenitor cells [388-390].

Gelatin is another natural polymer that was hybridised with organosilane components. A condensed structure of gelatin, for instance, was fabricated in the presence of GPTMS [422]. In this process, the epoxy functional group of GPTMS grafted to the amino acid groups of gelatin. The self-condensation of activated silane groups, moreover, acted as a crosslinking agent to form a hydrogel. Despite the significant enhancement of the mechanical performances, GPTMS crosslinking remarkably decreased the physicochemical properties and biological behaviours of these hydrogels compared to the other crosslinking methods [394, 395]. The inorganic proportion of these hybrids, moreover, could not be varied independently of the organosilane coupling agent. This restriction was addressed by the incorporation of different inorganic compounds such as calcium nitrate [398, 399, 423], TEOS [397, 401, 402], and TMOS [403] into the alkoxysilyl derivatives of gelatin. A gelatin-silica hybrid with tailorable physicochemical properties and mechanical performances was fabricated by incorporation of TEOS solution into the pre-functionalised solution of gelatin [400, 401]. The molecular weight of gelatin and the degree of organosilation were paramount factors to mimic the physicochemical and mechanical properties of these cytocompatible hybrids for an extensive range of applications [400, 401].

Poly(γ-glutamic acid) (PGA) is a biocompatible, natural-based polymer with a controllable profile of degradation. The sequence of glutamic acid residues presents in the collagen fibrils of bone and plays a significant role in the

nucleation of hydroxyapatite [424]. A bioactive hybrid of PGA and TEOS with an enhanced degree of cell proliferation was fabricated in the presence of GPTMS as a coupling agent [408]. The incorporation of different calcium sources into the inorganic phase of these hybrids, moreover, had a significant effect on their mechanical performances and degradation profiles [409, 410]. The ultimate compressive strain of these hybrids, for instance, was tuned in the range of 15-32 % upon the addition of different concentrations of calcium chloride [409]. Despite the significant improvements in the mechanical performance of hybrids, the presence of organic solvents in the fabrication process and restricting the encapsulating of biological motifs are the main drawbacks of these hybrids.

**Formation of Covalent Bonding between Synthetic Polymers and Inorganic Precursors**

The fabrication of organic-inorganic hybrids from synthetic polymers has a vast application in tissue engineering. PCL, for instance, was chemically modified in the presence of (3-isocyanatopropyl) triethoxysilane to form a covalent bond with silica [425-430]. The incorporation of MSC cells within these hybrids displayed a significant enhancement on their *in vivo* osteoconductivity in rabbit [404]. The organic-inorganic hybrids were also fabricated from the APTES-functionalised poly($_L$-lactic acid) in the presence of different bioactive glass solutions [412, 413]. The improved bioactivity of these hybrids in addition to the enhancement of cell proliferation introduced them as suitable candidates for bone tissue engineering.

Poly(alkyl methacrylate)s such as poly(methyl methacrylate) (PMMA) and poly((dimethylamino) ethylmethacrylate) (PDMAEMA) are the other examples of synthetic polymers used for fabrication of organic-inorganic hybrids. The presence of methacrylate functional group in the backbone of these polymers facilitates the organosilation reaction in the presence of methacryloxy-possessed coupling agents. For instance, (3-methacryloxypropyl) trimethoxysilane as an organosilane coupling agent

functionalised PMMA [431] and PDMAEMA [407] polymers prior to hybridisation. The addition of silica [414] or zirconia [405-407] into respectively PMMA and PDMAEMA solutions yielded to bioactive hybrids with enhanced mechanical performance and cell proliferation. The polymer-hybridisation has extensive applications in bone tissue engineering. Regardless their natures (*i.e.* type I or II), these organic-inorganic hybrids are fabricated through sol-gel method. The chemistry of this approach is described in the next session.

### 2.5.3 The Mechanism of Sol-Gel Process

A homogeneous organic-inorganic hybrid is fabricated through the mild conditions of the sol-gel method. This approach is based on the hydrolysis and condensation reactions of an organosilane precursor in an aqueous solution of polymer [19]. The presence of polymer solution does not interfere with hydrolysis and condensation of an inorganic compound. In this session, therefore, the mechanism of a sol-gel method for a pure inorganic compound is reviewed in detail.

In the first stage of the sol-gel process, the tetraalkyl orthosilicate as a precursor of BG goes through a hydrolysis reaction. The fabricated sol is a colloidal suspension of nanoparticles (size 1-100 nm) in an aqueous media supplemented with an acidic or basic catalyst. The condensation of these particles forms an interconnected network of submicron pores. This rigid network is converted into the gel structure in the second stage of the sol-gel process [432]. The physicochemical properties of the resulting hybrids depend upon the chemical composition of the catalyst, reactivity of inorganic compounds and the rates of hydrolysis and condensation reactions. The basic catalysed hybridisation, for instance, leads to the formation of multi-branched clusters [433]. The highly ramified structure is formed in the presence of acidic catalysts [434]. At low pH, moreover, the rate of hydrolysis is fast relative to condensation while using the basic catalyst reverses these relative rates and results in the formation of colloidal particles. The difference in cluster formation is also due to the higher

solubility of silicon oxide in alkaline media that enhances their inter-linking compared to acidic media [317].

Regardless of the chemical composition of the catalyst, the sol-gel process is a nucleophilic substitution reaction and comprises from hydrolysis and condensation reactions. The partial hydrolysis of tetraalkyl orthosilicate in the presence of various catalysts, as shown in Scheme 2-2, forms different silanol functional groups.

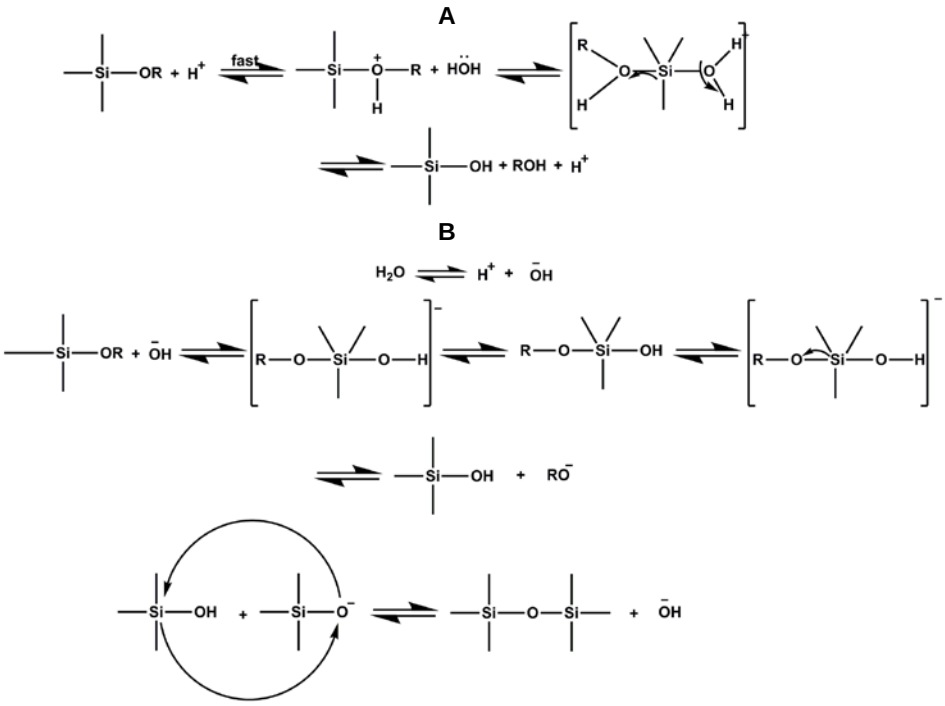


**Scheme 2-2 The schematic of acid- (A) and base-catalysed (B) hydrolysis reactions of silicate-based BG in the sol-gel process [19].**

The condensation of these partially hydrolysed intermediates, as shown in Scheme 2-3, forms bridging oxygen and liberates water, ethanol, or methanol. These hydrolysis and condensation reactions are initiated at different sites of the solution with complicated kinetics. When a sufficient number of interconnected siloxane is formed in a particular region; their cooperative interactions turn to colloidal particles and form a 3D network of gel over time.

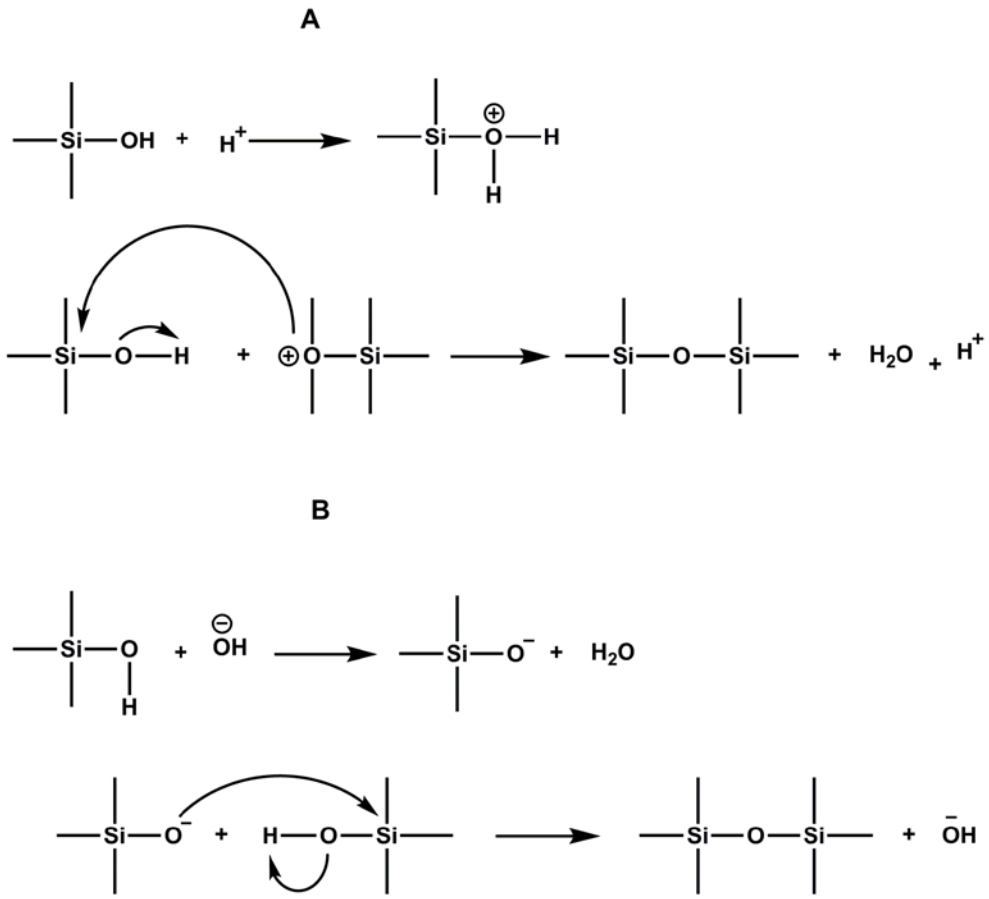


**Scheme 2-3 The schematic of acid- (A) and base-catalysed (B) condensation reactions of silicate-based BG in the sol-gel process [19].**

Following the gel formation, the condensed network goes through an ageing process to increasing the degree of condensation. The resulting materials then expulse the liquid phase, in the process called syneresis [435]. This drying process effectively prevents the formation of a 3D to the tendency of the hybrid network to shrink, crack and shatter [436, 437]. The large capillary forces generated within the pores of hybrid contribute to the drying stresses and yield to the shrinking and cracking of hybrid networks. The shattering, on the other hand, attributes to the solvent evaporation via either opening the reaction vessel at the ambient temperature or by placing the sample under mild vacuum [317]. These unfavourable side effects, however, can be minimised in different ways such as the controlled drying of a hybrid over the period of weeks or months. The addition of the pre-fabricated silica seeds during the sol-gel process, lyophilisation of the hybrid, the use of surfactant, control of drying step, and the presence of chemical additives are

the other approaches that can be used to increase the average pore size of condensed network and prevent the formation of cracks [438, 439]. Despite the formation of crack-free monoliths, the structure of the hybrid is still extensively shrunk (50-70 % of volume fraction) due to the presence of abovementioned capillary forces [317]. Therefore, it is critical to developing a new approach to addressing this issue and fabricating an organic-inorganic hybrid with enhanced physicochemical properties and mechanical performance.

## 2.6 Summary

This chapter described the demand for a new therapeutic approach to regenerating the bone. The current bone treatment techniques are entangled with several complications such as a donor site morbidity, disease infections, and deficient supply. Tissue engineering as a new approach was considered to overcome these burdens and regenerate bone structure. Among different approaches for bone regeneration, nanocomposite hydrogels have high potential to mimic the chemical composition of bone. The heterogeneous distribution of inorganic compound may have an adverse impact on biological behaviours of these hydrogels. This shortfall might be overcome by fabrication of organic-inorganic hybrid hydrogels. This approach, however, has not been exploited for bone tissue engineering.

Different organic-inorganic hybrids with enhanced mechanical properties and bioactivity have been developed to mimic the bone structure. These biomaterials were fabricated through sol-gel method to distribute the bioactive glass homogeneously within the polymer phase. Different aqueous solutions of natural or synthetic polymers have been incorporated into hydrolysed solutions of bioactive glass to form a synergistic hybrid upon the condensation of bioactive glass. In particular, a collagen-inorganic hybrid could be the most favourable biomaterials for musculoskeletal tissue engineering, as these components comprise the chemical structure of bone. However, the limited mechanical properties of these hybrids may evoke severe clinical complications. Despite the nature of organic and inorganic components, the complete condensation of the inorganic phase carries out

through drying and aging steps and yields to the formation of brittle structures. The fabrication of two-dimensional monolith with very limited water uptake capacity is their main drawbacks for bone tissue engineering.

## 2.7 Aim and Objectives

The aim of this study was to develop a unique structure for reconstruction of bone and its interface with soft tissues. It was hypothesised that the fabrication of an organic-inorganic hybrid with elastic mechanical performance and high swelling ratio might enhance the proliferation of bone progenitor cells. To achieve this objective, a covalently bonded hybrid of gelatin-bioactive glass was fabricated through the sol-gel method. It was hypothesised that polymer-crosslinking could control the condensation of the inorganic phase and prevent the formation of brittle structure. In addition, it was anticipated that the addition of the secondary crosslinking agent might improve the mechanical performance of hydrogels without interfering with hybridisation. The effect of variables such as chemical structure and composition of hybrids on their physicochemical properties, mechanical performance, degradation profile and biological performance were examined.

To achieve abovementioned objectives, it was planned to: (1) control the over condensation of inorganic phases in polymer-bioactive glass hybrids, (2) investigate the effect of covalent bond formation between gelatin and bioactive glass through organosilane coupling agents, (3) evaluate the impact of secondary polymer crosslinking on the physicochemical and mechanical properties of hybrid hydrogels, (4) study the impact of incubation media on the degradation profile and the mechanical performance of hybrid hydrogels, (5) conduct *in vitro* bioactivity and biological activity of these hybrid hydrogels, and (6) conduct animal study to assess their cytocompatibility, biological and biodegradable properties for bone repair.

# Chapter 3. Materials and Methods

## 3.1 Introduction

The intrinsic brittleness of pure bioactive glasses (BG) significantly restricts their biomedical applications [5, 297, 303]. Recent studies show that chemical bonding of BG with a polymer and fabrication of organic-inorganic hybrids addresses this shortcoming of bioactive glasses and promotes their physicochemical and mechanical properties [428, 440]. While these hybrids were less brittle, over-condensation of silica networks may still lead to acquiring the brittle monolithic structure. The aim of this study was to reduce the risk of over-condensation and fabricate a 3D structure of polymer-BG hybrid with enhanced physicochemical and mechanical properties. It was hypothesised that the polymer crosslinking can interfere with silica network formation and could be used as a method to control the condensation of the inorganic phase. To assess this hypothesis, gelatin was selected as a polymer phase due to its capacity to form hydrogel through different approach: physical [441], chemical [156, 173, 223] and photocrosslinking [235]. In this chapter, various methods for the fabrication of different types of the gelatin-BG hybrid hydrogel are described. In addition, the characterisation techniques that were used to assess mechanical performance, physicochemical and biological properties of these hybrids are described in detail.

## 3.2 Materials

Gelatin type A, soluble starch, poly(ethylene glycol) diacrylate (PEGDA, Mn 700), methacrylate anhydride (MA, 99%), (3-aminopropyl)-triethoxysilane (APTES), (3-glycidoxypropyl)-trimethoxysilane (GPTMS), tetraethyl orthosilicate (TEOS), tetramethyl orthosilicate (TMOS), and all other chemicals and solvents were in reagent grade and purchased from Sigma-Aldrich (USA) unless specifically mentioned. 2-hydroxy-1-(4-(hydroxyethoxy)phenyl)-2-methyl-1-propanone (Irgacure 2959®) as a photoinitiator was supplied by Ciba Geigy. Genipin was purchased from Wako Chemicals (Japan). Phosphate buffer saline (PBS, pH 7.4 and 0.1 M) was prepared by dissolving PBS tablets (Medicago, Sweden) in 100 ml of deionised water (Millipore, USA). Simulated body fluid (SBF, pH 7.42) was

prepared based on the method described by Kokubo *et al.* [442]. Briefly, proper amounts of sodium chloride and sodium sulphate (Merck Chemicals), potassium chloride and calcium chloride (Silform Chemicals), sodium bicarbonate, potassium phosphate dibasic and magnesium chloride (Sigma-Aldrich) were dissolved in deionised water at 36°C and the pH was adjusted between 7.42 and 7.45 by addition of Tris (Plus one) and 1 M solution of hydrochloric acid (HCl 32 %, Merck Chemical). All these chemicals and reagents were used without further purification.

McCoy's 5A medium modified, propidium iodide and paraformaldehyde were purchased from Sigma-Aldrich. Alkaline phosphate assay kit was purchased from Abnova®. Fetal bovine serum, $_{L}$-Glutamine, Antibiotic-Antimycotic, trypsin-EDTA, and 4', 6-diamidino-2-phenylindole (DAPI) and all other reagents for *in vitro* biocompatibility assays were supplied by Life Technologies unless specified.

## 3.3 Synthesis of Photocrosslinkable Gelatin

Photocrosslinkable gelatin was synthesised by converting the gelatin to its methacrylated derivative (GelMA) by using the method described by Van *et al.* [443]. Briefly, MA (13.4 mmol, 20 ml) was added drop wise (0.4 ml/min) to a 100 mg/ml solution of gelatin in PBS at 50°C to control the pH of the final product. The precise amounts of gelatin and MA were presented in *Appendix A, Table 1*. After one hour, the reaction ceased by the addition of 500 ml pre-heated PBS media. The GelMA solution was then dialysed against distilled water using 12-14 kDa cutoff dialysis tubes at 37°C until the pH was increased to 6. The purified GelMA solution was then lyophilised at -80°C and the resulting foams were kept in the dry and cool environment to avoid moisture absorption.

The degree of methacrylation in GelMA was quantified using proton nuclear magnetic resonance ($^{1}$HNMR) analysis (Varian INOVA NMR, USA). The $^{1}$HNMR spectra were collected at 35°C in deuterium oxide at a frequency of 500 MHz. Phase and baseline correction were applied before obtaining the integral of peaks, and the analysis was repeated at least triple.

It was found that GelMA with 80% degree of methacrylate was synthesised [254].

## 3.4 Synthesis of Photocrosslinkable Starch

Starch was converted to its methacrylated derivative (StaMA) using the method described by Caldwell *et al.* [444]. Briefly, the slurry of 400 mg/ml of starch in PBS was prepared at room temperature. The pH of the slurry was increased to 8-9 by the addition of 3 wt% solution of sodium hydroxide (NaOH, Merck Chemicals). Methacrylic anhydride in 4.5:1 molar ratio of starch: MA was added to the slurry drop wise (0.3 ml/min), and pH was adjusted to 8-9 using NaOH solution. The precise amounts of starch and MA were presented in *Appendix A, Table 2*. Following 1 h agitation at room temperature, pH was decreased to 6.5-7. The StaMA was then dialysed against deionised water for 3 days and then separated by centrifugation at 3500 rpm for 30 min. The sediments were then lyophilised at -80°C and the resulting powders were kept in a desiccator.

## 3.5 Preparation of Bioactive Glass Solution

Bioactive glass (BG) was prepared using the sol-gel method, in which TEOS was dissolved in 40 mM hydrochloric acid (HCl) in 8:1 molar ratio of TEOS: HCl solution. The precise amounts of these precursors were presented in *Appendix A, Table 3*. The mixture was stirred for one hour at room temperature to prepare a homogeneous solution. This solution was then used for the formation of either the interpenetrated gelatin-BG hydrogel or hybrid hydrogels.

## 3.6 Fabrication of Interpenetrated Gelatin-BG Hybrid Hydrogels

The interpenetrated network of gelatin-BG hydrogel was fabricated by the sol-gel method followed by different methods of polymer crosslinking. For the fabrication of all hydrogels, 100 mg/ml solution of gelatin was prepared in PBS at 50°C. Prior to the fabrication of interpenetrated gelatin-BG network, the temperature of the reaction was set at 37°C. Different concentrations of BG (0-6 µl BG per milligram of the organic phase) were

incorporated into the solutions immediately followed by addition of crosslinking agents. Genipin in the different final concentrations (1-7.5 mg/ml) and Irgacure (1 mg/ml) were added to the gelatin-BG solutions to form respectively chemically- and photocrosslinked hydrogels. The precise amounts of gelatin, crosslinking agents and BG were presented in *Appendix A, Table 4*. The BG-gelatin solutions were then poured into custom-made moulds to form different incorporated BG-gelatin hydrogels. While the physically crosslinking process was accomplished at room temperature in the absence of crosslinking agents, the genipin-contained solutions were kept at different temperatures (37°C -60°C) to complete the chemical crosslinking reaction. The photocrosslinking, on the other hand, was accomplished by irradiation of the GelMA-BG solution supplemented by Irgacure under ultraviolet light (UV, 365 nm, 6.9 $mW/cm^2$).

## 3.7 Fabrication of Covalently-Bonded Gelatin-BG Hybrid Hydrogels using Organosilation Technique

Prior to the hybrid formation, GelMA was functionalised with different organosilane coupling-agents to prepare a silane group in GelMA (Fn-GelMA) for covalent bonding with BG. Therefore, GPTMS or APTES was added to different concentrations of GelMA (75, 100 and 150 mg/ml) in PBS and stirred for at least 12 h at 40°C. The molar ratio of 2:1 between hydroxylysine, lysine and arginine amino groups of GelMA and organosilane coupling agents was obtained through addition of 92 µl of these agents per each gram of GelMA. The constant concentration of Irgacure (1 mg/ml) as a photo-initiator was then added to the GelMA-based solutions. Subsequently, different amounts of BG with respect to organic phase, *i.e.* GelMA, (0-1 µl per each milligram of GelMA) were added to the photocrosslinkable solution to form a hybrid solution. The precise amounts of GelMA, organosilane agents and BG were presented in *Appendix A, Table 5*.

The degree of crosslinking was also increased upon conjugation of different photocrosslinkable polymers. To this end, various concentrations of StaMA (0-20 mg/ml) or PEGDA (0-100 mg/ml)) were added to the GelMA solution

(100 mg/ml). The effect of secondary crosslinking on the covalently bonded hybrids was also investigated by the addition of these polymers to Fn-GelMA. Different amounts of BG (0-1 µl) were incorporated into conjugated solution with respect to the amount of organic content (*i.e.* the mass of GelMA and secondary crosslinking agent). The chemical composition of various hydrogels is determined in Table 3-1 and *Appendix A (Tables 6 and 7).* Despite their chemical compositions, the prepared photocrosslinkable solution was poured into a custom-made mould (Plastic Petri Dish with an internal diameter of Φ=35 mm) to fill the mould up to 2 mm. The solution was then photocrosslinked under UV light (365 nm, 6.9 mW/cm$^2$) to form a hydrogel. The required time for hydrogel formation was measured while a solid 3D structure was fabricated.

**Table 3-1 The chemical composition of various covalently bonded hydrogels fabricated by 1 mg/ml Irgacure**

| **Hydrogel** | **GelMA (mg/ml)** | **Secondary Crosslinking Network** | | **BG: Polymer (µl/mg)** |
|---|---|---|---|---|
| | | **StaMA (mg/ml)** | **PEGDA (mg/ml)** | |
| **Fn-GelMA** | 75-150 | - | - | - |
| **Fn-GelMA-BG** | 75-100 | - | - | 0-1 |
| **Fn-GelMA-StaMA-BG** | 100 | 0-20 | - | 0-1 |
| **Fn-GelMA-PEGDA-BG** | 100 | - | 0-100 | 0-1 |

## 3.8 Attenuated Total Reflection Fourier Transform Infrared Spectroscopy

Attenuated total reflection Fourier transform infrared (ATR-FTIR, Varian 660 IR, 4000–650 cm$^{-1}$) at a 4 cm$^{-1}$ resolution and 32 scans in absorbance mode was conducted to evaluate the chemical structures of dried hydrogels and also methacrylated starch.

## 3.9 Thermal Gravimetric Analysis

The effect of methacrylation on the thermal properties of starch was investigated by thermal gravimetric analysis (TGA, Q500) with the

assistance of Mr. Ehsan Pourazadi, School of Chemical Engineering. The thermal stability of starch was monitored while the temperature was increased from ambient temperature to 500°C with a ramping rate of 2.5°C/min under $N_2$ stream of 60 ml/min.

## 3.10 Quantification of amine functional groups

The mechanism of organosilation was determined using colorimetric quantification of amine functional groups on GelMA structure. In this well-established method, the amine functional group in a biopolymer is measured quantitatively using UV spectroscopy via observing the conversion of the yellowish colour of ninhydrin solution to the dark purple. In each run, 1 ml of 2 wt% ninhydrin in ethanol solution was added to 1 ml of 1.5 wt% solutions of plain and Fn-GelMA at 37°C. The temperature was then gradually increased to 80°C under mild stirring. The solution was kept at this temperature for 15 min to complete the reaction and then cooled down to ambient temperature. The degree of amine functional group (Da) was calculated by Equation 1 based on the recorded light absorbance at 410 nm (Bio-Rad 680 microplate reader).

$$D_a = [(B - A)/A] \times 100 \qquad \textbf{Equation 1}$$

where A is the mole fraction of free amine functional groups in GelMA and B represents the mole fraction of Fn-GelMA. The Da of functionalized GelMA by APTES in the abovementioned conditions (16 %) was used as a control to determine the mechanism of GPTMS functionalisation. The amine functional groups of APTES formed a covalent bond with carboxylic acid groups of GelMA.

The presence of amine functional groups in Fn-GelMA hydrogel was also determined qualitatively using fluorescein isothiocyanate (FITC, Sigma-Aldrich) assay. In this method, the sample was incubated in 1 mg/ml solution of FITC in PBS in the dark container. After 24 h incubation at ambient temperature, the hydrogel was washed against deionised water, and the absorbance of FITC was collected at 495 nm. A cylindrical sample was

fabricated from poly($_L$-lactic acid) (PLLA) to use as a positive control. This sample was incubated in the abovementioned conditions in FITC solution.

## 3.11 Swelling Properties

The swelling behaviour of hydrogel was measured at 37°C in PBS. The dry weight of hydrogels ($W_d$) was recorded after lyophilizing overnight. Subsequently, the hydrogels were immersed in excessive PBS overnight followed by weighting ($W_s$). The equilibrium swelling ratio (ESR) was then calculated using Equation 2**.**

$$ESR\left(\frac{mg}{mg}\right) = \frac{W_s - W_d}{W_d} \qquad \textbf{Equation 2}$$

## 3.12 Mechanical Properties

The mechanical performance of hydrogels was investigated using uniaxial compression tests (Instron 5943, 100 N load cell). The hydrogels were punched using 8 mm biopsy to form disks (Φ= 8 mm, h=2 mm) and swelled for 2 h in PBS at 37°C unless specifically mentioned. The hydrogels underwent 3 cycles of compression-decompression with a compression rate of 0.05 mm/min in the hydrated state at 37°C. The compressive modulus was then obtained from the tangent slope of the stress–strain curve in the linear strain range (10-20%). In addition, for all samples, the energy loss based on the compression cycle was computed.

## 3.13 Degradation Profile of Hydrogels

The degradation profiles of samples were measured based on the released protein and silicate anions in different media (*i.e.* PBS and SBF). The lyophilized samples were weighed prior to the test and incubated in different media at 37°C for a period of time. The protein concentration of each sample was measured using Qubit® Protein Assay Kits (Invitrogen) with considering the media absorbance as a background. The protein calibration curves were linear for known concentrations of GelMA in different media (PBS: $R^2$=0.99; SBF: $R^2$=0.98). The degree of protein release was calculated based on the concentration of protein with respect to the dried weight of samples.

The profile of silica degradation was also monitored using spectrophotometric analysis as described by Coradin *et al.* [445]. In each particular time interval, 1 ml of media was diluted with 15 ml deionised water. The diluted media were then mixed with 1.5 ml of 102 mM ammonium molybdate solution in 2.45 mM HCl. After 10 min vigorous shaking of this solution at room temperature, the released silica ions were conjugated with molybdate anions and formed a yellowish solution. This solution, however, could be formed due to the formation of phosphomolybdate or the possible reaction between GelMA and molybdate ions. These unfavourable salts, therefore, were eliminated from the solution by addition of 7.5 ml of secondary solution contained 22 mM oxalic acid, 32 mM sodium sulphite and 39 mM metol in 1.9 mM sulphuric acid [445]. The colour of the solution was changed to blue upon addition of the secondary solution. After 2 h agitations at ambient temperature, the amount of released silica was measured at 810 nm using UV-Vis spectroscopy (Cary 60, Agilent Technologies). In this study, the calibration line was prepared for known concentrations of TEOS ($R^2$=0.99) prior to analysis and SBF solution was used as the background. The degree of Si release was calculated based on the concentration of Si with respect to the dried weight of samples.

## 3.14 Bioactivity of Hydrogels

Scanning electron microscopy with energy dispersive X-ray spectroscopy (SEM-EDS, Zeiss EVO) at 15 KV was used to determine the bioactivity of hydrogels following SBF incubation at 37°C. Hydrogels were removed from SBF at a specific time, washed with deionised water, lyophilized, mounted on aluminium stubs and then carbon sputtered prior to SEM-EDS analysis. The AZtec software (Oxford Instruments, UK) was integrated to SEM to identify the chemical composition of hydrogels before and after SBF immersion. At least three different images with similar magnifications were collected to measure the amount of precipitated ions on their surfaces.

## 3.15 *In Vitro* Cell Culturing

Saos-2 osteoblast cells were cultured in McCoy's 5A medium supplemented with 10% fetal bovine serum, 1% $_{L}$-Glutamine and 1% Antibiotic-Antimycotic in 75 $cm^2$ tissue culture flasks (BD Biosciences, USA). Cells were passaged weekly, and media was changed every two days. Cells were incubated at 37°C with 0.5% $CO_2$ (Incubator Thermo Fisher Heracell 150i).

### 3.15.1 Cell Seeding of Hydrogels

The hydrogels were fabricated in aseptic condition with pre-sterilised components to eliminate the sterilization with ethanol. The presence of ethanol within hydrogels may have adverse effects on their degradation profile and also cell viability. Prior to cell seeding, the hydrogels were cut into small disks (Φ= 8 mm, h=2 mm) and transferred to 48-well plates. The prepared hydrogels were then rinsed with sterilized PBS followed by incubation in prepared media overnight. Saos-2 cells were trypsinised, counted and resuspended in fresh media at a density of 200,000 cells/ ml. The pre-determined amounts of cells were then seeded onto the surface of hydrogels and were placed in a $CO_2$ incubator at 37°C.

### 3.15.2 Live-Dead Assay and Bone Specific Analyses

The cell viability and proliferation were measured by double staining of the cells cultured on the surface of hydrogels. After 14, 21 and 28 days of incubation, hydrogels were transferred to the new well-plate contained 1 ml of fresh media. The nuclear of dead cells was stained by addition of 1 µl propidium iodide solution (PI, 1 mg/ml) followed by 30 min incubation at 37°C. The PI-stained hydrogels were thoroughly rinsed with PBS and then fixed by 10 min soaking in 4% paraformaldehyde (PFA) at 37°C. The residue of PFA was then removed by several rinsing steps of hydrogels with PBS. The DNA-specific 4', 6-diamidino-2-phenylindole (DAPI) was used to stain the nuclear of cells. The samples were then placed on a glass slide for confocal laser scanning microscopy (LeicaSP5, Germany) examination. The confluence of cells on the hydrogel was determined by analysing fluorescent images using the Fiji-ImageJ software.

The differentiation of Saos-2 osteoblast cells was determined using alkaline phosphate assay (ALP). After 14, 21 and 28 days cell culturing, the cells were trypsinised from the surface of hydrogels, and their ALP activities were evaluated based on manufacture's procedure.

## 3.16 *In Vivo* Animal Study

The *in vivo* cytocompatible, degradation and the biological properties of the hybrid hydrogels were studied by using mice subcutaneous implantation model. These hydrogels were pre-fabricated *in vitro* as described in 3.15.1. The surgeries were carried out in ANZAC Research Institute in Concord Hospital with the direct assistance of Dr. Yiwei Wong.

Nine pathogen-free, male BALB/c mice, aged 6 months with 28±1.7 g were acquired, housed and studied under a protocol approved by SLHD Animal Welfare Committee in Sydney, Australia (#2013/019A). Each mouse was anesthetised individually by intraperitoneal injection of a mixture of ketamine (75 mg/ml) and xylazine (10 mg/ml) at 0.01 ml/g of body weight. The dorsal hair was shaved and skin was cleaned with Betadine solution and washed with sterile saline. The incision was created surgically in the dorsal area and dissected to create a subcutaneous pouch into which the hydrogel was inserted. The wounds were then closed with 5-0 silk sutures and covered by Atrauman® (Hartmann, Australia) and IV3000 wound dressings (Smith & Nephew) for 7 days. Carprofen (5 mg/kg) was given at the time of anaesthesia and then on the following day post-surgery for analgesia. After surgery, each mouse was caged individually for the first two days and then three mice per cage thereafter with free access to water and food. Skin biopsies were collected for histological analysis at 1, 2 and 4 weeks post-implantation.

### 3.16.1 Haematoxylin and Eosin Staining

Skin biopsies with implanted conjugated hybrid hydrogels were fixed in 100 mg/ml formalin for 24 h. All samples were then dehydrated and embedded in paraffin. The 5 µm sections were deparaffinised in xylene and stained with Haematoxylin and Eosin (H&E).

## 3.17 Statistical Analysis

All experiments were repeated at least for three times. Data was reported as mean±STD. A one-way analysis of variance (ANOVA) for single comparisons and Bonferroni Post-Hoc tests for multiple comparisons were performed, using IBM SPSS software for Windows, version 21. Statistical significance is accepted at $p<0.05$ and indicated in the Figures as * ($p<0.05$), ** ($p<0.01$) and *** ($p<0.001$), no star represents no statistical significance.

# Chapter 4. Fabrication of an Interpenetrated Network of Organic-Inorganic Hybrid Hydrogel

## 4.1 Introduction

The polymer-bioactive glasses formed through sol-gel method are commonly brittle monoliths with low water uptake capacity due to the over-condensation of their inorganic phases [414]. The aim of this study was to fabricate 3D networks of polymer-BG with enhanced swelling properties and mechanical performance. In this part of the study, it was hypothesised that the combination of sol-gel method and polymer crosslinking can control the condensation of the inorganic phase and thus prevents the formation of brittle structure. In this study, gelatin was used as a polymer model due to its intrinsic capacity to form a hydrogel through different methods of crosslinking [446-448]. The gelatin solution in constant concentration (100 mg/ml) was prepared at 37°C and turned to the hydrogel using different methods. The physically crosslinked hydrogel was formed by cooling the solution at room temperature. The genipin, however, was used to crosslink the gelatin chains chemically. Finally, a photoinitiator was used to rapidly crosslink a gelatin that was methacrylated. In this chapter, the effects of different processing parameters, such as temperature and the concentration of crosslinking agents on the interpenetrated gelatin-BG network structure were examined.

## 4.2 The Effects of External Stimuli on the Gelatin Hydrogel Formation and the Gelation of BG

Prior to the fabrication of gelatin-BG hybrids, the rates of both BG condensation and the gelatin crosslinking were measured. It was ideal to select the conditions that both these compounds simultaneously are forming the gel to prepare a homogeneous macrostructure. To this end, two critical factors, the reaction temperature, and the concentration of crosslinking reagents were optimised [449-451].

The temperature was varied between 25°C and 60°C. The pure BG turned to a brittle structure after 3 h incubation at room temperature. Increasing the temperature to 37°C and 60°C, however, resulted in the formation of condensed networks of BG within 10 min and 2 min, respectively. This remarkable increase in the rate of BG condensation was due to the higher

rates of aggregation and collisions of activated silanol groups at elevated temperatures [452].

Genipin crosslinking resulted in a change of colour of solution from clear to dark blue and also converting liquid to highly viscous gel. These are simple tests for determining the degree of crosslinking while the darker blue colour is an indication of stronger crosslinking reaction. In fact, other methods such as FTIR were not that sensitive due to the fact that the carboxylate functional groups and also amino acid were still present in the final crosslinked hydrogels.

The temperature had a significant impact on the hydrogel formation as the gelatin solution formed a physically crosslinked hydrogel below 35°C [453, 454]. While the physically crosslinked hydrogel was formed after 10 min incubation of gelatin solution at room temperature, at least 30 min was required to form a hydrogel when using different concentrations of genipin as a chemical crosslinking agent at 37°C. Data in Figure 4-1A show that the concentration of genipin and the temperature had significant effects on the gelation time of hydrogels. Despite the temperature of the reaction, increasing the concentration of genipin had a significant impact on the hydrogel formation. For instance as shown in Figure 4-1A, when the concentration of genipin was increased from 1 mg/ml to 2.5 mg/ml, the gelation time at 37°C was decreased 6-fold from 180 min to 30 min ($p<0.001$).

Increasing the concentration of genipin at a constant temperature or elevating the temperature of the reaction for similar concentrations of genipin significantly decreased the gelation time of hydrogels. The statistical analyses through Bonferroni Post-Hoc tests, however, revealed that the effect of temperature on the gelation time of hydrogels ($p<0.05$) was marginally significant compared to the genipin concentration ($p>0.05$). Increasing the concentration of genipin from 2.5 mg/ml to 5 mg/ml at 37°C, for instance, did not have a significant effect on the gelation time of hydrogels. Incubation of these hydrogels at 60°C, however, significantly decreased their gelation times from 60 min to 30 min (Figure 4-1A, $p<0.05$).

The physicochemical properties of hydrogels were also dependent upon these two key factors (*i.e.* reaction temperature and the concentration of crosslinking agent). Increasing the concentration of genipin at a constant temperature significantly decreased the physicochemical properties of hydrogels. The swelling ratio of hydrogels, however, did not significantly alter by increasing the reaction temperature for a constant concentration of genipin (Figure 4-1B). For instance, the swelling ratio of hydrogels fabricated at 37°C was remarkably decreased from 6.7±0.3 mg/mg to 5.8±0.1 mg/mg upon increasing the concentration of genipin from 2.5 mg/ml to 5 mg/ml ($p<0.05$). Elevating the incubation temperature to 60°C, however, did not have a significant effect on their swelling ratios ($p>0.05$). Data in Figure 4-1 reveal that the optimum hydrogel with proper swelling ratio and fast gelation time was formed upon the incubation of gelatin solution supplemented with 2.5 mg/ml genipin at 60°C.

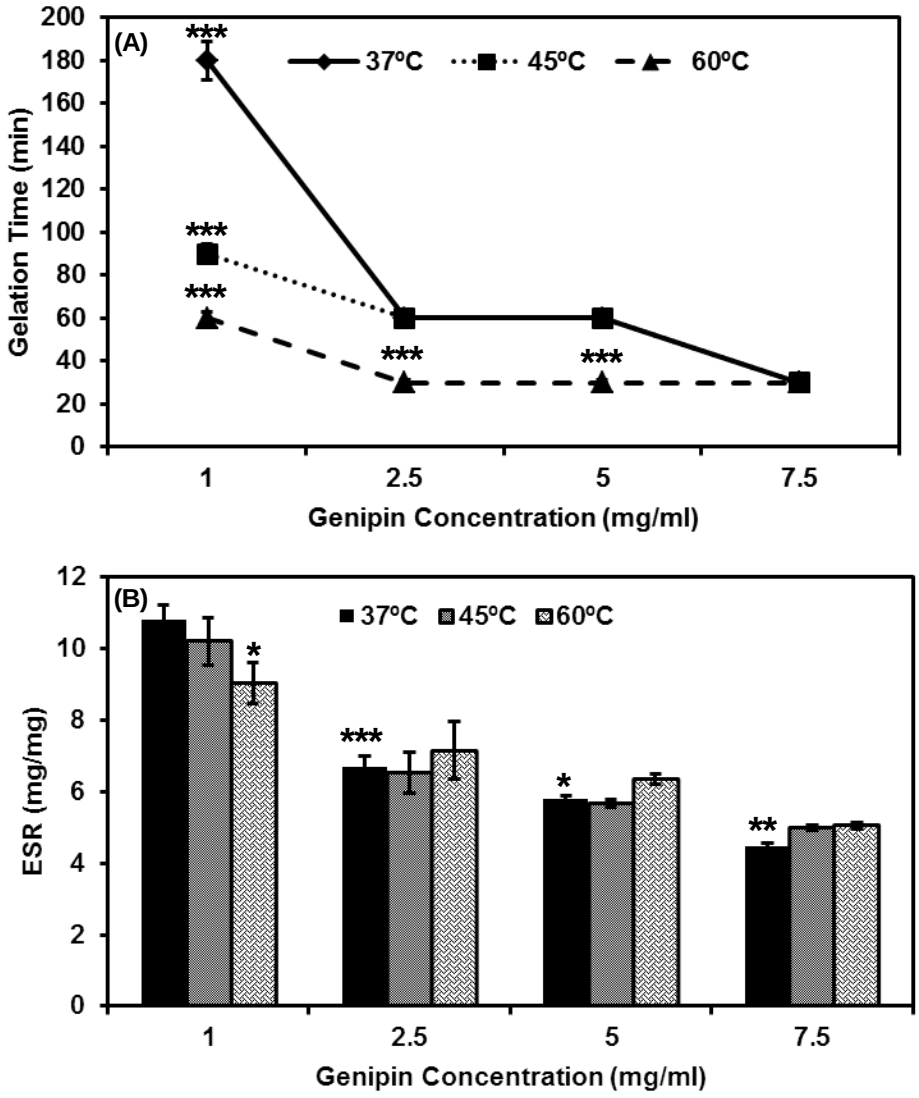


**Figure 4-1 The effects of genipin concentration and crosslinking temperature on the hydrogel formation (A) and swelling ratio (B) of gelatin hydrogels. Data presented in *, ** and *** represent $p<0.05$, $p<0.01$ and $p<0.001$, respectively.**

The photocrosslinking of methacrylated gelatin (GelMA) in the presence of Irgacure as a photoinitiator was a fast method to form a hydrogel within 2 min. The temperature has a negligible effect on the gelation time of photocrosslinked hydrogels. In addition, when using more than 0.25 mg/ml the residue of Irgacure evokes significant drawbacks on biocompatibility and physicochemical properties of hydrogels [455-457]. Therefore, it was attempted to use the minimal amount of Irgacure required for photocrosslinking.

The different methods of crosslinking provided the particular conditions to investigate the effect of polymer crosslinking on the controlling of BG condensation and thus the formation of an interpenetrated network of BG and gelatin.

## 4.3 Fabrication of Interpenetrated Gelatin-BG Hybrid Hydrogel through Physical or Chemical Crosslinking of Polymer

The effects of polymer crosslinking on the formation of interpenetrated network of gelatin-BG were studied. The physical and chemical methods of crosslinking were used to form hydrogels before or after the condensation of BG. Despite the method of crosslinking, different concentrations of BG (0-6 µl/mg) were incorporated into the gelatin solution at 37°C. It was found that the brittle structure was immediately formed upon the addition of high concentration of BG (more than 2 µl/mg) in the gelatin solutions prior to crosslinking. In these arbitrary structures, gelatin was entrapped within the condensed network of BG, and this network did not lose its integrity upon increasing temperature to 60°C. It seems that this entrapment was due to the differences in the isoelectric points (IEP) of gelatin and BG.

Gelatin with IEP of 8.6 possesses the positive charges in the PBS media (pH 7.4), while BG with IEP of 2.6 represents the negative charges in the environment with pH higher than its IEP [458, 459]. The interactions between gelatin and BG, therefore, enhanced the condensation of silicate anions and formed the brittle structures. This result was in agreement with the previous study by Heinemann *et al.* while their collagen solutions simultaneously solidified upon the incorporation of higher concentration of pre-hydrolysed tetramethyl orthosilicate due to increasing the rate of aggregation [348]. The degree of silica-condensation was decreased through the incorporation of lower concentration of BG. The polymer crosslinking, therefore, had the dominant role in the formation of gelatin-BG hybrid hydrogels and might control the degree of BG-condensation.

The different concentrations of BG (0-2 µl/mg) were mixed with gelatin solution to physically crosslink the gelatin-BG hybrids. Despite the concentration of BG, the transparent hybrid hydrogels were formed after 10

min incubation at ambient temperature and no phase separation was observed. These hybrid hydrogels, moreover, have lost their physical integrities during the incubation at 37°C prior to assessing their physicochemical and mechanical properties. The lack of chemical bonding between interpenetrated gelatin-BG networks led to the rapid release of gelatin into solution and acquiring the fragile structure.

Genipin as a biocompatible chemical crosslinking agent was used to form a gelatin-BG hybrid hydrogel. The distribution of silica within this hybrid hydrogel was monitored by electron microscopy. The SEM-EDS analyses in Figure 4-2 showed that silicate anions were homogeneously distributed within the gelatin-BG hydrogels.

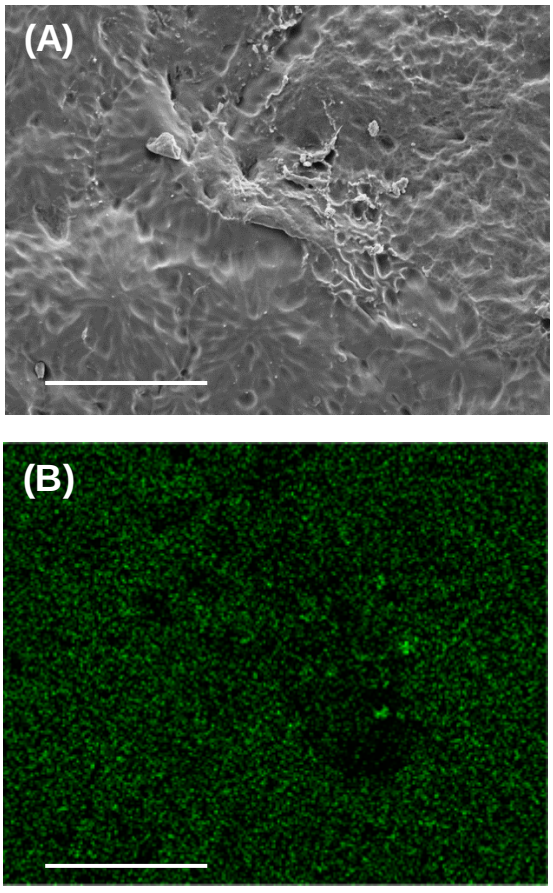


**Figure 4-2 SEM image (A) and the distribution of Si ions (B) on the surface of genipin-crosslinked gelatin-BG hybrid hydrogels. The scale bars represent 100µm.**

The physicochemical properties of BG and pure hydrogels were significantly altered upon the formation of these hybrids. The incorporation of 1 µl/mg of BG into genipin-crosslinked hydrogels, for instance, significantly decreased the swelling ratio of pure hydrogels from 7.15±1.59 mg/mg to 3.64±0.28 mg/mg. Data in Figure 4-3A show that further increase of BG concentration remarkably decreased the swelling ratio of hydrogels ($p$<0.001). This significant reduction was due to the intrinsic hydrophobic nature of BG, which had the water uptake capacity of 0.35±0.01 mg/ml. These results were in the agreement with the literature where the conjugation of silica increased the hydrophobicity of gelatin powders by demonstrating the contact angle of ~45° [460].

The formation of the interpenetrated gelatin-BG hybrid had a significant impact in the mechanical performances of hydrogels. As shown in Figure 4-3B, the compressive modulus of hydrogels, for instance, was significantly increased from 1.00±0.12 kPa to 26.67±6.31 kPa after incorporation of 2 µl/mg BG compared to pure gelatin hydrogels. The condensed silica network structurally reinforced the gelatin hydrogels upon van der Waals forces and the formation of hydrogen bonds between silanol functional groups of BG and free amines and/or carbonyl units of gelatin [461].

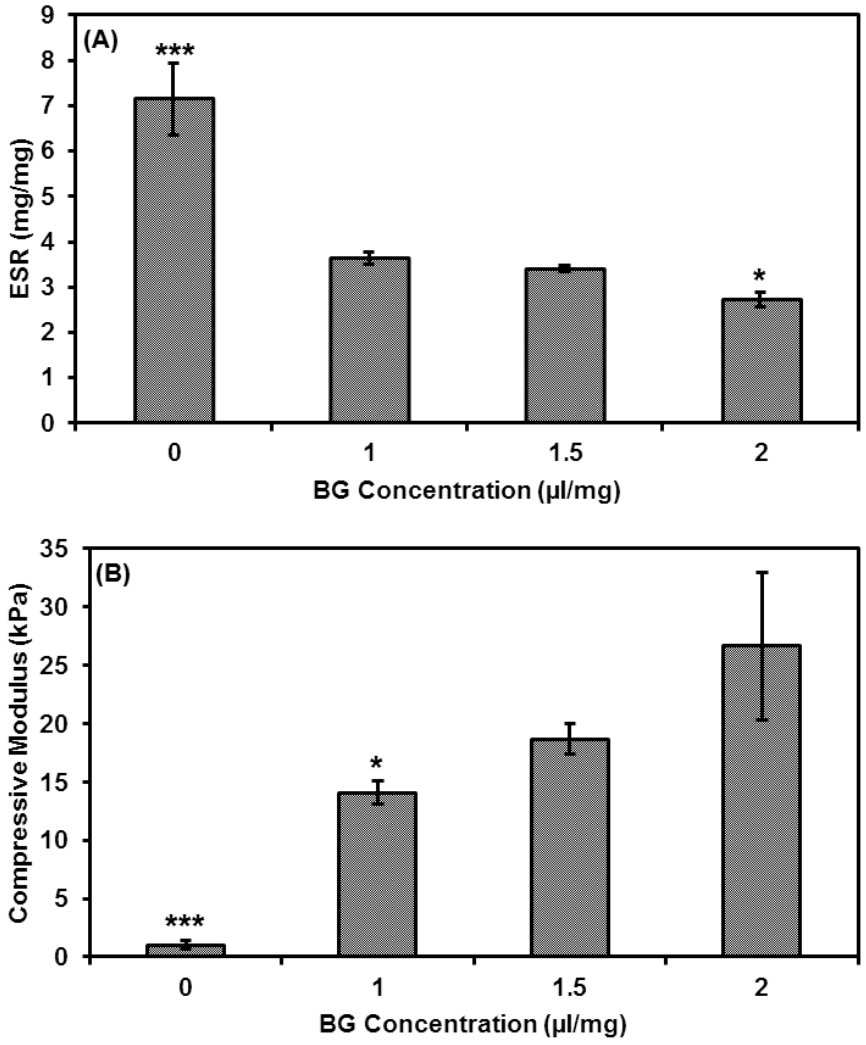


**Figure 4-3 The effect of BG conjugation on swelling ratio (A) and compressive modulus (B) of genipin-crosslinked hybrid hydrogels. Data presented in * and *** represent $p<0.05$ and $p<0.001$, respectively.**

Despite the significant improvement on the mechanical properties of hydrogels, genipin-crosslinking did not significantly control the over-condensation of the silica network. The results showed that when using genipin as a crosslinking agent, increasing the temperature significantly decrease the gelation time of hydrogels. For instance, the hydrogel was fabricated at 60°C after 30 min incubation of gelatin solution. At this condition, however, BG was condensed within 2 min. The significant effect of temperature on the hydrogel formation, the condensation of silica, and the differences between gelation time of BG and genipin-crosslinking resulted in the formation of brittle structures. These data implicitly suggested that it

was favourable to form the gelatin hydrogel prior to BG networking to overcome these limitations.

## 4.4 Fabrication of a Photocrosslinked Gelatin-BG Hybrid Hydrogel

The interpenetrated gelatin-BG hybrid hydrogels with different concentrations of BG were fabricated after 2 min UV-irradiation of gelatin-BG solutions. The methacrylated derivative of gelatin (GelMA) was used to form a photocrosslinkable hydrogel in the presence of Irgacure as a photoinitiator. It was found that the pre-matured structures were formed immediately after the addition of 1.5 µl of BG per each mg of GelMA. It seems that the presence of methyl methacrylate groups in the structure of GelMA enhanced the hydrogen bond formation between silica and gelatin and thus facilitated the formation of pre-matured structure. Data in Figure 4-4 show that the conjugation of low concentration of BG (0.5 µl/mg) in GelMA hydrogels did not have significant effects on the physicochemical properties and mechanical performances of hydrogels ($p$>0.05). Incorporation of 1 µl/mg BG, on the other hand, significantly decreased the swelling ratio of hydrogels from 7.51±0.08 mg/mg to 5.43±0.34 mg/mg.

The interpenetration of the photocrosslinked hydrogel within BG network enhanced the mechanical performance of hydrogels. Data in Figure 4-4B show that these hydrogels could withstand under uniaxial cycles of compression-decompression. However, their energy loss were significantly increased by the incorporation of BG due to the intrinsic brittleness of silica. The addition of 1 µl/mg BG into pure GelMA hydrogels, for instance, significantly increased their energy loss from 23.44±4.86 % to 62.25±5.4 %. The compressive modulus of these hydrogels, as shown in Figure 4-4C, was improved from 39.44±4.86 kPa to 79.89±5.3 kPa upon interpenetrating of BG precursor (1 µl/mg) within their structure ($p$<0.001).

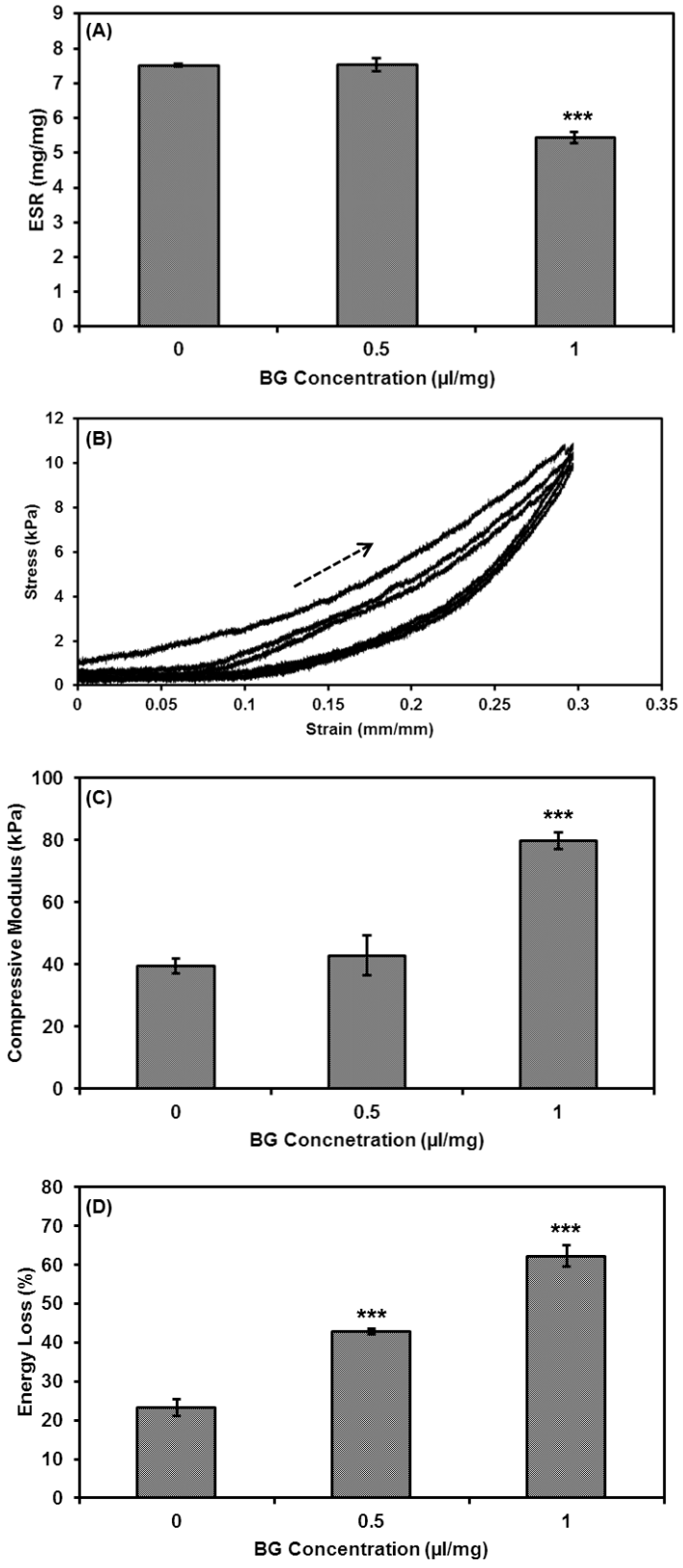


**Figure 4-4 The effect of BG conjugation on swelling ratio (A), cyclic compression (B), compressive modulus (C) and energy loss (D) of photocrosslinked Gelatin-BG hybrid hydrogels. Data presented in *** represents $p<0.001$.**

Despite the significant effect of photocrosslinking on controlling the condensation of BG, the interpenetrated network of gelatin-BG did not possess acceptable mechanical properties for bone tissue engineering due to the lack of covalent bonding between gelatin and BG.

## 4.5 Summary

This chapter described the formation of interpenetrated network of organic-inorganic hybrid hydrogels upon the combination of the sol-gel method and polymer crosslinking. It was hypothised that polymer crosslinking prior to the condensation of BG was vital to eradicating the formation of brittle structures. In addition, external stimuli such as temperature and the isoelectric point of polymer and BG, the mechanism of polymer crosslinking, and the concentration of the inorganic component are the significant governing factors for tuning the formation of the interpenetrated networks. The mechanical performance and physicochemical properties of fabricated gelatin-BG were superior to BG. The problems associated with this method, however, was the insufficient mechanical strength of these hydrogels for bone tissue engineering applications. In the next chapter, the effect of using different organosilane coupling agents for covalent bonding of gelatin to BG would be examined. In addition, the impact of organosilation and further organic-inorganic hybrid formation on the physicochemical and mechanical properties of photocrosslinkable hydrogel would be discussed.

# Chapter 5. Fabrication of Covalently-Bonded Organic-Inorganic Hybrid Hydrogels

## 5.1 Introduction

An interpenetrated network of gelatin-BG can be produced by the sol-gel method. In Chapter 4, it was demonstrated that crosslinking of polymer phase has an impact on condensation of BG. Fast gelation of polymer phase expedited the condensation of BG and enhanced the mechanical strength of this interpenetrated structure. Among different method of crosslinking, the photocrosslinking was favourable as it controlled the condensation of BG and prevented the formation of brittle structure. The mechanical strength of GelMA-BG, however, was not within the acceptable range for bone tissue engineering. To address this shortfall, it was hypothesised that the formation of covalent bonds between GelMA and BG may enhance the mechanical strength and physical stability of these constructs.

Different organosilane coupling agents have been selected for covalent bonding between the polymer and inorganic phases [408, 410, 462]. The fabricated hybrid, however, formed the brittle monolith due to the complete condensation of inorganic compounds through drying and aging steps [431]. In this chapter, the feasibility of organosilation of GelMA through different coupling agents and their mechanisms are investigated. The resulting functionalised GelMA was then chemically conjugated to BG to form a covalently bonded hybrid hydrogel. The effects of organosilation and hybrid formation on the physicochemical properties, mechanical strength, and the degradation behaviour of the resulting hybrids were then investigated.

## 5.2 Organosilation of GelMA

Different concentrations of GelMA (75-150 mg/ml) were functionalised with various organosilane coupling agents including APTES and GPTMS to form covalent bonds between gelatin backbone and BG. The organosilation reaction was accomplished in PBS (pH 7.4) at 40°C to control the hydrogel formation and gelation of BG. The hydrolysis of APTES and GPTMS liberated ethanol and methanol, respectively. The functionalisation of GelMA with organosilane was not feasible when using a high concentration of GelMA (150 mg/ml) due to the high viscosity of the solution. Therefore,

the lower concentrations of GelMA (75 mg/ml and 100 mg/ml) were used for this reaction.

It was anticipated that by using APTES for GelMA functionalisation, the biological activity of this hydrogel is preserved due to the presence of this amine-coupling agent. The functionalisation occurs through direct condensation between amine groups of APTES and carboxylic acid groups of GelMA at 40°C for 20 h. However, the functionalisation of GelMA with APTES retard the gelation time of this hydrogel from 2 min to 10 min due to the steric hindrance effect of APTES chains and its interference with methacrylate group. This hydrogel, moreover, had lower structural integrity, and mechanical properties compared to neat GelMA.

GPTMS was another organosilane coupling agent that was used to form a covalent bridge between GelMA and BG. GPTMS as a heterobifunctional agent undergoes competitive reactions between epoxy-ring hydrolysis and polycondensation of activated silanol groups. At 40°C and neutral pH, the kinetics of epoxide ring-opening reaction is slow [169]. The preliminary results showed that less than 14 h was not adequate for this reaction and above this period, there was a premature condensation of GPTMS. The faster self-condensation of GPTMS compared to APTES was due to the presence of methoxy pendant group in this coupling agent, which are more reactive than ethoxy functional groups of APTES [463]. The reaction time observed in this study was in agreement with the results of $^{29}$Si nuclear magnetic resonance ($^{29}$Si-NMR) spectroscopy by Gabrielli *et al*. [464]. Their study confirmed that pure GPTMS is condensed after 16 h in neutral pH [464]. The presence of GPTMS had a negligible effect on the properties and gelation time of GelMA (Fn-GelMA) hydrogel. Therefore, GelMA was functionalised with GPTMS at 40°C for 14 h for the rest of the study.

Glycidoxy functional group of GPTMS can form a covalent bond with either amine [395] or carboxylic acid [400] groups in amino acid residues of gelatin [465, 466]. The results of ATR-FTIR analyses in Figure 5-1A show the appearance of new bands at 970 $cm^{-1}$ (silanol) and 1020 $cm^{-1}$ (methoxysiloxane) in Fn-GelMA, which endorsed the complete

functionalisation of GelMA with GPTMS [467]. These results, however, did not disclose the mechanism of organosilation. Colorimetric ninhydrin assay was therefore used to quantify the amine groups in Fn-GelMA hydrogels to determine the mechanism of GPTMS-functionalisation. The results show that the amount of the free amine functional group in GelMA was 15%, which was in agreement with $^{1}$H-NMR results [254]. However, the fraction of amine functional groups in GelMA was decreased to 13% following the functionalisation with GPTMS ($p$<0.001). This reduction of the percentage of free amine groups in Fn-GelMA confirmed that the glycidoxy functional groups of GPTMS formed covalent bonds with amine groups of GelMA during functionalisation reaction (Figure 5-2). The biological activity of GelMA might be slightly decreased due to decreasing the free amine groups [468].

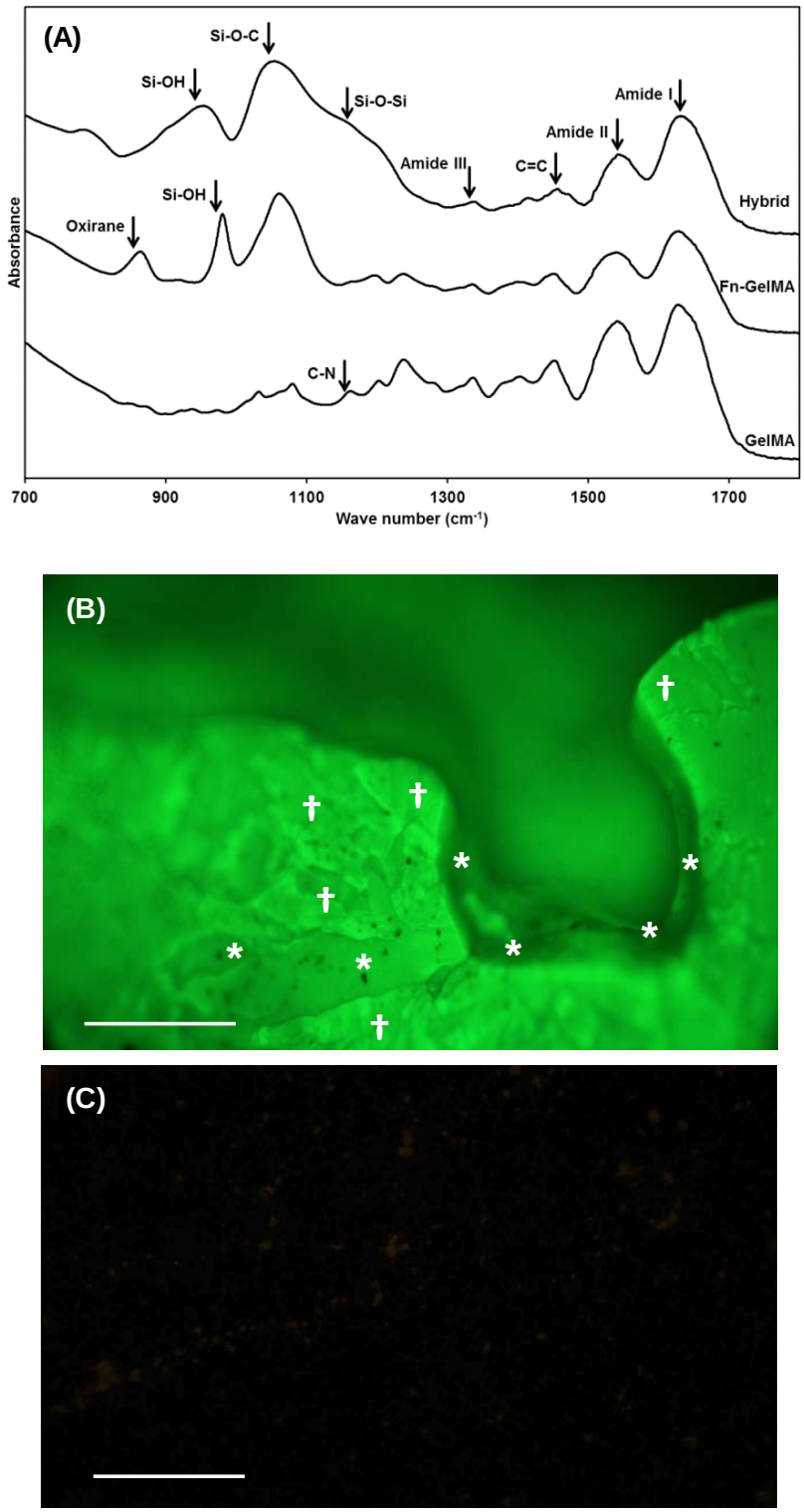


**Figure 5-1 FTIR spectra of various hydrogels (A) the distribution of FITC-labelled amine groups (green) in Fn-GelMA hydrogel (B) and PLLA sample (C). PLLA was used as a positive control to show the absence of green fluorescence in this sample due to the absence of amine functional groups. The daggers and asterisks respectively represent to the presence and absence of amine functional groups. Scale bar represents 200 µm.**

The presence of the free amine groups in the backbone Fn-GelMA was visualised with FITC. The strong and uniform fluorescence in Figure 5-1B confirms the presence of these sequence motifs within the structure of Fn-GelMA hydrogels. The fabricated PLLA sample was also used as a positive control. Data in Figure 5-1C show that the PLLA sample did not illustrate any fluorescent light due to the absence of amine functional group in its structure. This result suggested the negligible impact of the partial reduction of the amine group on the biological activity of GelMA hydrogels.

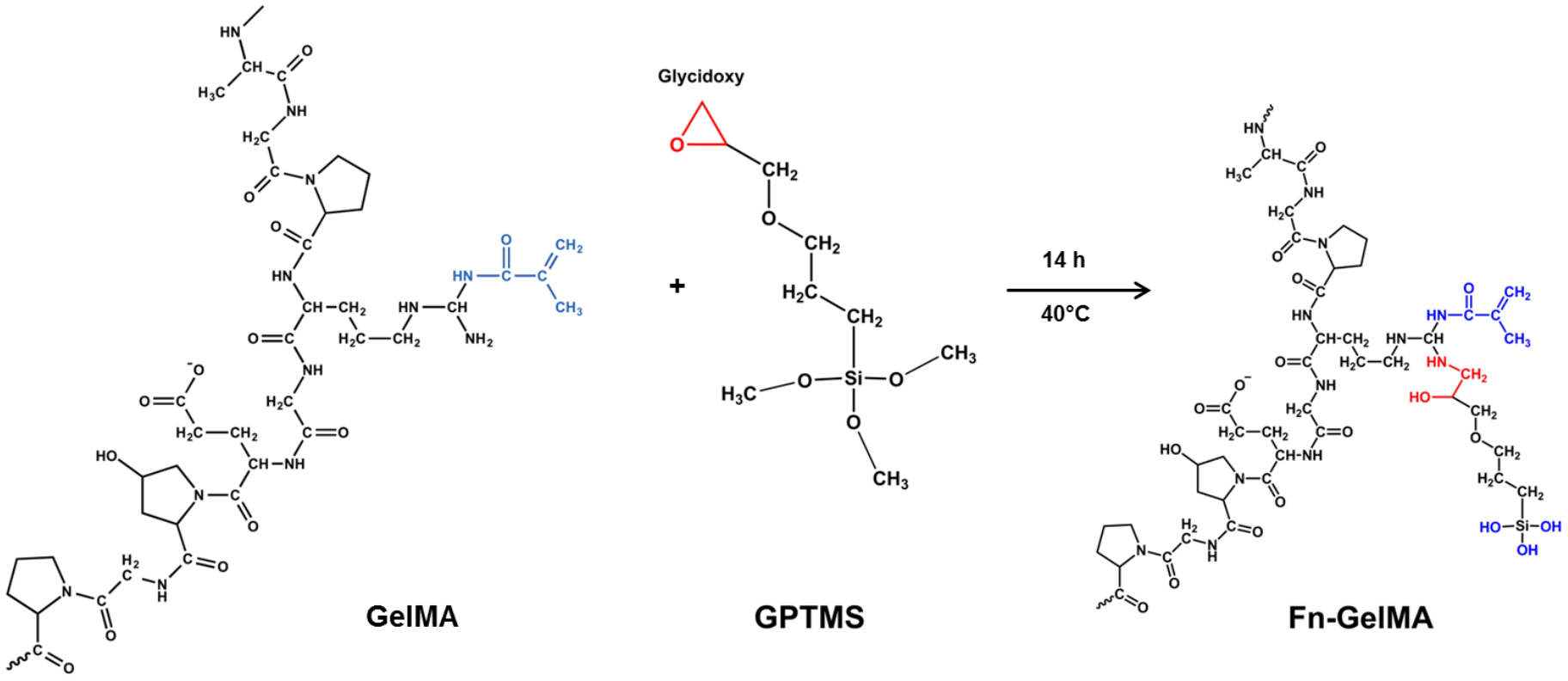


**Figure 5-2 The mechanism of organosilation of GelMA.**

## 5.3 Physicochemical and Mechanical Properties of Functionalised GelMA Hydrogels

The effect of GPTMS-functionalisation on the physicochemical properties and mechanical performance of hydrogels was studied. The molar ratio of 2:1 between hydroxylysine, lysine and arginine amino groups of GelMA and organosilane coupling agents was chosen to preserve the biological activity of hydrogels. Data in Figure 5-3 show that the organosilation did not have a significant impact on swelling ratio and mechanical performance of hydrogels with a similar concentration of GelMA ($p$>0.05). On the other hand, increasing the concentration of GelMA significantly modified the physicochemical properties of hydrogels. The swelling ratio of Fn-GelMA hydrogels, for instance, was significantly decreased from 12.32±0.36 mg/mg to 9.41±0.20 mg/mg by increasing the concentration of GelMA from 75 mg/ml to 100 mg/ml. The compressive modulus of the functionalised hydrogels, moreover, was remarkably enhanced from 19.47±4.59 kPa to 42.39±3.58 kPa by increasing the concentration of GelMA ($p$ <0.001). These results were in agreement with previous data presented by Nichol *et al.* who observed that by increasing the GelMA concentration the degree of crosslinking was increased [241]. Therefore, the swelling ratio of hydrogels decreases upon increasing the GelMA concentration while their compressive modulus increases [241].

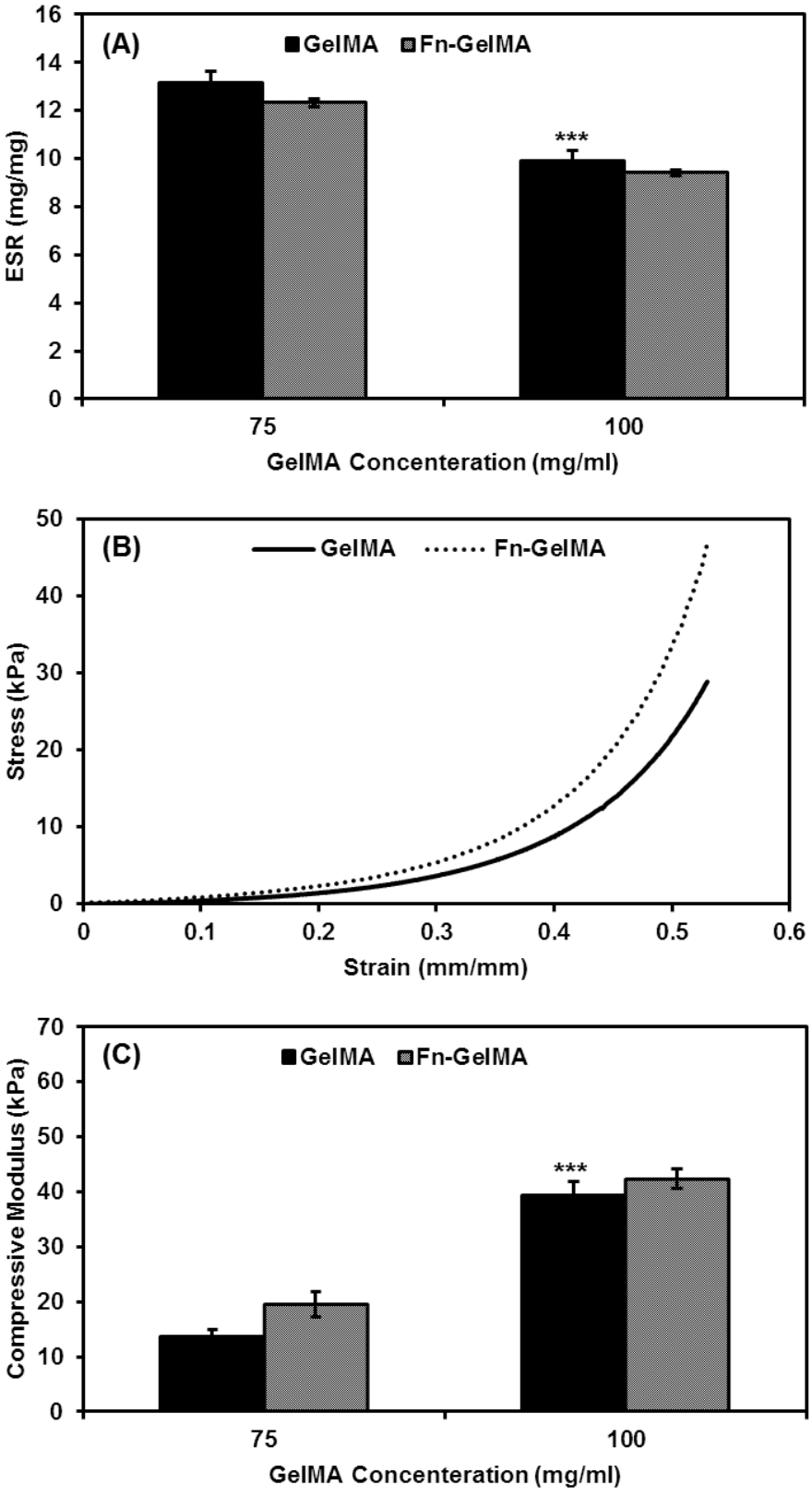


**Figure 5-3 The effect of GPTMS-functionalisation on swelling ratio (A), Compression profile (B) and compressive modulus (C) of GelMA hydrogels with different concentration of GelMA. Data presented in *** represented $p<0.001$.**

## 5.4 Fabrication of Fn-GelMA-BG Hybrid Hydrogels

The covalently bonded organic-inorganic hybrid was fabricated by incorporation of BG precursors into an aqueous solution of Fn-GelMA. A preliminary test was performed to determine the concentration of BG (TEOS or TMOS) that could be used for chemical bonding with Fn-GelMA. The concentration of BG was changed from 0.25 to 1 µl/mg (µl of BG solution per mg of polymer). The hybridization reaction did not occur at low BG ratio (0.25 µl/mg). On the other hand, increasing the concentration of BG to 1 µl/mg led to the formation of the brittle structure due to the self-condensation of silica networks. The BG ratio of 0.5 and 0.75 µl/mg were therefore used to fabricate the Fn-GelMA-BG hybrid hydrogels.

The hybrid hydrogel was formed after 2 min UV crosslinking of the conjugated Fn-GelMA-BG solution in the presence of Irgacure. The chemical composition of BG precursors had a significant effect on the physicochemical properties of hydrogels due to the different steric hindrance and hydrolysis rates of their alkoxysilanes groups. The methoxy functional groups of TMOS, for instance, were hydrolysed 6-10 times faster than ethoxy functional groups of TEOS [463]. The higher hydrolysis rate and lower steric hindrance of these functional groups led to the faster condensation of TMOS, also expedited the covalent bonding with Fn-GelMA and thus hybrid formation.

The TMOS-based hybrid hydrogels showed brittle structures with insufficient swelling properties. For instance, the hybrid hydrogels fabricated from 100 mg/ml Fn-GelMA and 0.5 µl/mg TMOS displayed only 2.91±0.1 mg/mg swelling ratio and 68.23±5.29 kPa compressive modulus. The further increase in the concentration of TMOS, as shown in Figure 5-4, did not have a significant effect on the physicochemical and mechanical properties of hydrogels. TEOS was therefore used as a BG precursor for chemical bonding with Fn-GelMA and formation of an Fn-GelMA-BG hybrid.

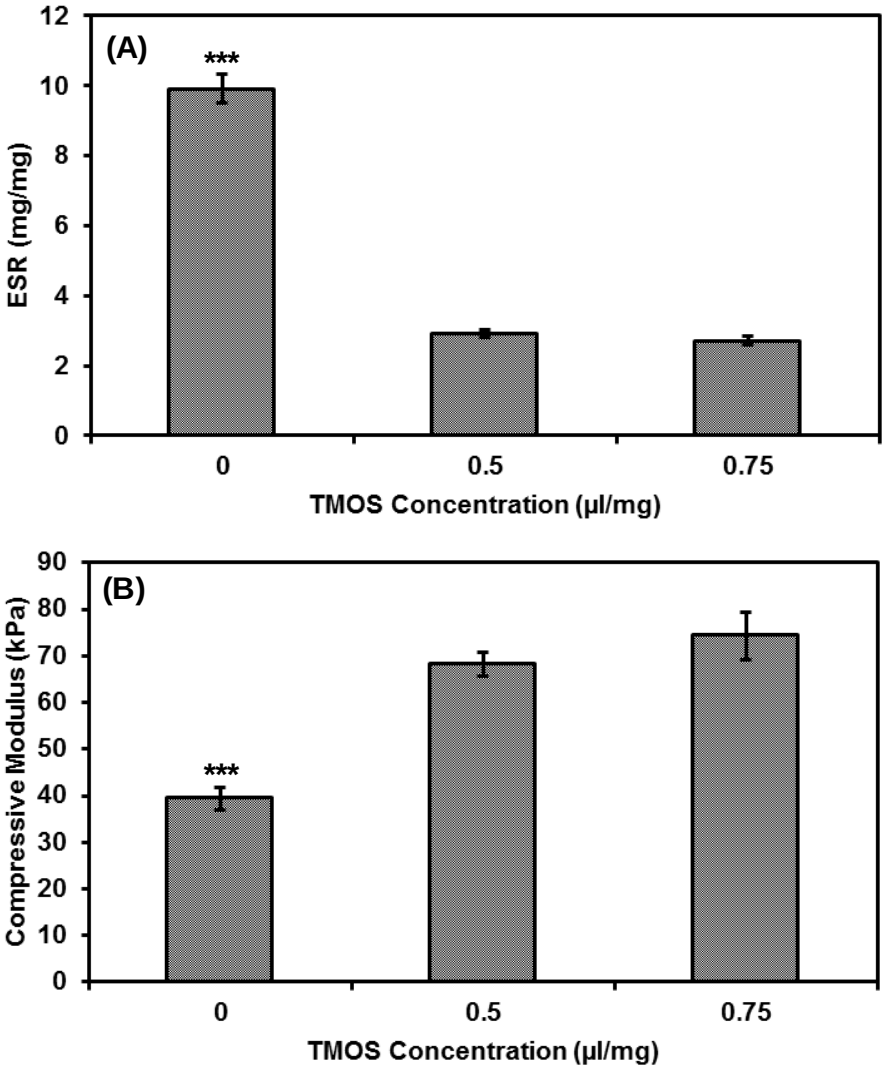


**Figure 5-4 The effect of TMOS concentration on the swelling ratio (A) and compressive modulus (B) of Fn-GelMA-BG hydrogels. Data presented in *** represented $p<0.001$.**

The complete conjugation of Fn-GelMA and BG was confirmed by ATR-FTIR spectra (Figure 5-1A). Upon the addition of BG and hybrid formation, the silanol band (at 970 $cm^{-1}$) was shifted to 950 $cm^{-1}$ and a new band was observed at 1150 $cm^{-1}$ corresponding to silica structure [461, 469]. The distribution of silica within hybrid hydrogel structure was also monitored by SEM-EDS. The SEM image of Fn-GelMA-BG hybrid hydrogel is shown in Figure 5-5A. The homogeneous distribution of Si elements on the surface of this hybrid hydrogel was shown by SEM-EDS analysis as depicted in Figure 5-5B. The ATR-FTIR spectroscopy and SEM-EDS analyses confirmed the formation of a covalent bond between Fn-GelMA and BG,

and also the homogeneous distribution of BG on the surface of hybrid hydrogels.

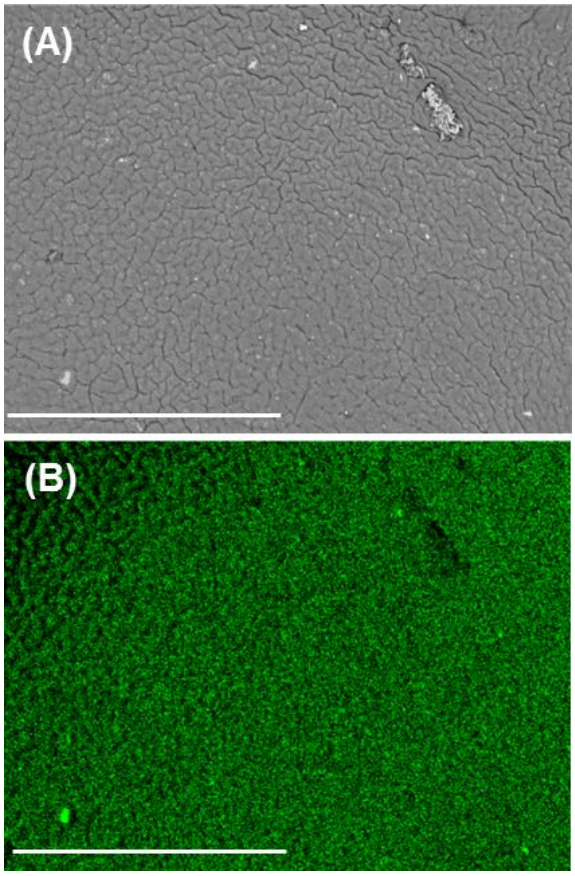


**Figure 5-5 SEM image (A) and the distribution of Si ions (B) on the surface of Fn-GelMA-BG hybrid hydrogels. The scale bars represent 500μm.**

## 5.5 Physicochemical and Mechanical Properties of Fn-GelMA-BG Hybrid Hydrogels

The formation of the hybrid structure of Fn-GelMA and BG (*i.e.*, TEOS solution) had significant impacts on the physicochemical and mechanical properties of hydrogels. Data in Figure 5-6A show that increasing Fn-GelMA concentration did not have a significant effect on swelling ratio of hybrid hydrogels ($p>0.05$). Incorporation of BG into hydrogels, on the other hand, significantly decreased their swelling ratios due to increasing the degree of crosslinking and also the hydrophobic nature of BG (TEOS) [470, 471]. For instance, the conjugation of 0.5 µl/mg BG into the hydrogels with 75 mg/ml concentration of Fn-GelMA significantly decreased their swelling ratio from 13.16±1.0 mg/mg to 9.55±1.46 mg/mg. Further increasing the concentration of BG remarkably decreased the swelling ratio of hydrogels to 2.21±0.16 mg/mg ($p<0.001$).

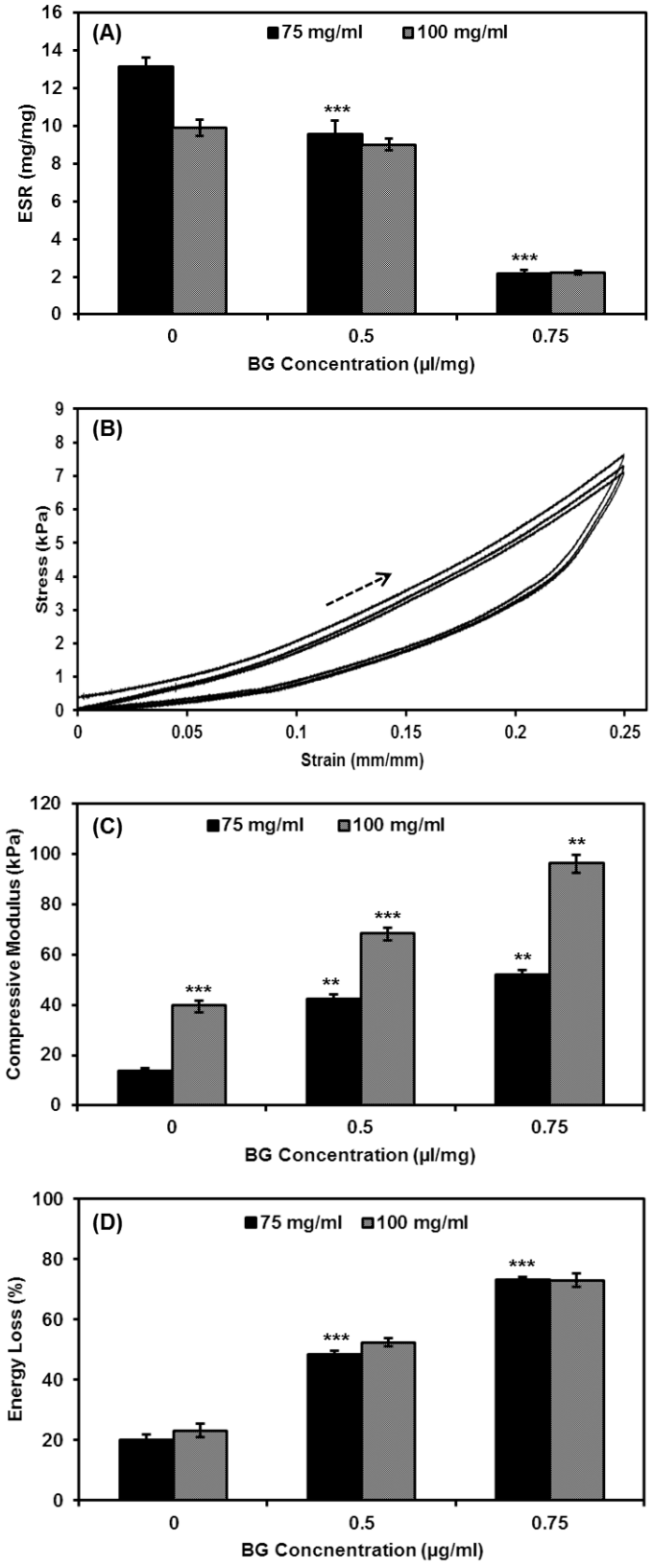


**Figure 5-6 The effect of hybrid formation on swelling ratio (A), cyclic compression-decompression (B), compressive modulus (C) and energy loss (D) of Fn-GelMA-BG hydrogels. Data reported as ** and *** represent $p<0.01$ and $p< 0.001$, respectively.**

The effect of hybrid formation on the mechanical performance of hydrogels was evaluated to optimise the concentration of Fn-GelMA and BG. As shown in Figure 5-6B, hybrid hydrogels could withstand continuous cycles of compression-decompression without any deformations. The mechanical performance of hydrogels, moreover, was significantly enhanced by the conjugation of BG (Figure 5-6C) due to the formation of both covalent bonds and weak van der Waals interactions between Fn-GelMA and BG. The compressive modulus of hydrogels fabricated from 100 mg/ml Fn-GelMA, for instance, significantly enhanced from 39.44±4.85 kPa to 68.23±5.3 kPa upon the incorporation of 0.5 µl/mg BG. Further increasing the concentration of BG to 0.75 µl/mg remarkably elevated their compressive modulus to 96.08±5.28 kPa ($p$<0.01). Despite the significant increase in compressive modulus of hydrogels by hybrid formation, the presence of silica in their structure had a significant effect on their energy loss as depicted in Figure 5-6D. The incorporation of BG in 0.5 µl/m and 0.75 µl/mg ratios into Fn-GelMA hydrogels (100 mg/ml), for instance, significantly increased the energy loss of Fn-GelMA hydrogels from 23.28±2.16 % to respectively 52.39±2.74 % and 73.04±4.34 % ($p$<0.001).

The outcomes of this study revealed that the concentration of BG has the paramount effect on the physicochemical and mechanical properties of hybrid hydrogels. The concentration of BG was kept below 0.5 µl/mg to minimise the risk of acquiring the brittle structure. Increasing the concentration of Fn-GelMA, on the other hand, significantly enhanced the mechanical properties of hydrogels, while their swelling ratio was not changed remarkably. The optimum hybrid hydrogel was therefore fabricated from 100 mg/ml Fn-GelMA and 0.5 µl/mg of BG.

## 5.6 Degradation Profile of Hybrid Hydrogels

### 5.6.1 The Accuracy of Analysis Method

The gravimetric technique is an established method to determine the degradation profile of hydrogels [354, 448, 472]. This method, however, was not accurate in this study due to the poor structural integrity of GelMA

hydrogel that was used as a control sample. On the other hand, the possible precipitation of calcium phosphate particles on the surface of hybrid hydrogels could interfere with the actual mass of hydrogels. Hence, the mass loss ratio was not an accurate and practical method for monitoring the degradation profile of these hydrogels. The main components of the fabricated hybrid hydrogels were protein and silica. In here, the release of protein from the hybrid structures was measured to determine their degradation profiles.

The degradation profiles of hydrogels were usually measured in phosphate buffer saline (PBS) to eliminate the effects of osmotic pressure between the hydrogel and its environment. The chemical composition of this media, however, differs from biological body fluids (Table 5-1). The ionic strength (mol/kg) of these media was calculated using $I = {}^{1}/_{2} \sum_{i=1}^{n} b_i \times z_i^2$ equation, where b and z represented the molarity and the charge of different ions in these media. Data in Table 5-1 show that the chemical composition and ionic strength of simulated body fluid (SBF), compared to the PBS, is closer to the human blood plasma.

Particularly for bone tissue engineering, the *in vitro* bioactivity of scaffolds and formation of calcium phosphate particles are measured in SBF [473]. These differences between chemical composition and ionic strengths might have a significant effect on the *in vitro* performance of hydrogels. However, there is no study to evaluate the effect of incubating media on the degradation profile of hydrogels.

**Table 5-1 Chemical composition of human blood plasma [474], simulated body fluid (SBF) [475] and phosphate buffer saline (PBS) [476]**

| Ion | Human Blood Plasma (mM) | SBF (mM) | PBS (mM) |
|---|---|---|---|
| $HCO_3^-$ | 27 | 4.2 | - |
| $K^+$ | 5 | 5 | 2.7 |
| $Cl^-$ | 103 | 147.8 | 140.7 |
| $Na^+$ | 142 | 142 | 148 |
| $Ca^{+2}$ | 2.5 | 2.5 | - |
| $Mg^{+2}$ | 1.5 | 1.5 | - |
| $HPO_4^{-2}$ | 1 | 1 | 8.1 |
| $H_2PO_4^-$ | - | - | 1.9 |
| $SO_4^{-2}$ | 0.5 | 0.5 | - |
| **Ionic Strength** | **0.150 (mol/kg)** | **0.160 (mol/kg)** | **0.163 (mol/kg)** |

### 5.6.2 The Effect of Incubation Media on the Degradation of Hydrogels

The effect of incubation media on the degradation profile of hydrogels in PBS and SBF was investigated. In both systems, as shown in Figure 5-7, the degradation rate of hybrid samples was lower than pure GelMA hydrogel. This significant stability and lower degradation were due to the formation of network structure between Fn-GelMA and BG [470]. The hybrid formation significantly decreased the amount of the released proteins ($p$<0.001) after 14 days incubation in PBS from 92.92±2.74 % to 34.21±3.55 % for pure GelMA and hybrid samples fabricated from 0.5 µl/mg ratio of BG, respectively.

As it was speculated, the incubation media had a significant effect on the degradation rate of hydrogels ($p$<0.001). For instance, the amount of the released proteins from hybrid hydrogel after one-day incubation was significantly decreased from 8.98±1.36 % to only 5.48±0.23 % by changing the media from PBS to SBF. This effect was due to the chemical compositions and ionic strength of these media [477]. Further incubation of

hybrid hydrogels revealed that only 22.26±0.85 % of their proteins was released after 14 days soaking in SBF. This amount was significantly lower than the cumulative amount of released proteins from hybrid hydrogels incubated in PBS in the same time point (34.21±3.55 %, $p$<0.001). Data in Figure 5-7 show that the hybrid formation significantly enhanced the integrity of gelatin hydrogel in the media and more than 60% of GelMA remained in hybrid hydrogels after 28 days incubation in SBF. The improvement in stability of the hydrogels is of great importance for *in vitro* regeneration of bone as Patterson *et al.* showed that osteoblasts formed more orientated structures on the scaffolds degraded within 6-8 weeks [478]. Therefore, it was concluded that the hybrid hydrogels formed with 100 mg/ml Fn-GelMA and 0.5 µl/mg BG displayed the favourable degradation behaviour compared with pure GelMA hydrogels in different media.

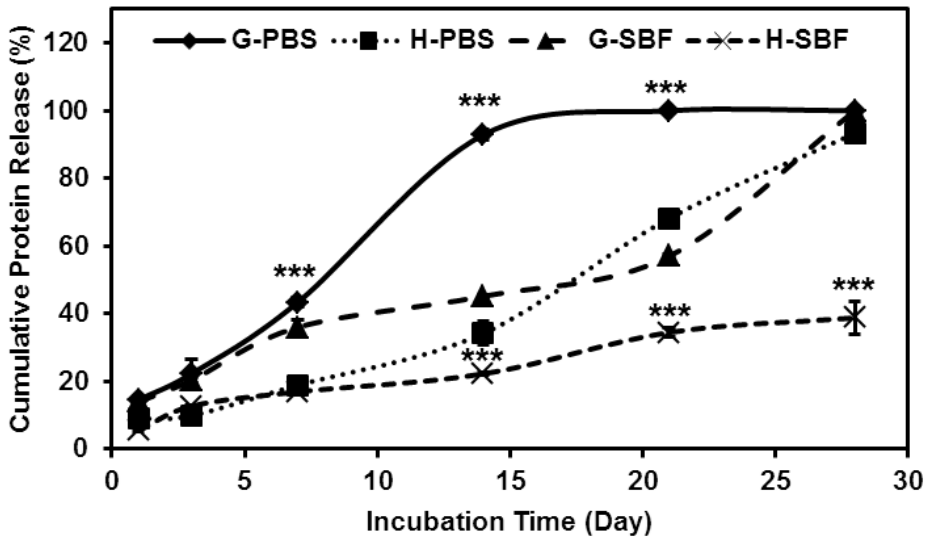


**Figure 5-7 Degradation profile of various hydrogels in different media with respect to their protein release in particular days, G and H represent to GelMA and hybrid hydrogels fabricated with 100 mg/ml Fn-GelMA and 0.5 µl/mg BG, respectively. Data reported as *** $p$< 0.001.**

The formation of the hybrid structure of Fn-GelMA and BG had significant impacts on physicochemical properties, degradation profile, and mechanical strength of the hydrogel. For a bone application, however, the scaffolds with the compression modulus higher than 300 kPa are favourable [479]. Increasing the methacrylation fraction, the concentration of GelMA and photoinitiator could increase the degree of crosslinking and thus improve the mechanical properties of hydrogels

The effect of methacrylation fraction on the mechanical and biological properties of GelMA-based hydrogels was previously investigated [241, 254]. It was found that upon the methacrylation, the free amine groups of gelatin formed a chemical bond to methacrylate groups [241]. Increasing the degree of methacrylation, therefore, enhanced the degree of crosslinking and elevated the mechanical properties of hydrogels. On the contrary, decreasing the biological motif sites of gelatin, *i.e.* free amine groups had a significant impact on the biocompatibility of GelMA hydrogels [254]. The degree of methacrylation of GelMA in this study was 80%. The further increase in the content of methacrylate might have a negative impact on the biological activity of hydrogels.

The preliminary results showed that increasing the GelMA concentration led to the formation of premature silica network during the functionalisation process due to increasing the viscosity of the solution. Increasing the concentration of Irgacure, on the other hand, decreased the pore size of hydrogels and had significant drawbacks on biocompatibility and physicochemical properties of hydrogels [455-457]. Incorporation of GelMA hydrogel within prefabricated scaffolds is another approach to improving the mechanical properties [248]. The compressive modulus of these reinforced hydrogels, however, only depends on the concentration of GelMA. Therefore, this strategy was not used in this study to enhance the mechanical property of hybrid hydrogel.

## 5.7 Summary

In this chapter, the feasibility of functionalised GelMA for chemical bonding to BG was examined. The favourable organosilane coupling agent was GPTMS due to complete functionalisation of GelMA. This organosilation reaction, moreover, did not interfere with crosslinking of the polymer phase. After this, the concentration of GelMA, GPTMS, and BG was optimised to acquire stronger mechanical strengths and suitable swelling properties compared to an interpenetrating hybrid of GelMA-BG. The hydrogels fabricated from 100 mg/ml GelMA functionalised with GPTMS, and 0.5 µl TEOS solution per each milligram of the organic component had superior properties. Despite the significant enhancement of physicochemical properties, mechanical strength, and degradation behaviours of these hydrogels their compressive modulus still was not adequate for bone tissue engineering. In the next chapter, a new approach would be proposed to enhance the mechanical properties of these hybrids.

# Chapter 6. Fabrication of Bioactive Hybrid Hydrogel for Bone Tissue Engineering

## 6.1 Introduction

The covalently bonded hybrid hydrogel with enhanced physicochemical properties and degradation behaviour was fabricated in Chapter 5. The mechanical performance of these hydrogels was significantly enhanced by the formation of covalent bonds between Fn-GelMA and BG. Their compressive modulus, however, was still insufficient for bone tissue engineering. The aim of this study was to enhance the mechanical strength and stability of hybrid hydrogels. Several approaches including composite formation [480-482], double network formation [248, 483-485] and fibre reinforcement [486-488] have been attempted to improve the mechanical strength of hydrogels. The heterogeneous distribution of secondary phases within the hydrogel, however, is the paramount issue of these approaches. It was speculated that introducing a secondary crosslinking agent might have significant impacts on the mechanical strength and degradation profile of hybrid hydrogels.

The feasibility of the formation of conjugated hybrid hydrogels with enhanced physicochemical properties and mechanical performances is investigated in this chapter. It is important to note that the secondary polymers should not interfere with organosilation reaction. Therefore, the absence of carboxylic acid and amine functional groups in their structures is the prerequisite criteria for the secondary crosslinking agents. The effect of the secondary polymer conjugation on the mechanical performance, physicochemical properties, degradation behaviour, and *in vitro* and *in vivo* biological performances of hybrid hydrogels are investigated.

## 6.2 Fabrication of Natural-Based Photocrosslinkable Hybrid Hydrogel

The photocrosslinkable derivatives of natural polymers such as alginate [232], chitosan [233, 489], Gellan gum [490], hyaluronic acid [227], and starch [491, 492] were extensively used to form a biocompatible hydrogel. It was speculated that the conjugation of these biopolymers into Fn-GelMA solution could enhance the mechanical properties and stability of hybrid hydrogels. A scaffold with enhanced mechanical properties, for instance,

has been fabricated using double network formation of GelMA and methacrylated derivative of Gellan gum [484]. The presence of carboxylic acid in the backbone of Gellan gum, however, could interfere with GelMA in organosilation reaction. The nucleophilic functional groups such as amine and carboxylic acid are found in the structure of other biopolymers including chitosan (amine), alginate and hyaluronic acid (carboxylic acid). Starch, on the other hand, only possesses electrophile functional groups (*i.e.* hydroxyl) in its structure. Therefore, the mechanical properties of GelMA-BG hybrids might improve by conjugation of methacrylated derivative of starch (StaMA) within Fn-GelMA solution without any interference in GPTMS-functionalisation. Prior to the fabrication of bioconjugated hybrid hydrogels, the methacrylation process of starch was characterised.

### 6.2.1 Characterisation of StaMA

The effect of methacrylation on the chemical structure and thermal stability of starch was investigated. ATR-FTIR spectroscopy in Figure 6-1A confirms the synthesis of StaMA by the appearance of a characteristic band at 1670 $cm^{-1}$ correspondence to alkenyl carbon (C=C) in its spectra [469]. The methacrylation, moreover, did not shift other characteristic bands of starch spectra. Data in Figure 6-1B show that the thermal stability of starch was significantly modified by methacrylation. The decomposition of StaMA, for instance, was initiated at 255°C, which was considerably lower than the decomposition temperature of pure starch (280°C).

The slope of the thermogravimetric cure during decomposition period was calculated as a rate of decomposition [493]. It was found that the rate of decomposition was significantly improved from -0.287 (%/°C) to -0.128 (%/°C) after methacrylation. The decomposition of StaMA was finished at 305°C while more than 70% of StaMA remained untouched. On the other hand, 40% of the pure starch was remained after complete thermal decomposition at 310°C. These outcomes confirmed the complete methacrylation of starch.

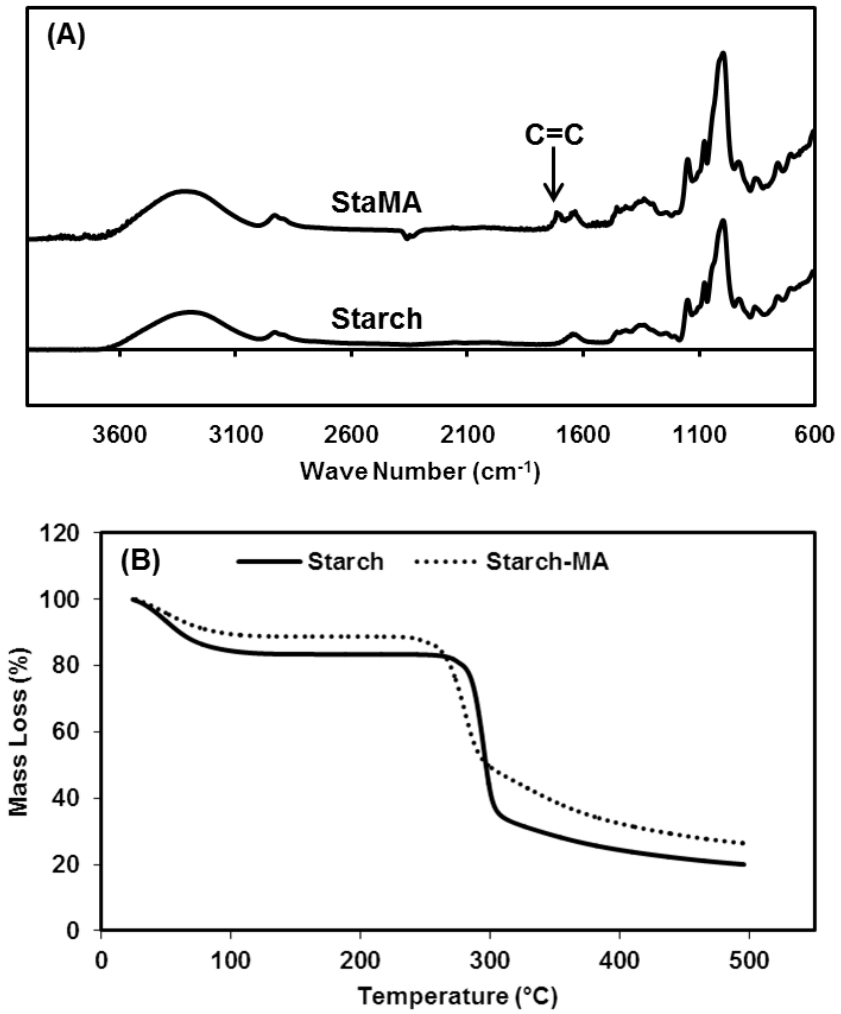


**Figure 6-1 The effect of methacrylation on ATR-FTIR (A) and TGA (B) of starch.**

The highest concentration of starch to form an aqueous solution is 20 mg/ml. This concentration was therefore used to form a bioconjugated solution of StaMA and Fn-GelMA to form an organic-inorganic hybrid in the presence of BG. The temperature was set at 40°C to prevent over-condensation of BG and also gelatinization of starch [494]. The presence of hydroxyl as an electron-donating group in the backbone of StaMA might form weak van der Waals interactions and hydrogen bonding with electron-withdrawing functional groups of GelMA. StaMA, therefore, could entangle within GelMA chains and act as a filler to form a composite upon photocrosslinking. This hypothesis was evaluated by the formation of composite from 100 mg/ml GelMA and 20 mg/ml starch. It was found that UV irradiation of this solution did not form a hydrogel even after 10 min

due to the steric hindrance of starch molecules. The bioconjugation of 20 mg/ml StaMA into GelMA solution, on the other hand, formed a hydrogel within 1 min UV irradiation due to increasing the degree of photocrosslinkable functional groups.

The presence of MA functional groups in the structure of StaMA could form a chemical bond with other MA groups in StaMA and GelMA chains. The formation of these chemical bonds forms a crosslinked structure or an interpenetrated polymer network (IPN) with GelMA solution. The specific clarification between these two networks (*i.e.,* crosslinked or IPN) was not possible due to the appearance of similar functional groups in FTIR-ATR of GelMA-StaMA hydrogels (data not shown). In this study, therefore, the term of bioconjugation was used to covering both crosslinking and IPN formation in GelMA-StaMA hydrogels.

### 6.2.2 Physicochemical and Mechanical Properties of Bioconjugated Hybrid Hydrogels

The effects of StaMA bioconjugation on the physicochemical properties and mechanical performance of GelMA hydrogels are shown in Figure 6-2. It was found that the bioconjugation of StaMA significantly decreased the swelling ratio of GelMA hydrogels from 9.92±0.42 mg/mg to 6.25±0.9 mg/mg ($p$<0.001) due to increasing the degree of crosslinking. The incorporation of BG solution (0.5 µl per each milligram of Fn-GelMA and StaMA) into these hydrogels significantly decreased their swelling ratio to 4.06±0.6 mg/mg due to intrinsic hydrophobicity of silica and formation of more compact structures.

Despite the significant decrease in the swelling ratio of bioconjugated hybrid hydrogels, their mechanical performances were remarkably enhanced. The Fn-GelMA-StaMA-BG hydrogels, as shown in Figure 6-2B, could withstand the uniaxial cycles of compression-decompression loads without deformation. The compressive modulus of hydrogels, moreover, was enhanced 1.7-fold upon StaMA conjugation. Further incorporation of BG into bioconjugated hydrogel significantly improved its compressive

modulus from 67.57±1.96 kPa to 198.75±24.2 kPa ($p$<0.001). The previous outcomes in Chapter 5 showed that the hybrid formation had a significant effect on the energy loss of pure GelMA hydrogels. The further bioconjugation of StaMA within these hydrogels significantly increased their energy loss ($p$<0.001). The hybrid formation, however, did not have significant impacts on the energy loss of the bioconjugated hydrogels. The energy loss of all hydrogels, as shown in Figure 6-2D, was less than 50% that underpin the elasticity of all hybrid hydrogels [495].

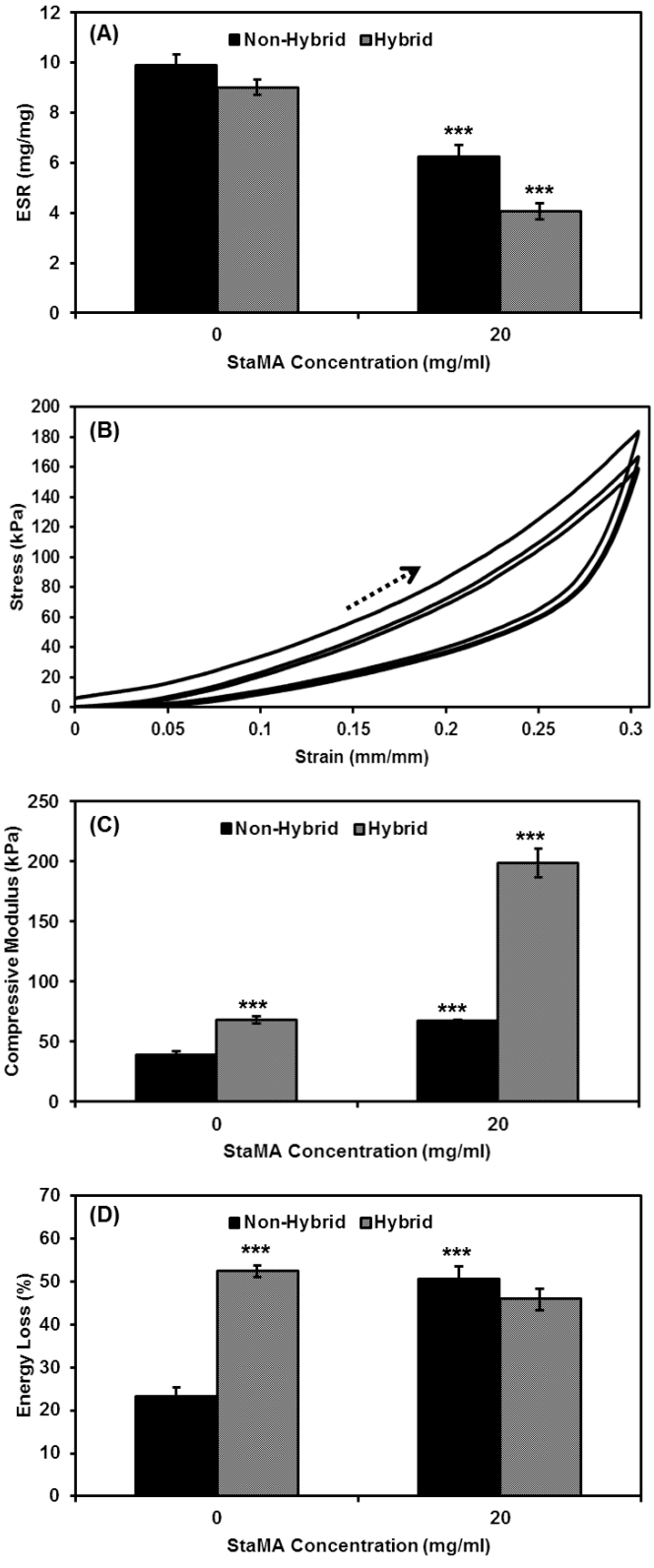


**Figure 6-2 The effect of StaMA bioconjugation and hybrid formation on swelling ratio (A), cyclic compression-decompression (B), compressive modulus (C), and energy loss (D) of GelMA-based hydrogels. Non-Hybrid refers to polymeric hydrogels without organosilation. Data presented as *** represented $p<0.001$.**

Despite the significant improvements on the physicochemical and mechanical properties of hybrid hydrogels upon StaMA conjugation, the further modification of these complexes was restricted due to the limited solubility of starch in PBS. Therefore, another photocrosslinkable polymer was conjugated to Fn-GelMA-BG hybrid hydrogels to enhance their physicochemical and mechanical performances.

## 6.3 Conjugation of PEGDA within GelMA Hydrogels

The application of poly(ethyleneglycol) diacrylate (PEGDA) as inert biomaterials in hydrogel formation is widespread due to its hydrophilic nature and tailorable physicochemical and mechanical properties [496-503]. The lack of nucleophilic functional groups in the structure PEGDA prevents any interfere with organosilation of GelMA. Different concentration of PEGDA, therefore, was conjugated within the GelMA-based hydrogel, and their physicochemical and mechanical properties were studied. Data in Figure 6-3A show that the swelling ratio of hydrogels was significantly decreased upon the conjugation of PEGDA within their structures ($p$ <0.001) due to increasing the degree of crosslinking [471]. Conjugation of 50 mg/ml PEGDA to GelMA solution, for instance, significantly decreased the swelling ratio of hydrogels to 7.26±0.34 mg/mg. The further increasing in the concentration of PEGDA to 200 mg/ml in conjugated hydrogels remarkably decreased their swelling ratio to 2.83±0.08 mg/mg ($p$<0.001).

Despite the remarkable decrease in swelling ratio of conjugated hydrogels, their mechanical performances were significantly improved. It was found that elevating the concentration of PEGDA from zero to 50 mg/ml, and 100 mg/ml increased the mechanical strength of these conjugated hydrogels by five- and seven-fold, respectively. The conjugated hydrogel with 50 mg/ml concentration of PEGDA, for instance, displayed elastic performances under uniaxial cycles of compression-decompression and possessed the compressive modulus of 211.16±14.2 kPa (Figure 6-3B and C). The further increasing of the concentration of PEGDA significantly enhanced the compressive modulus of hydrogels to 342.97±17.3 kPa.

The conjugation of PEGDA also had a significant effect on the mechanical properties of hydrogels. The addition of 50 mg/ml PEGDA to GelMA, for instance, significantly increased the energy loss of hydrogels from 23.27±4.32 % to 38.67±1.4 %. This effect might be due to the random conjugation of PEGDA chain within GelMA network. Further increase of PEGDA concentration, as shown in Figure 6-3C and D, remarkably decreased the energy loss of hydrogels. The conjugation of 200 mg/ml PEGDA into GelMA solution, as an example, led to the formation of an elastic hydrogel with a compressive modulus of 1181.71±394.8 kPa and 17.41±1.8 % energy loss.

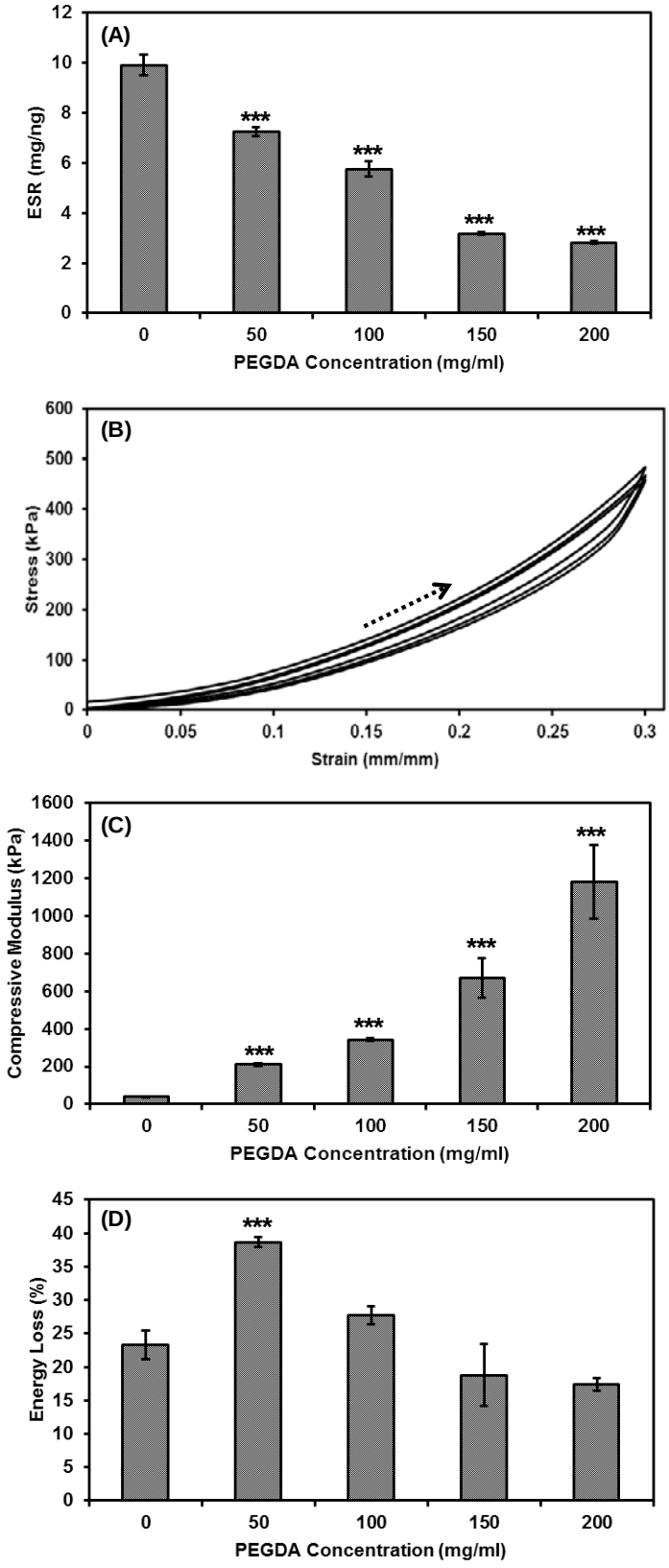


**Figure 6-3 The effect of PEGDA concentration on swelling ratio (A) cyclic compression-decompression (B), compressive modulus (C) and energy loss (D) of conjugated GelMA hydrogels. Data presented in *** represented to $p<0.001$.**

The previous outcomes in Chapter 5 revealed that the hybrid formation was the prosperous method to enhance the compressive modulus of hydrogels. The swelling ratios of those hybrid hydrogels, however, were significantly decreased due to the hydrophobic nature of BG and also increasing their degree of crosslinking. The concentration of PEGDA in conjugated hydrogels, therefore, must be optimised prior to the incorporation of BG and the hybrid formation. Despite the significant improvement in the mechanical performance of hydrogels, conjugation of high concentration of PEGDA significantly decreased the swelling ratio of hydrogels. The lower concentrations of PEGDA (50-100 mg/ml) were therefore conjugated within Fn-GelMA to form an organic-inorganic hybrid with proper swelling ratio properties.

## 6.4 Fabrication of Photocrosslinkable Hybrid Hydrogels with Enhanced Physicochemical and Mechanical Properties

The effects of hybrid formation on the swelling ratio and mechanical performance of PEGDA-conjugated hydrogels were investigated. As it was expected, the swelling ratio of hydrogels dramatically decreased upon incorporation of BG ($p<0.01$). Data in Figure 6-4A reveal that the swelling ratio of hydrogels conjugated with 50 mg/ml PEGDA was significantly decreased from 7.26±0.34 mg/mg to 4.35±0.44 mg/mg after hybrid formation. Increasing the concentration of PEGDA in the hybrid hydrogel, however, did not significantly decrease their swelling ratio ($p>0.05$).

Upon the incorporation of BG, the compression modulus of PEGDA-conjugated hydrogels was further increased by 1.5-fold. These results endorsed that regardless of PEGDA concentration, the formation of the silica network reinforced the compressive modulus of hydrogels. For instance, the fabricated hybrid hydrogel from 100 mg/ml PEGDA displayed the compression strength of 528.9±32.67 kPa that was within the acceptable range for bone regeneration applications [479]. The compression strength of this hybrid hydrogels is remarkably higher than previously developed interpenetrated polymer network (IPN) hydrogels from GelMA and PEGDA [235, 254, 256]. For instance, the IPN hydrogel fabricated from similar

concentrations of GelMA and PEGDA using thiol click chemistry technique showed the compressive modulus of 80 kPa [235]. The conjugation of poly (lactide-*co*-ethylene oxide-*co*-fumarate) (PLEOF) and PEGDA was another attempt to improve the mechanical properties of GelMA hydrogels [254]. The hydrogel fabricated from 300 mg/ml PLEOF, 100 mg/ml PEGDA and 100 mg/ml GelMA possessed the compressive modulus of 250 kPa that was lower than hybrid hydrogels fabricated in this study. In addition to enhancement of compressive modulus of hydrogels, the energy loss of conjugated hydrogels was increased upon hybrid formation. The energy loss of all hybrid hydrogels, as shown in Figure 6-4D, was less than 50% that underpins their elasticity [495].

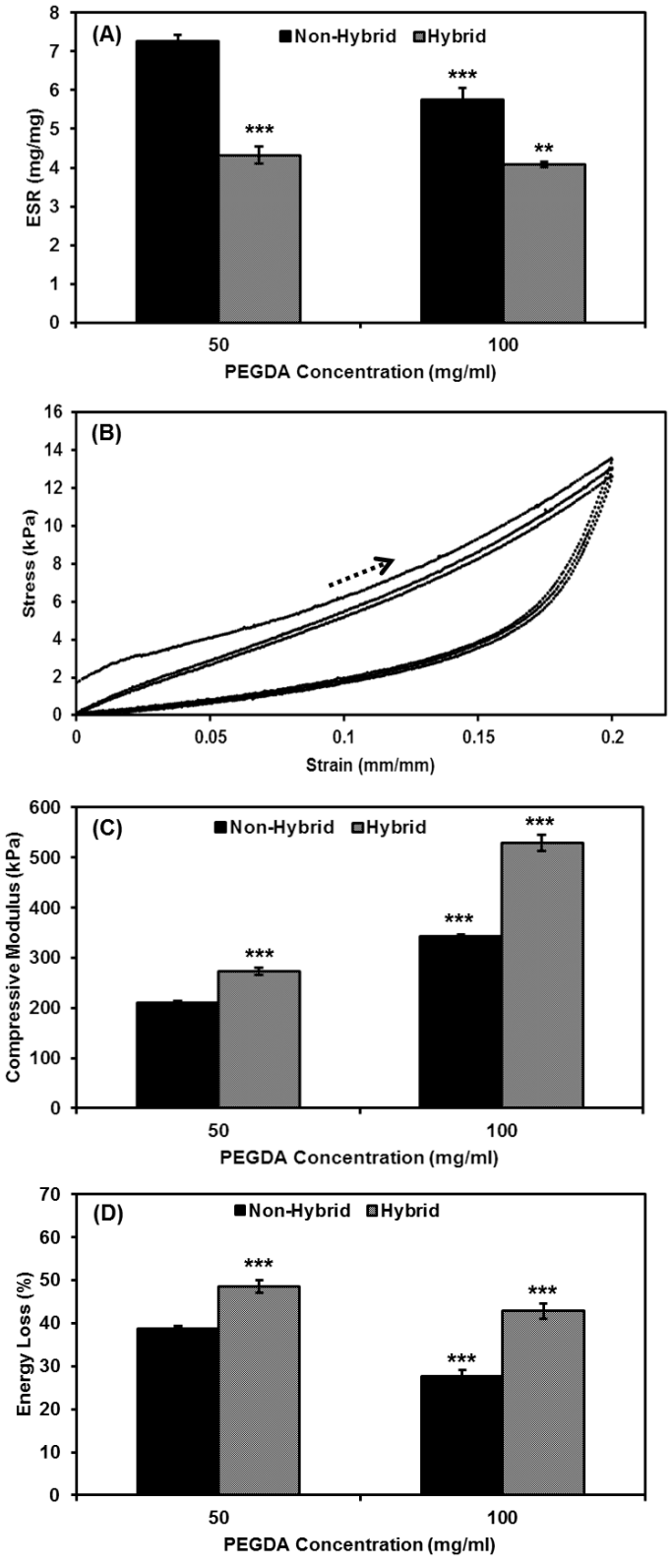


**Figure 6-4 The effect of PEGDA conjugation and hybrid formation on swelling ratio (A), cyclic compression-decompression (B), compressive modulus (C) and energy loss (D) of GelMA-based hydrogels. Non-Hybrid refers to polymeric hydrogels without organosilation. Data presented in ** and *** represented to $p<0.01$ and $p<0.001$.**

The results of this study in Chapter 5 showed that the degradation profile of hydrogels was a function of incubation media. It was hypothesised that the incubation media also has a significant impact on the mechanical performance of hydrogels. The GelMA-based hydrogels were prepared in PBS solution and their mechanical properties in this media were shown in Figure 6-4. The ultimate application of these hydrogels is bone tissue engineering. In order to stimulate the physiological environment of the bone, these hydrogels were incubated in SBF at 37°C. The presence of inorganic compounds in the structure of hybrid hydrogels acted as a nucleation site and thus could enhance the precipitation of ionic components on the surface of hydrogels [504]. Hence, the topography of hydrogels would change upon the sedimentation of ionic compounds that further alters the mechanical performances of hybrid hydrogels. No attempt, however, has been approached to investigate the effect of incubation media on the mechanical performance of hydrogels.

## 6.5 The Effect of Incubation Media on Mechanical Properties of Hydrogels

Different concentrations of PEGDA were conjugated within GelMA-based hydrogels before and after hybrid formation, and all hydrogels were incubated in SBF media at 37°C. The effects of media incubation, PEGDA conjugation, and hybrid formation on the mechanical properties of hydrogels, therefore, were specifically distinguished. As shown in Figure 6-5A, the compressive modulus of hydrogels was significantly decreased upon incubating in SBF ($p$<0.001). The continuous decrease in the compressive modulus of hydrogels was in agreement with the results of Jeon *et al.* while their photocrosslinked alginate hydrogels lose their compressive moduli in deionised water over time [232].

The compressive modulus of pure GelMA hydrogels, for instance, decreased from 39.44±4.85 kPa to 29.23±2.3 kPa after one-day incubation in SBF. The compressive moduli of other hydrogels were similarly decreased after 1 day incubation that was due to the osmotic pressure between hydrogels and SBF. Further incubation of hydrogels in SBF media

significantly decreased their compressive moduli ($p$<0.001). The pure GelMA, for instance, possessed 19.59±2.90 kPa compressive modulus after 3 days incubation in SBF. The seven days incubated GelMA hydrogels lost their physical integrity during the compression test, and thus their compressive moduli were excluded.

The previous data in Chapter 5 revealed that 20.38±1.6 % and 36.02±4.18 % of proteins were released from pure GelMA hydrogel within respectively 3 and 7 days incubation in SBF. The bulk hydrolysis of hydrogels, therefore, was the particular aspect on decreasing of mechanical properties of GelMA hydrogels overtime.

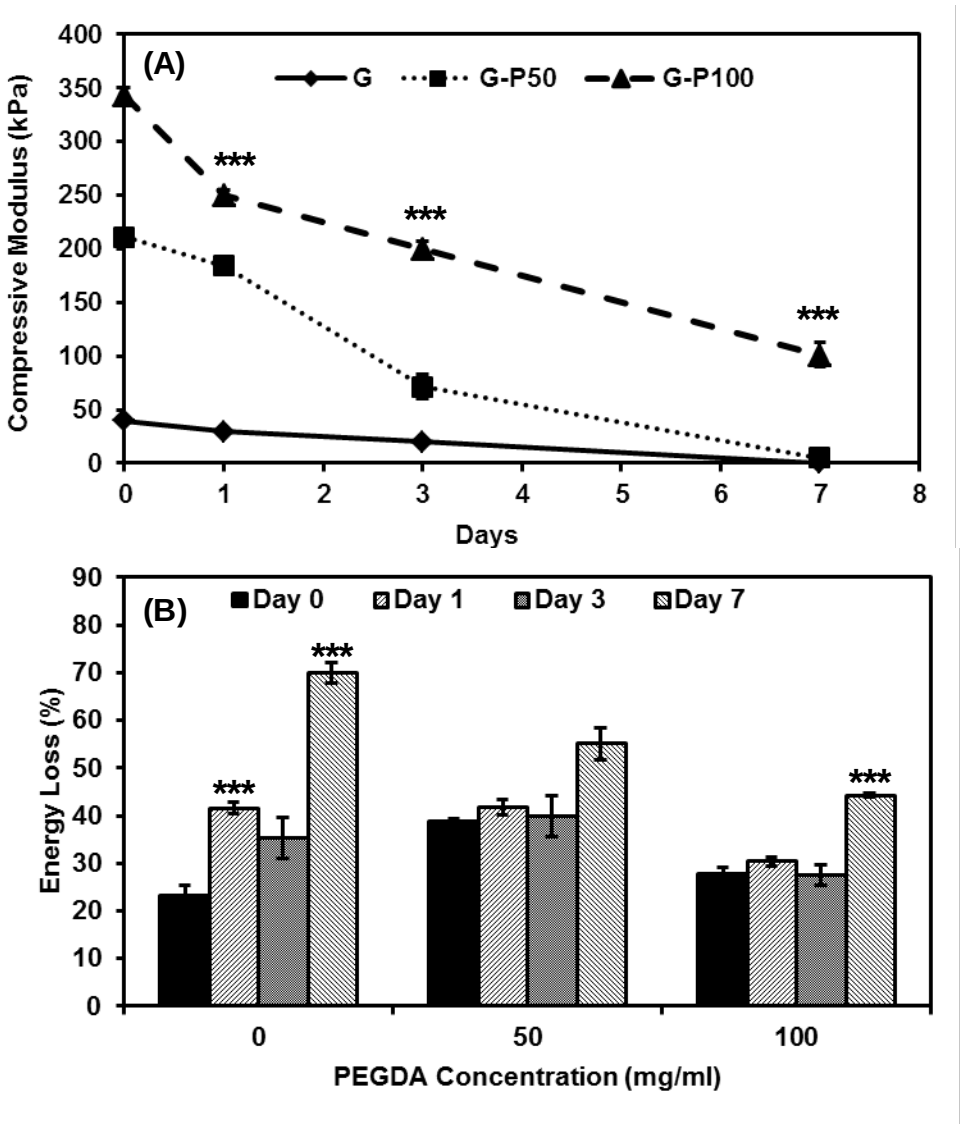


**Figure 6-5 The Compressive modulus and energy loss of GelMA-PEGDA hydrogels after incubation in SBF at different times G and P represented to GelMA and PEGDA, respectively. Data reported as *** $p < 0.001$.**

The mechanical properties of GelMA-PEGDA hydrogels displayed similar trend with pure GelMA hydrogels as depicted in Figure 6-5A. For example, the hydrogels contained 50 mg/ml PEGDA significantly lost their compressive modulus from 211.16±7.09 kPa to 71.46±22.32 kPa after 3 days incubation in SBF. The compressive modulus of these hydrogels was dramatically decreased to 4.89±.038 kPa after 7 days incubation in SBF. It was concluded that mechanical strength was gradually decreased due to the degradation of hydrogels.

Increasing the concentration of PEGDA had a significant impact on the mechanical stability of these hydrogels. After 7 days incubation in SBF, for instance, the 100 mg/ml PEGDA-conjugated hydrogels displayed the compressive modulus of 100.87±22.64 kPa which was significantly lower than its modulus prior SBF-incubating (342.98±15.42 kPa, $p<0.001$).

Despite the significant effect of incubating media on the compressive modulus of conjugated hydrogels, the SBF incubation up to 3 days did not have a remarkable impact on the energy loss of GelMA-PEGDA hydrogels ($p>0.05$). Data in Figure 6-5B show that these hydrogels kept their elastic performance under cycles of compression-decompression loads, while their energy loss was less than 50 % after 3 days incubation in SBF. After 7 days incubation in SBF, however, these hydrogels could not withstand under cyclic compression-decompression loads. It was concluded that the mechanical properties of hydrogels were a factor of incubating media and the period of incubation.

The mechanical stability of hydrogels over time is a crucial factor for bone tissue engineering since the callus formation in a bone defect site is a protracted process and begins 7 days post-culture [505]. The hybrid formation significantly improved the mechanical stability of hydrogels over time (Figure 6-6). Prior to conjugation of PEGDA, for instance, the Fn-GelMA-BG hybrid hydrogels kept their mechanical stability after 7 days incubation in SBF. Their compressive modulus was continuously decreased from 70.18±4.56 kPa to 58.06±1.46 kPa and 40.18±0.96 kPa after respectively 1 and 7 days incubation. These hydrogels, however, lost their physical integrities under the compression loads after 14 days incubation in SBF. Similar to non-hybrid hydrogels, the osmotic pressure and bulk degradation of these hybrid hydrogels were the main aspects on the continuous decrease of their mechanical performances.

The bioactive scaffold with continuous mechanical stability was fabricated by conjugation of PEGDA within the hybrid hydrogels. Data in Figure 6-6A demonstrate that the conjugated hybrid hydrogels contained 100 mg/ml PEGDA displayed an elastic performance with a compressive modulus of

101.66±6.82 kPa after 7 days incubation in SBF. These hydrogels, moreover, represented the compressive modulus of 51.09±13.68 kPa after 21 days incubation in SBF, which is still favourable for osteoblasts to proliferate [506]. The conjugated hybrid hydrogels with a lower concentration of PEGDA (50 mg/ml), on the other hand, lost their mechanical stability over time. These hydrogels displayed 1.37±0.84 kPa compressive modulus after 7 days incubation in SBF (Figure 6-6B). Regardless the concentration of PEGDA, the elastic performance of all conjugated hybrid hydrogels was confirmed by measuring their energy loss. Data in Figure 6-6C show that the energy loss of all hydrogels did not significantly change during SBF incubation.

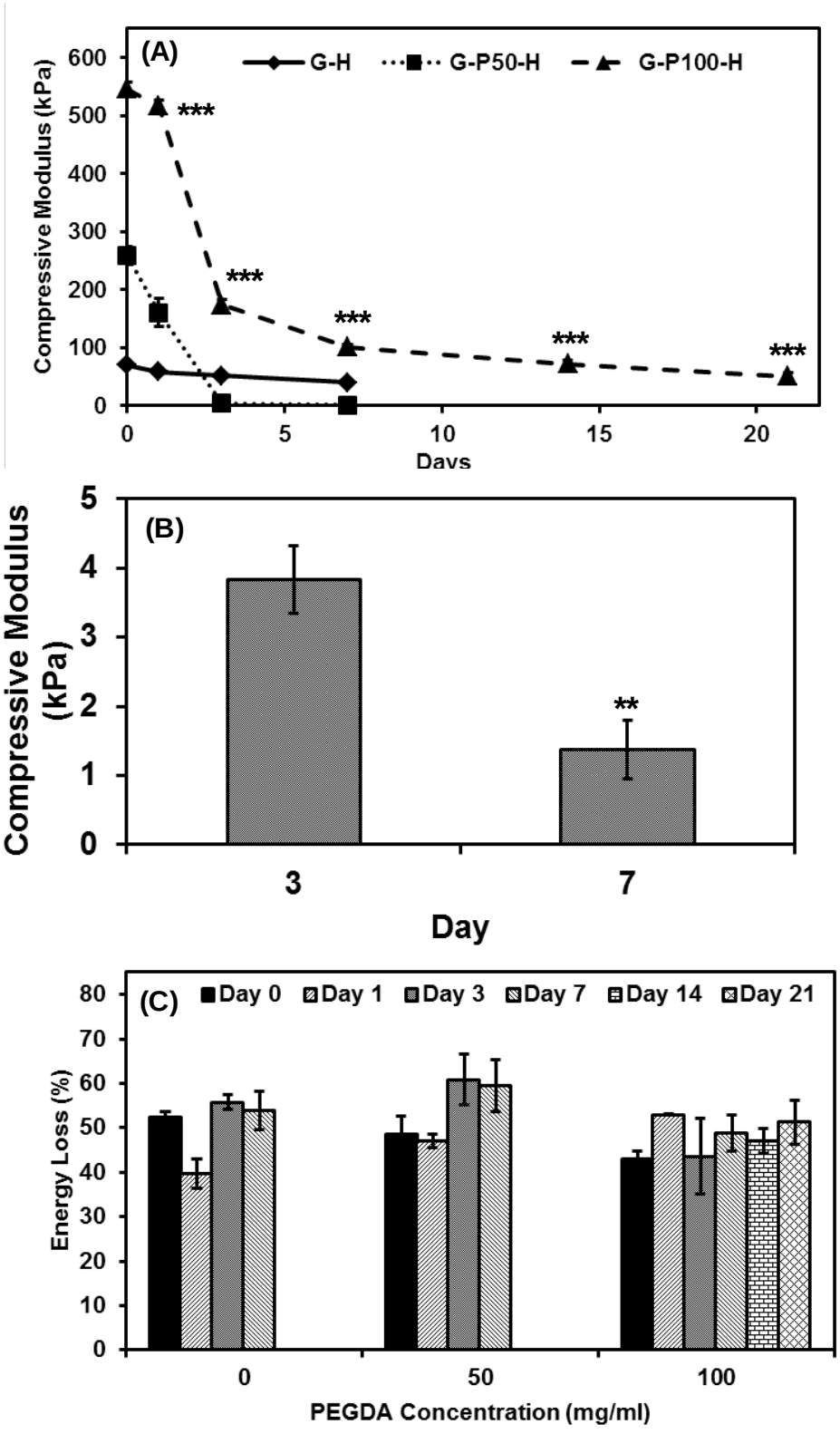


**Figure 6-6 The Compressive modulus(A and B) and energy loss (C) of Fn-GelMA-PEGDA-BG hybrid hydrogels after incubation in SBF at different times. G, P and H represented to Fn-GelMA, PEGDA and Hybrid hydrogel, respectively. Data reported as ** $p < 0.01$ and *** $p < 0.001$.**

The comparison between these outcomes revealed that the introducing the secondary polymer into hybrid hydrogels significantly increased their degree of crosslinking. The hybrid hydrogel with a higher concentration of PEGDA, for instance, demonstrated the highest mechanical stability over time. The swelling ratio of hydrogels, on the other hand, was remarkably decreased by PEGDA conjugation. Their swelling ratio, however, was still in the acceptable range for biomedical applications including bone regeneration or controlled release of pharmaceutically active proteins [507-510]. The results of this study demonstrated that 100 mg/ml PEGDA was sufficient to achieve the desirable mechanical strength and also swelling property of hybrid hydrogels.

## 6.6 Physical Stability of Conjugated Hybrid Hydrogels

Previous outcomes in Chapter 5 showed that regardless the chemical composition of incubation media, the physical stability of hydrogels was enhanced by hybrid formation. The similar chemical composition of SBF, moreover, stimulated the degradation of hydrogels in body fluid. The degradation profile of conjugated hybrid hydrogels was therefore investigated in SBF media with respect to the cumulative degree of released proteins and silicate ions from these hydrogels.

The conjugated hybrid hydrogels were fabricated from GelMA, PEGDA, and BG. The degradation profile of PEGDA chains has been investigated *in vitro* [511] and *in vivo* [512]. It was found the molecular weight of PEGDA has a significant impact on the hydrolytic resorption of PEGDA [513]. In this study, low-molecular weight PEGDA (Mn= 700) was used. Therefore, it can be exerted from the body through metabolism and show a minimal impact on the biocompatibility of hybrid hydrogels [514]. The amounts of released protein and silicate anions were therefore quantified to determine the profile of degradation of hydrogels.

It was found that the conjugation of PEGDA into GelMA hydrogels dramatically enhanced their structural integrity. Data in Figure 6-7A show that the protein release from GelMA hydrogels after seven days incubation

in SBF was decreased from 36.02±2.09 % to 25.86±0.90 % by conjugation of 100 mg/ml PEGDA within their structure ($p<0.05$). The hybridization of the hydrogel with BG further enhanced their structural stability and caused a 2-fold decrease in the protein release. The protein release from hybrid hydrogel was only 11.92±1.72 % after seven days, which confirmed their high structural stability and protein retention capacity.

Previous studies showed that the retention of proteins within the structure of hydrogels is essential to acquire favourable biological responses for a long-term *in vitro* [131, 135, 232]. After 21 days, nearly 75% of GelMA was maintained within the structure of hybrid hydrogel due to chemical bonding between GelMA and BG that reduced the degradation rate of gelatin. Indeed, this enhancement of structural stability was remarkably higher than previous studies that attempted different approaches for preserving GelMA in hydrogel structure. For instance, at the same period, it was reported that more than 45% of GelMA was leached out from IPN hydrogel fabricated from GelMA, PLEOF and PEGDA [254]. Therefore, the presence of silica network structure in these hybrid hydrogels has a paramount role in enhancing the physical integrity of hydrogel.

The amount of silicate anions released from hybrid hydrogels in SBF was monitored to assess their degradations. As shown in Figure 6-7B, the conjugation of PEGDA in hybrid hydrogels did not have a significant impact on degradation of silicate anions ($p>0.05$). For instance, less than 1.2 % of silicate anions were released from hybrid hydrogels after 28 days incubation in SBF. The substantial integrity of silica within hybrid hydrogels could enhance the bioactivity of hydrogels; hence, it promotes the precipitation of calcium phosphate particles on the surface of hydrogels for a longer period.

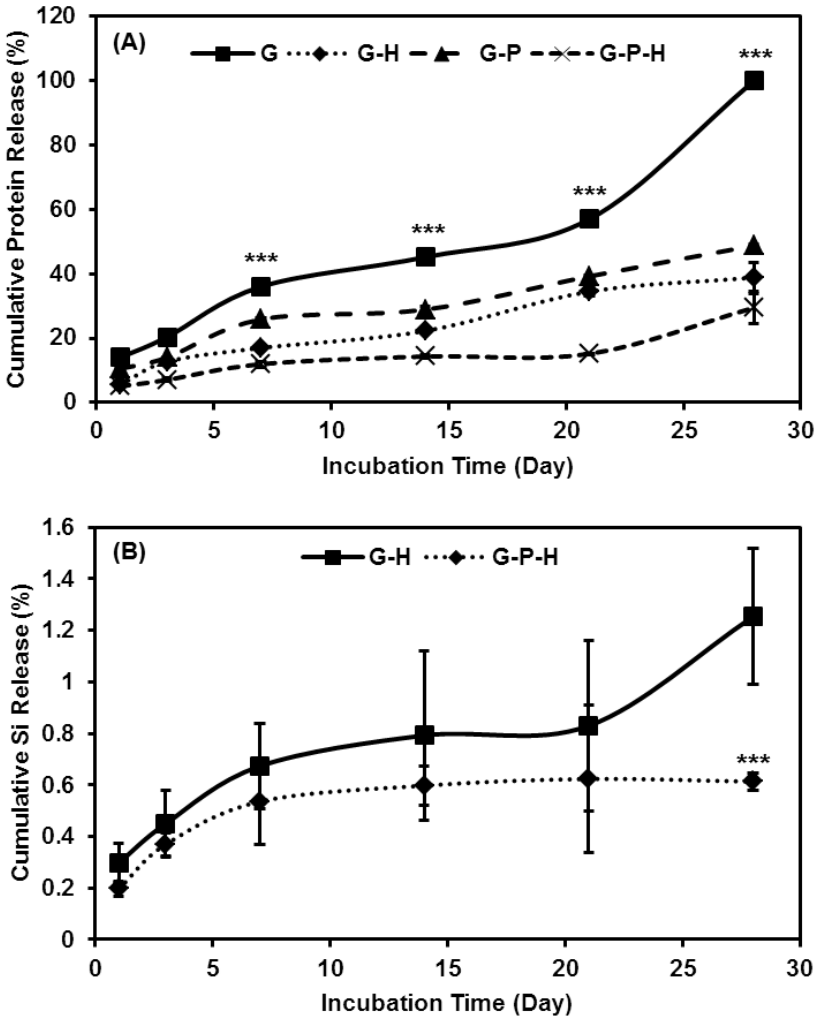


**Figure 6-7 The cumulative protein release (A) and cumulative silicate degradation (B) from different hydrogels. G, P and H represent to GelMA (100 mg/ml), PEGDA (100 mg/ml) and Hybrid (0.5 µl/mg BG), respectively. Data presented in *** represents $p$<0.001.**

## 6.7 *In vitro* Bioactivity of Conjugated Hydrogels

The *in vitro* bioactivity of hybrid hydrogels was assessed upon soaking these hydrogels in SBF media at 37°C. The pure GelMA hydrogel as a control was incubated in the similar condition. The results of SEM-EDS microscopy in Figure 6-8 revealed that no calcium (Ca) or phosphate (P) ions were precipitated on the surface of GelMA hydrogels. However, the results in Figure 6-9 shows the presene of Ca and P ions on the similar position of the surface of hybrid. The calcium phosphate (Ca-P) particles were therefore formed on the surface of hybrid hydrogels. The presence of

silanol functional groups in these hydrogels acted as the nucleation sites and thus enhanced the precipitation of Ca-P particles from SBF solution on their surfaces [504]. The distribution of Ca and P particles on the surface of hybrid hydrogels after 21 days SBF incubation at 37°C is shown in Figure 6-8. Moreover, it was found that the ratio of Ca to P ions in the precipitated particles was increased over time and approached 1.84±0.15 after 21 days incubation in SBF. This ratio was not further increased significantly, and it was close to Ca/P ratio in a typical adult female bone (1.71) [515].

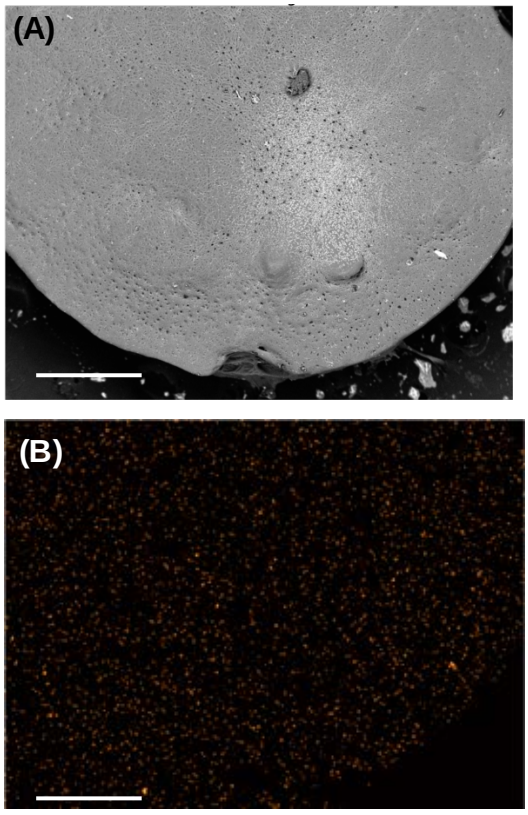


**Figure 6-8 SEM image (A) and the distribution of Ca ions on the surface of GelMA hydrogel after 3 weeks incubation in SBF at 37°C. Scale bar represents 500 µm**

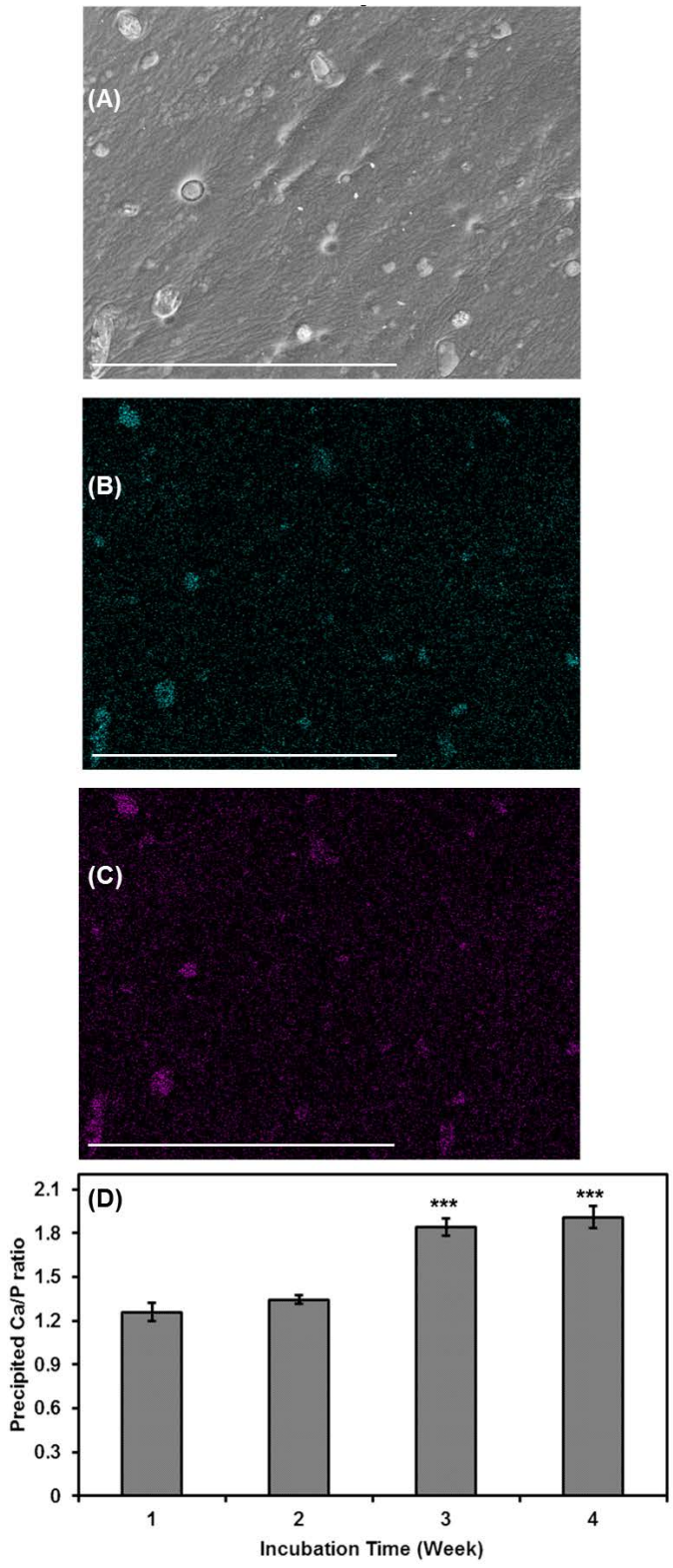


**Figure 6-9 SEM image (A), the distribution of calcium (B) and phosphate (C) particles on the surface of hybrid after 3 weeks incubation in SBF at 37°C, and the ratio of precipitated Ca-P particles on the surface of Fn-GelMA-PEGDA-BG hybrid hydrogels in different time (D). Data presented in *** represented $p<0.001$. Scale bars represent 500 µm.**

## 6.8 *In vitro* Cell Studies

The precipitation of Ca-P particles on the surface of hybrid hydrogels can promote the proliferation of osteoblasts. This hypothesis was studied by comparing the proliferation and alkaline activity of osteoblasts on the surface of pure GelMA and hybrid hydrogels for up to 28 days. The confocal laser scanning microscopy (CLSM) images (Figure 6-10A and B) revealed that the viability of osteoblast cells was significantly improved on the surface of hybrid hydrogels. This enhancement was due to the stiffness improvement of hybrid hydrogels and more importantly the precipitation of Ca-P particles on their surfaces as the two main components of natural bone extra cellular matrix. The CLSM images also revealed that the osteoblast cells diffused within hydrogels. Three-dimensional conversion of CLSM images (Figure 6-10C) showed that the Saos-2 cells lost their vitality upon diffusing within GelMA hydrogels 28-days post-seeding. The viability of the diffused cells within hybrids, however, was remarkably enhanced, and the cells proliferated progressively through these hydrogels (Figure 6-10D). Despite the evaluation of vitality and proliferation of osteoblasts, their phenotype was also examined upon alkaline phosphatase assay (ALP).

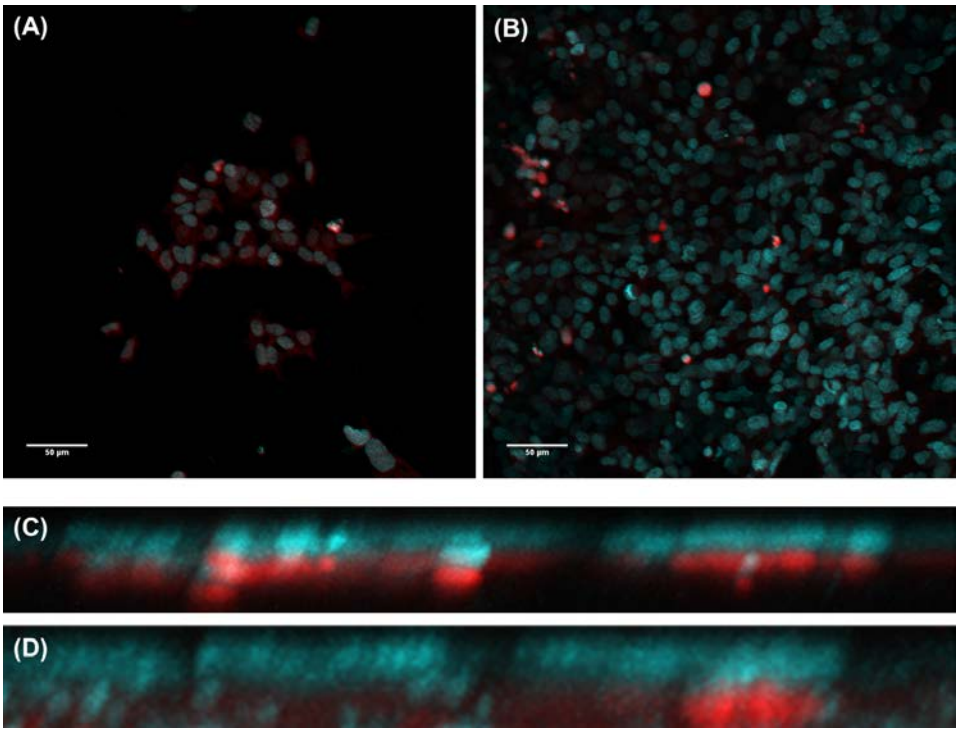


**Figure 6-10 Proliferation of osteoblast cells cultured on the surface of GelMA (A) and hybrid (B) hydrogels after 14 days (scale bar=50 µm) and their diffusion within GelMA (C) and hybrid (D) hydrogels 28-days post-culturing. Cells were stained using PI (red) and DAPI (cyan) and images were analysed using Fiji-ImageJ software.**

The release of ALP from osteoblasts is the well-known assay to assess their osteogenic phenotypes. As shown in Figure 6-11, the ALP activity of the cells on the hybrid GelMA-PEGDA-BG structures was significantly higher than GelMA hydrogels ($p$<0.001). In addition, the cultured cells on the surface of hybrids kept their phenotypes at least for 21 days since their alkaline phosphatase activity was significantly increased over time. This result confirmed that the chemical conjugation of BG imparted osteoconductivity behaviour to the hydrogel structures.

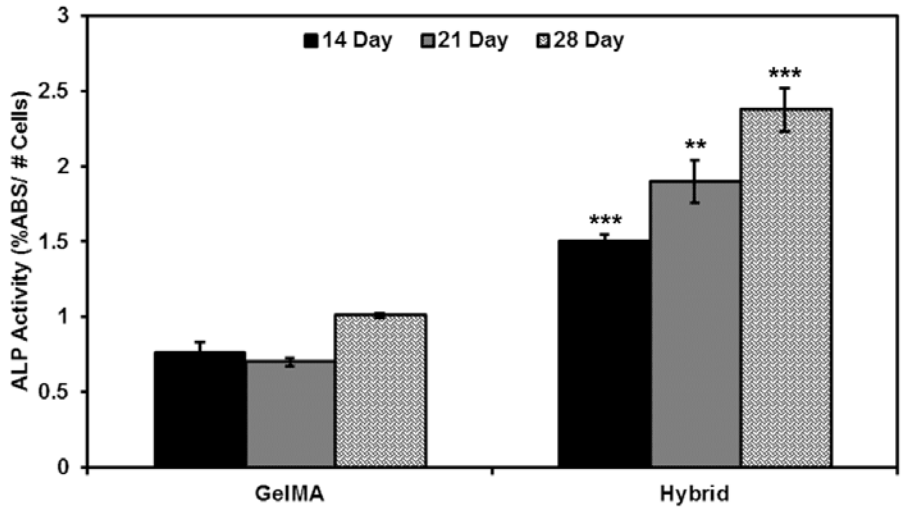


**Figure 6-11 The alkaline phosphatase activity (ALP) of cells cultured on the surface of different hydrogels. Data presented as ** and *** respectively represent $p<0.01$ and $p<0.001$.**

## 6.9 *In vivo* Animal Study

The *in vivo* cytocompatibility, degradation and the biological properties of hybrid hydrogels were studied by using mice-subcutaneous implantation model. These hydrogels were pre-fabricated *in vitro* by photocrosslinking of 100 mg/ml Fn-GelMA with 100 mg/ml PEGDA covalently bonded to 0.5 µl of BG per each milligram of polymer content, in the presence of Irgacure. The surgeries were accomplished in ANZAC Research Institute in Concord Hospital with direct assistance of Dr. Yiwei Wong.

Nine pathogen-free, male mice, aged 6 months were acquired, housed, and studied under a protocol approved by SLHD Animal Welfare Committee in Sydney, Australia (2013/019A). After the surgery, in the period of the test for 4 weeks, the animal behaviour was monitored for signs of pain/distress, restlessness, depression, and lack of appetite. Heart and respiratory rates, body temperature, and their activities were also monitored. The mice maintained their well-being throughout the period of study. All wounds healed favourably by secondary intention and with no scarring. Regular and comfort movements of mice were noticed in the housing facility.

At different time points, up to 4 weeks post-surgery, the hybrid hydrogels were successfully excised. It was found that the explanted hydrogels retained their shapes and structures for more than four weeks. The *in vivo* degradation profile of these hydrogels also confirmed that hybrid formation has a significant impact on their *in vivo* stability. The pure GelMA hydrogel, for instance, lost its integrity after two weeks subcutaneously implantation in mice [516, 517]. The magnetic resonance imaging (MRI) of subcutaneously implanted PEGDA hydrogels, moreover, confirmed that these hydrogels lost more than half of their volume after 25 days implantation [518]. The *in vivo* resorption profile of hybrid hydrogels revealed that their physical stability was significantly enhanced by hybrid formation, which was in agreement with their *in vitro* degradation profile in SBF.

At different time points, the implanted hydrogels were successfully excised and underwent histology analyses. During the slide preparation for H&E staining, however, the hydrogels were washed away due to the prolonged ethanol washing cycles, e.g. 24 hours. Therefore, an empty gap was formed at the implantation site, as shown in Figure 6-12. An inflammatory response towards the hybrid hydrogels was observed during the first two weeks of implantation due to the formation of fibrotic tissues around the hybrids. It was found that the enormous foreign body giant cells (FBGC) were formed around the implanted hydrogels 1 week post-implantation. The extension of FBGCs, however, was significantly decreased up 14 days. This immunogenic response was due to the presence of PEGDA in the hybrid hydrogels since the MRI monitoring has confirmed the poor integration and rapid resorption of this polymer [518]

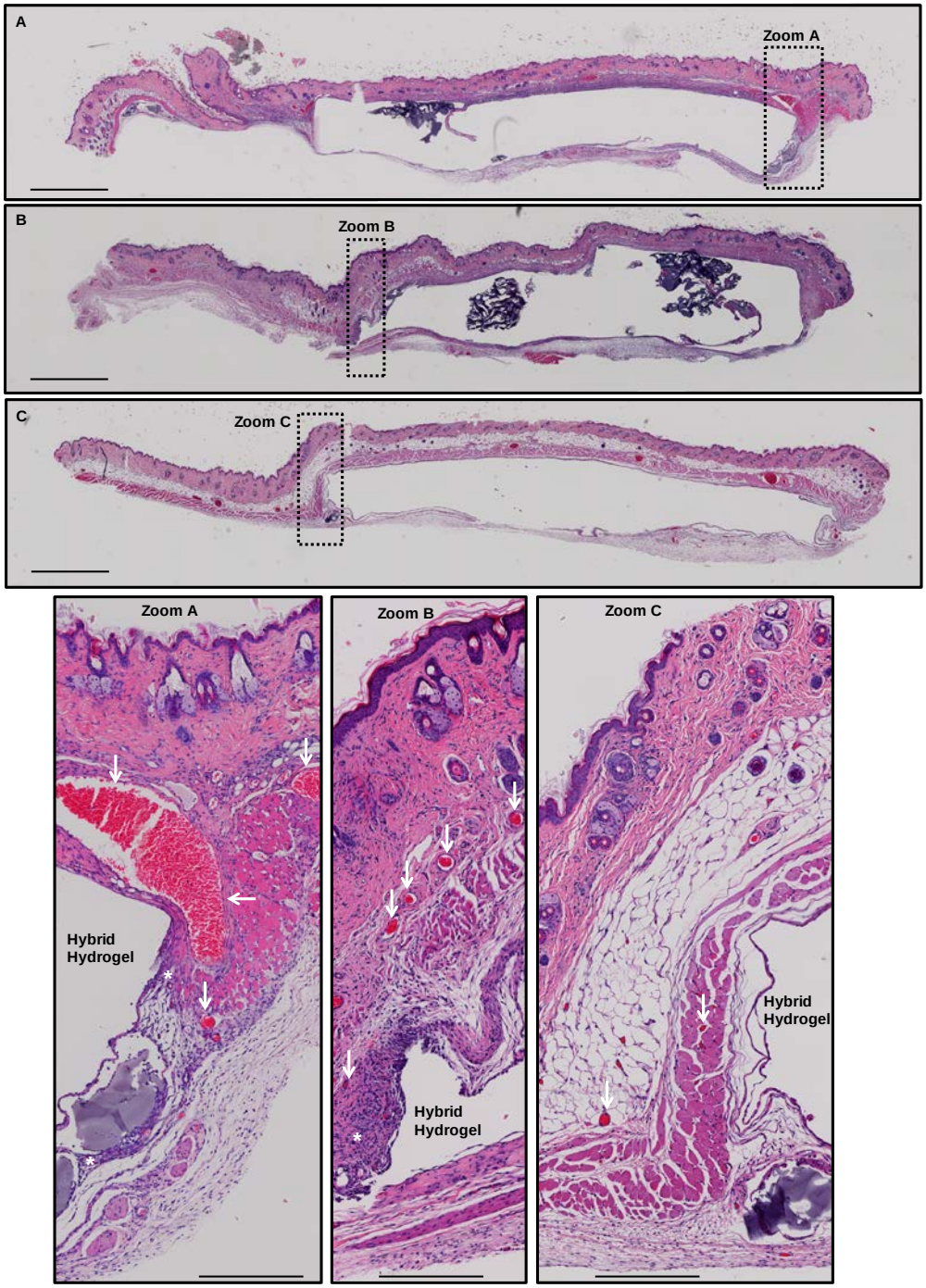


**Figure 6-12 H&E staining of implants after one (A), two (B) and four (C) weeks post-implantation with the scale bar of 100 µm. The progress of fibrotic tissues around the implanted hydrogels after different time points are illustrated in higher magnification (scale bars represent 200 µm). The white arrows and asterisks respectively represent to foreign body giant cells and lamina propria.**

In the period of two to four weeks post-operation, the immune response to the hybrid hydrogels was settled, as the fibrotic tissue around the implanted hydrogel was significantly decreased after 2 weeks. The histological analyses of the implanted hydrogels with their surrounded tissues were shown in Figure 6-12 A-C. In addition, the observed FBGCs was completely diminished after four weeks (the white arrows in Figure 6-12). The presence of lamina propria was another sign of inflammatory within the first couple of weeks post-implantation. These loose connective tissues contain various cell types including fibroblasts, lymphocytes, plasma cells, and macrophages to form the fibrotic tissue around the implanted hydrogels (white asterisks in Figure 6-12). This drop of lamina propria after four weeks implantation revealed that the hybrid hydrogels did not cause chronic inflammation.

One possible explanation for these behaviours is the chain relaxation behaviour of gelatin at physiological condition resulting from coil-to-triple helix conformation changes to promote its biocompatibility [519, 520]. The presence of bioactive glass on these hybrid hydrogels, moreover, have significant impacts on their interfacial reactions with surrounding tissue [330]. The formation of Ca-P particles on the surface of these hybrids, therefore, could promote the formation of ECM and improve the biocompatibility of hydrogels. The *in vivo* results of this study completely confirmed the accuracy of *in vitro* degradation profile of hybrid hydrogels in SBF and their biocompatibility towards different tissues and cell types. In addition to significant impacts of bioactive hybrid hydrogels on proliferation of osteo-progenitor cells and thus bone regeneration, the presence of GelMA in the backbone of these hybrids may promote the proliferation of soft tissues. The interface of soft-to-hard tissues therefore might be mimicked upon the fabrication of bioactive hydrogel with gradient of mineralisation.

## 6.10 Fabrication of Bioactive Hybrid Hydrogel with Gradient of Mineralisation

The shortcomings of current fixation methods for ligament reconstruction are insufficient mechanical stability [521], and the formation of non-

mineralised soft tissue within the bone tunnel [522]. It is critical to developing a new approach to addressing these issues and minimise the risk of failure of current ligament replacement at interface. To this end, a bioactive hydrogel with gradient of mineralisation was fabricated from GelMA that was covalently bonded with bioactive glass to mimic the structure of ligament interface. The optimum concentrations of GelMA, PEGDA, and BG were used to embed a silk fabric, as a ligament reconstruction graft, within the resulting scaffold. The physical integrity of these structures was tested for the ligament-to-bone interface tissue engineering.

### 6.10.1 Fabrication of Bioactive Hybrid Hydrogel with Gradient of Mineralisation

A bioactive hydrogel with gradient of mineralisation was fabricated that composed of three regions. This gradient hydrogel was fabricated in a custom-made mould that consisted of a removable slab made from poly(dimethyl siloxane) (PDMS). As shown in Figure 6-13, the slab was firstly inserted in the middle of the mould to form two distinct zones. In each run 1 mg/ml Irgacure was added as a photoinitiator for the fabrication of GelMA-PEGDA-BG hydrogel network. Different colour dyes were used for separate parts to demonstrate the integration of different regions. As shown in Figure 6-13, after filling the solution at two end parts, the mould was kept at -20°C to form physically crosslinked hydrogels. The PDMS slab was then removed from the mould, and the hybrid solution of GelMA-BG was poured between the physically crosslinked hydrogels at room temperature. The mould was then transferred under UV light to form a bioactive scaffold with gradient of mineralisation.

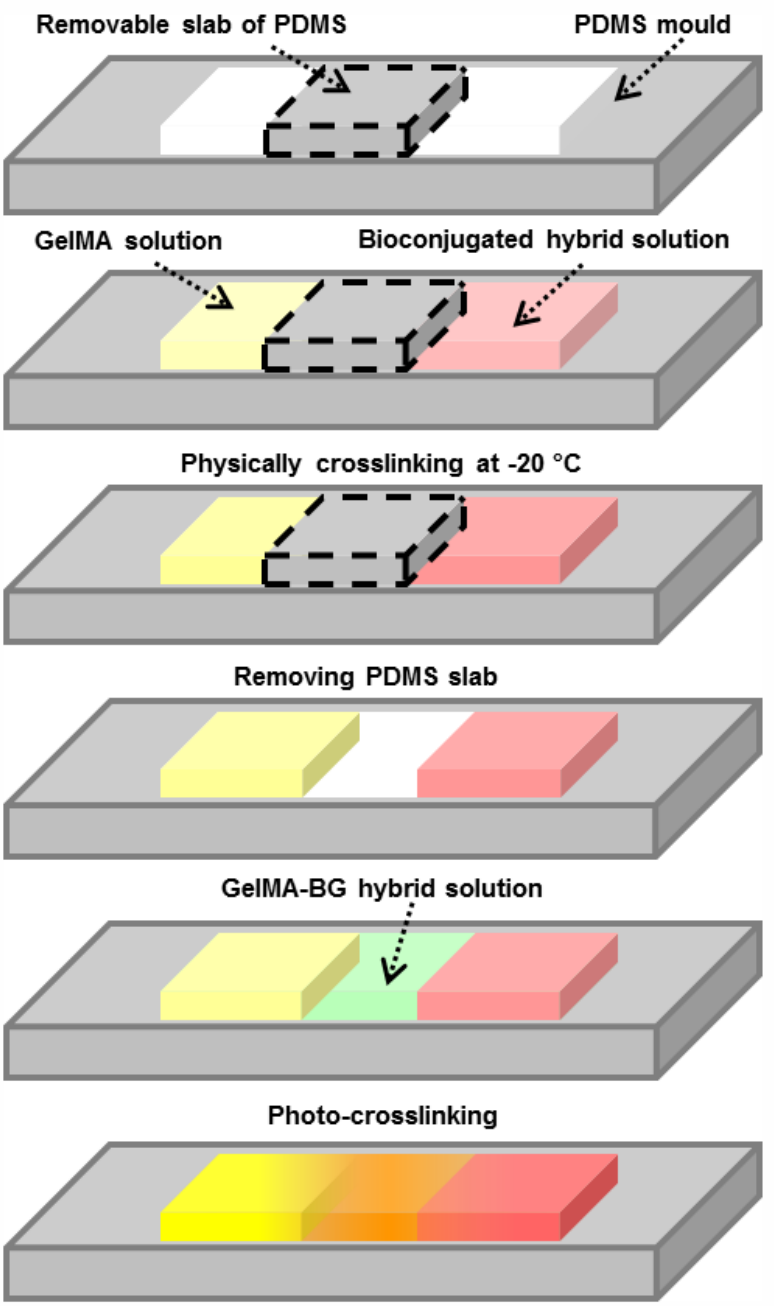


**Figure 6-13 The procedure for fabrication of bioactive scaffold with gradient of mineralisation**

The bioactive hydrogel with gradient of mineralisation was fabricated from the optimum concentrations of GelMA, PEGDA, and BG. As shown in Figure 6-14A, these materials were fully integrated within their boundaries and formed a unique structure with a gradient of chemical composition. The physical integrity of this bioactive hydrogel was qualitatively evaluated under different mechanical loads. As shown in Figure 6-14B, the gradient

hydrogel could withstand under bending loads without any deformation. The effect of elongation on the physical integrity of the gradient hydrogel was also examined. To this end, the hydrogels were fixed within the pneumatic grips and underwent tensile load with a rate of 0.05 mm/min in the hydrated state at 37°C. As shown in Figure 6-14C, the gradient hydrogel did not lose its physical integrity from its boundaries under the elongation loads.

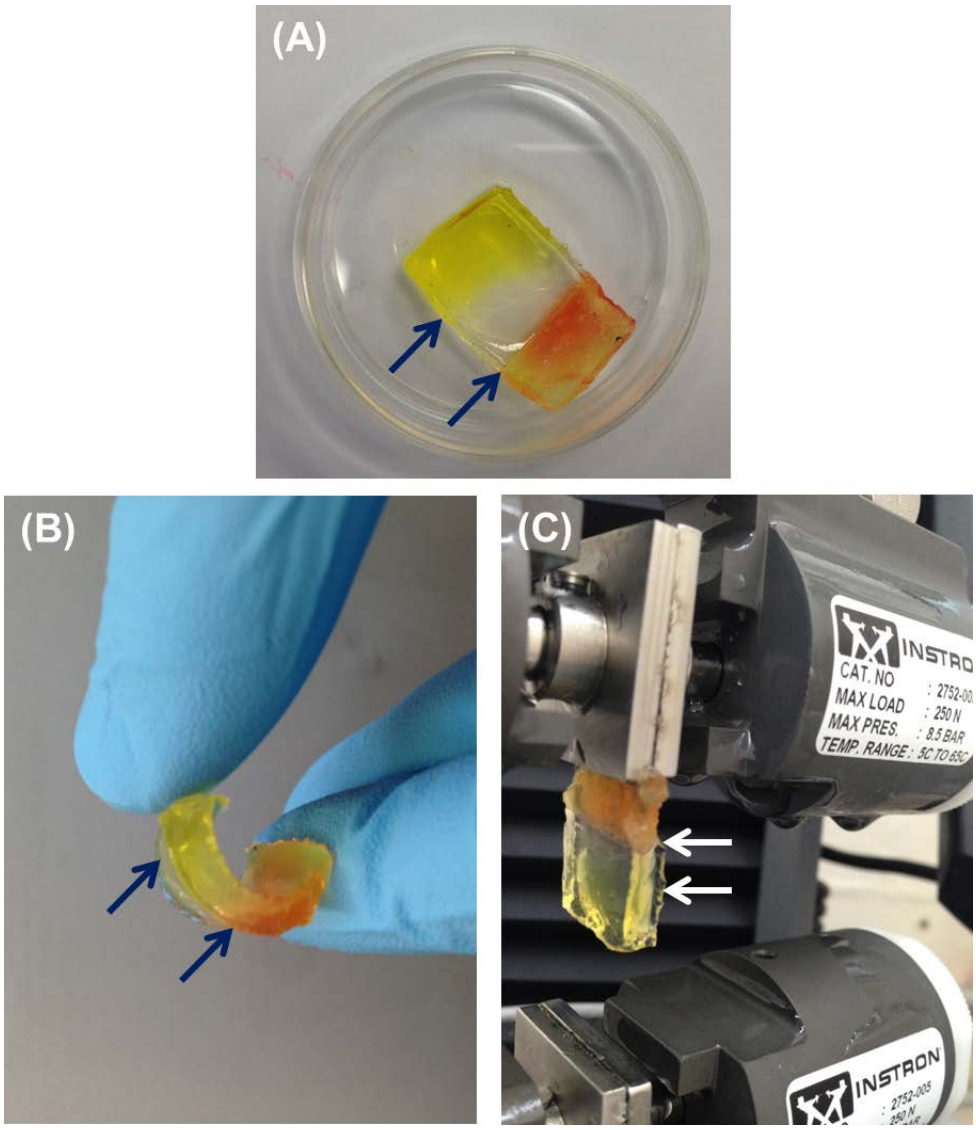


**Figure 6-14 The fabricated bioactive scaffold with a gradient of mineralisation (A) and its physical integrity under bending (B) and elongating loads (C). Arrows indicate the integration of hydrogels in their boundaries.**

The formation of bioactive hydrogel with gradient of mineralisation mimicked the chemical composition of ligament-to-bone interface. A reconstructive graft, moreover, needs to be fully integrated within the gradient hydrogel to resemble the chemical composition and mechanical performance of ligament tissue. Therefore, silk fabric as a ligament reconstruction graft was embedded within the gradient hydrogel and its physical integrity was qualified.

### 6.10.2 Fabrication of Gradient Hybrid Hydrogel Embedded with Silk Fabric

A gradient hydrogel embedded with silk fabric was fabricated based on the approach shown in Figure 6-13 with some modifications. The bioactive hydrogel with gradient of bioactive glass component was fabricated by transferring the mould to -20°C instead of photocrosslinking. The silk fabric was then settled on the top of physically crosslinked hydrogel and embedded with the secondary mould. The secondary layer of the gradient hydrogel was fabricated in the same method as shown in Figure 6-13. This complex was then transferred under UV light to form a gradient hydrogel embedded with silk fabric.

The integrity of silk fabric within the gradient hydrogel was investigated by using SEM-EDS. The white arrows in Figure 6-15A indicated the presence of silk fabric in the gradient hydrogels. The monitoring of the silicon distribution in this construct, moreover, confirmed the successful integration of the electrospun film within the hydrogel. The dash-lines in Figure 6-15B showed the boarders of silk-tropoelastin fabric within the hydrogels, as no silica has been detected in this region.

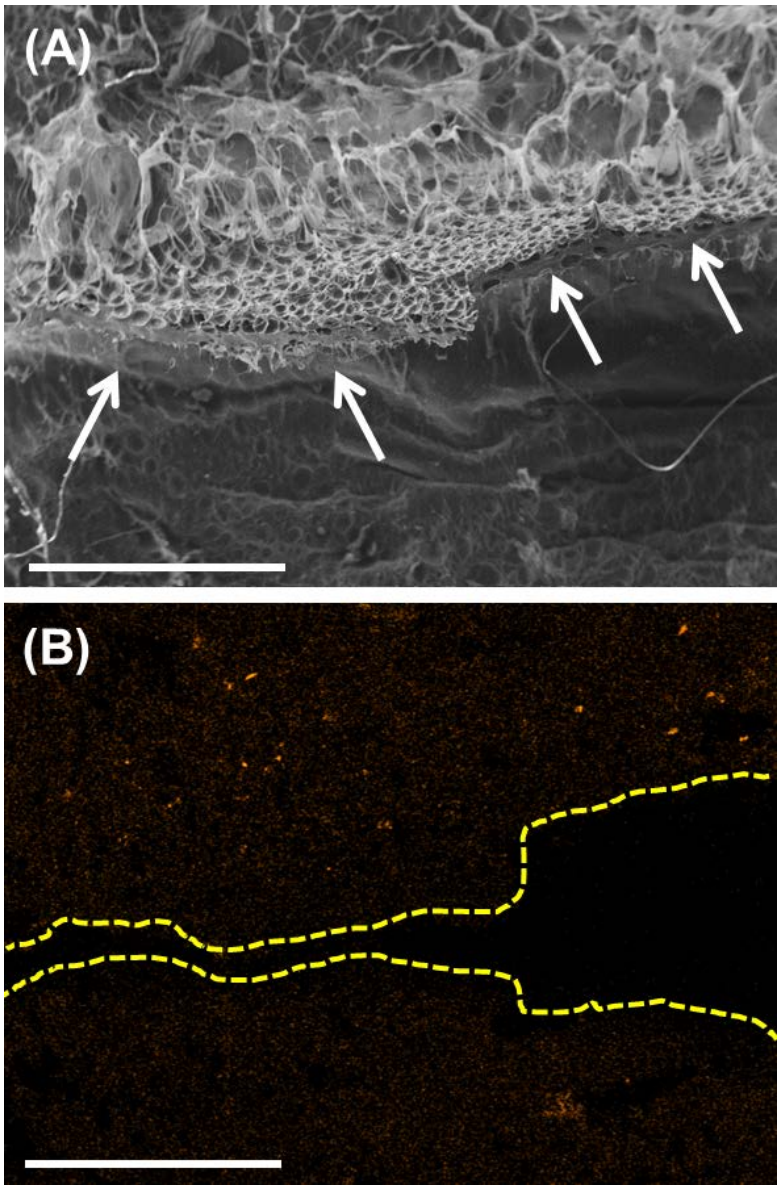


**Figure 6-15 SEM image (A) and the distribution of silicon (B) on the surface of the gradient hydrogel embedded with silk fabric. White arrows indicate to the electrospun film. Dash-lines in (B) represent to the boarders of silk fabric. Scale bars represent 1mm.**

## 6.11 Summary

In this chapter, the feasibility of secondary crosslinking agent for enhancing the mechanical properties and degradation profile of hydrogels was examined. The favourable polymer for bioconjugation with hybrid hydrogel was PEGDA. The inert nature of this photocrosslinkable polymer and its high solubility in water led to the formation of bioconjugated hybrid hydrogel with tuneable mechanical strength and degradation profile. This polymer, moreover, did not interfere with organosilation and hybridisation of GelMA.

The concentration of PEGDA was also optimised to acquire a hydrogel with enhanced mechanical stability and physical integrity over time compared to the covalently bonded GelMA-BG hybrid. The hydrogels fabricated from 100 mg/ml Fn-GelMA, 100 mg/ml PEGDA and 0.5 µl TEOS solution per each milligram of the organic component had superior properties. The *in vitro* bioactivity and biological properties as well as *in vivo* biocompatibility and degradation profile of bioconjugated hybrid hydrogels were also examined. The precipitation of Ca-P particles on the surface of these hybrids enhanced the *in vitro* proliferation of osteoblasts and the secretion of bone-specific enzymes.

The *in vivo* mice-subcutaneous implantation, moreover, confirmed the biocompatibility and bio-resorption of these hydrogels for bone tissue engineering. The feasible application of these hybrid hydrogels for interface tissue engineering was also investigated. The bioactive hydrogel with a gradient of mineralisation was fabricated from GelMA that was covalently bonded with bioactive glass. This gradient hydrogel could withstand the elongation loads without any deformation. These results demonstrated the potential of bioconjugated hybrid hydrogels for bone repair and engineering its interface with soft tissues.

# Chapter 7. Conclusions and Recommendations

## 7.1 Conclusions

The organic-inorganic hybrids fabricated by the sol-gel method are intrinsic bioactive materials with extensive applications in bone tissue engineering. The brittleness and limited water uptake capacity of these monoliths, however, restrict their applications for the interface of soft and hard tissues. The aim of this study was to develop a unique structure for reconstruction of bone structure and its interface with soft tissues. To this end, a new class of polymer-inorganic hybrid was developed in which polymer crosslinking ceased the over-condensation of a bioactive glass component and eradicated the formation of brittle structure.

The feasibility of this approach was confirmed by formation of covalently bonded hybrid hydrogels of gelatin and BG upon the combination of sol-gel method, organosilation process, and polymer-crosslinking. To this end, GelMA was functionalised with GPTMS for chemical bonding to BG through sol-gel method. This organosilation reaction and hybrid formation did not interfere with crosslinking of the polymer phase. Prior to the complete condensation of BG, GelMA sessions were photocrosslinked to eradicate the formation of brittle structures. The formation of these hybrid hydrogels was governed by the external stimuli such as temperature and the isoelectric point of polymer and BG, the chemical structure of organosilane coupling agent, and the concentration of the inorganic component. The physicochemical properties and mechanical strength of these hybrid hydrogels were then tuned by the incorporation of secondary crosslinking agents such as PEGDA. The resulting biodegradable hydrogels displayed elastic properties with ultimate elastic compression strain above 0.2 (mm/mm). Furthermore, the compression modulus of these hydrogels was tuned in the range of 42-530 kPa while they demonstrated the minimum swelling ratio of 400 %, which is still acceptable for tissue engineering applications.

The regulation of mechanical properties and degradation profile is a key factor for *in vivo* performance of hydrogels in tissue engineering applications. The hybrid hydrogels were therefore incubated in simulated

body fluid to evaluate their *in vitro* degradation profiles, as well as their mechanical properties over time. The optimum hybrid hydrogel comprised from 100 mg/ml Fn-GelMA, 100 mg/ml PEGDA and hybridised with 0.5 µl of bioactive glass solution per each milligram of polymer content. This hybrid hydrogel kept its structure 28 days post-incubation and displayed elastic properties. The presence of homogeneously distributed bioactive glass in these hydrogels, moreover, promoted the precipitation of calcium phosphate particles as the main inorganic compositions of the bone extracellular matrix. The continuous increase of alkaline phosphatase activity of bone progenitor cells for at least 28 days *in vitro* cell culturing confirmed the osteoconductive properties of these hybrid hydrogels. The *in vivo* mice-subcutaneous implantation, moreover, confirmed the biocompatibility and bio-resorption of these hydrogels. These biological behaviours showed the potential of hybrid hydrogels for the regeneration of bone fractures.

The chemical composition of ligament-to-bone interface was mimicked upon the fabrication of GelMA-based hydrogel with a gradient of covalently bonded bioactive glasses. This gradient hydrogel could withstand the elongation loads without any deformation. The feasibility of integration of a constructive graft was also evaluated by embedding a silk fabric within this gradient hydrogel. The results of this study confirmed that this bioactive scaffold had a great potential to engineer the interface of bone and soft tissues.

## 7.2 Recommendations

The main scope of this study was to develop a new approach to fabricating a non-brittle structure with a homogeneous distribution of inorganic compounds for regenerating the bone and its interface with soft tissues. The outcomes of this study broaden the application of organic-inorganic hybrids by controlling the over-condensation of the silica network *via* polymer crosslinking. This new class of hydrogels displayed tuneable physicochemical characteristics with superior structural integrity and remarkable bioactivity, cytocompatibility and bio-resorption properties.

The presence of photocrosslinkable polymer in this approach presents a great potential of these bioactive hybrids for *in situ* tissue engineering. The progenitor cells may suspend into a solution of organic-inorganic hybrid to form an injectable, cell-encapsulated hydrogel. Series of *in vitro* and *in vivo* studies need to be conducted to confirm the feasibility of cell-encapsulation with these hydrogels and their potential to maintain the metabolic activity for dental applications.

The solubility of these materials provides a huge potential for fabrication of hybrid hydrogels *via* 3D printing and stereolithography. The presence of the inorganic compound may promote the angiogenic behaviour of the hydrogels. The biological motifs, therefore, can be encapsulated within the organic-inorganic hybrids to form a 3D hydrogel with predetermined topography. Series of *in vitro* studies need to be conducted to confirm the angiogenicity of these hydrogels and their potential to maintain the metabolic activity and to support the proliferation cells.

The presence of a semi-conductive material (silica) in the hybrids may promote the electro-conductivity of these hydrogels. This class of hydrogels, therefore, is deemed to have a potential for nerve tissue engineering. Series of *in vitro* studies need to be conducted to confirm the feasibility of delivering neural stem cells with these hydrogels and their potential to maintain the metabolic activity and to support the proliferation cells.

These gelatin-bioactive glass hybrid hydrogels can be used for mimicking the bone structure and its interface with soft tissues. However, further studies should be conducted to assess the potential of hybrid hydrogels for interface tissue engineering, systematically:

- Co-culturing of ligament and bone progenitor cells on the gradient hydrogels. The potential of gradient hydrogels for mimicking the cellular constitution of ligament-to-bone interface needs to be fully assessed by simultaneous cultivation of fibroblast and osteoblast cells on the surface of gradient hydrogels to regenerate ligament and

bone sides, respectively. The cell proliferation and also migration of these progenitor cells on the gradient hydrogels need to be evaluated systematically.

- Encapsulating of mesenchymal stem cells in gradient hydrogels in the presence of biological motifs. The feasibility of cell encapsulation within GelMA-based hydrogels has been confirmed and thus the hydrogels with a gradient of mineralisation may display a high potential for differentiation of MSC cells to form a gradient of the cellular constitution. The presence of biological motifs such as growth factor, moreover, significantly promoted the proliferation of MSC cells. An engineered ligament-to-bone interface with a gradient of chemical composition and cellular constitution, therefore, can be fabricated upon the encapsulation of MSC cells in the presence of growth factors.
- Pilot *in vivo* animal studies on the potential of hybrid hydrogels for the regeneration of bone defects. The osteogenic properties of hybrid hydrogels have been confirmed and thus, gradient hydrogels may display a high potential for the regeneration of bone. Pig ligament-to-bone defect can be used to promote the migration of progenitor cells from bone marrow to the defected site and regeneration of ligament enthesis.

# References

[1] Salgado AJ, Coutinho OP, Reis RL. Bone tissue engineering: state of the art and future trends. Macromol Biosci. 2004;4:743-65.
[2] Sommerfeldt D, Rubin C. Biology of bone and how it orchestrates the form and function of the skeleton. European Spine Journal. 2001;10:S86-S95.
[3] Finkemeier CG. Bone-Grafting and Bone-Graft Substitutes. The Journal of Bone & Joint Surgery. 2002;84:454-64.
[4] Nandi SK, Roy S, Mukherjee P, Kundu B, De DK, Basu D. Orthopaedic applications of bone graft & graft substitutes: A review. Indian J Med Res. 2010;132:15-30.
[5] Rahaman MN, Day DE, Sonny Bal B, Fu Q, Jung SB, Bonewald LF, et al. Bioactive glass in tissue engineering. Acta Biomaterialia. 2011;7:2355-73.
[6] Wang C, Lin K, Chang J, Sun J. Osteogenesis and angiogenesis induced by porous β-CaSiO3/PDLGA composite scaffold via activation of AMPK/ERK1/2 and PI3K/Akt pathways. Biomaterials. 2013;34:64-77.
[7] Fei L, Wang C, Xue Y, Lin K, Chang J, Sun J. Osteogenic differentiation of osteoblasts induced by calcium silicate and calcium silicate/β-tricalcium phosphate composite bioceramics. Journal of Biomedical Materials Research - Part B Applied Biomaterials. 2012;100 B:1237-44.
[8] Gorustovich AA, Roether JA, Boccaccini AR. Effect of bioactive glasses on angiogenesis: a review of in vitro and in vivo evidences. Tissue engineering Part B, Reviews. 2010;16:199-207.
[9] Gerhardt L-C, Widdows KL, Erol MM, Burch CW, Sanz-Herrera JA, Ochoa I, et al. The pro-angiogenic properties of multi-functional bioactive glass composite scaffolds. Biomaterials. 2011;32:4096-108.
[10] Li H, Chang J. Stimulation of proangiogenesis by calcium silicate bioactive ceramic. Acta Biomaterialia. 2013;9:5379-89.

[11] Zhai W, Lu H, Chen L, Lin X, Huang Y, Dai K, et al. Silicate bioceramics induce angiogenesis during bone regeneration. Acta Biomaterialia. 2012;8:341-9.
[12] Li H, Xue K, Kong N, Liu K, Chang J. Silicate bioceramics enhanced vascularization and osteogenesis through stimulating interactions between endothelia cells and bone marrow stromal cells. Biomaterials. 2014;35:3803-18.
[13] Li H, Chang J. Bioactive silicate materials stimulate angiogenesis in fibroblast and endothelial cell co-culture system through paracrine effect. Acta Biomaterialia. 2013;9:6981-91.
[14] Hench LL. Bioactive Glass: Chronology, Characterization, and Genetic Control of Tissue Regeneration. In: Ben-Nissan B, editor. Advances in Calcium Phosphate Biomaterials. Berlin: Springer; 2014.
[15] Mammeri F, Bourhis EL, Rozes L, Sanchez C. Mechanical properties of hybrid organic-inorganic materials. Journal of Materials Chemistry. 2005;15:3787-811.
[16] Arcos D, Vallet-Regí M. Sol-gel silica-based biomaterials and bone tissue regeneration. Acta Biomaterialia. 2010;6:2874-88.
[17] Miguez-Pacheco V, Hench LL, Boccaccini AR. Bioactive glasses beyond bone and teeth: Emerging applications in contact with soft tissues. Acta Biomaterialia. 2015;13:1-15.
[18] Ciriminna R, Fidalgo A, Pandarus V, Béland F, Ilharco LM, Pagliaro M. The Sol–Gel Route to Advanced Silica-Based Materials and Recent Applications. Chemical Reviews. 2013;113:6592-620.
[19] Singh LP, Bhattacharyya SK, Kumar R, Mishra G, Sharma U, Singh G, et al. Sol-Gel processing of silica nanoparticles and their applications. Advances in Colloid and Interface Science. 2014;214:17-37.
[20] Salinas AJ, Vallet-Regí M. Bioactive ceramics: From bone grafts to tissue engineering. RSC Advances. 2013;3:11116-31.
[21] Kawai K, Larson BJ, Ishise H, Carre AL, Nishimoto S, Longaker M, et al. Calcium-Based Nanoparticles Accelerate Skin Wound Healing. PLoS ONE. 2011;6:e27106.
[22] Hench LL, Greenspan D. Interactions between bioactive glass and collagen: A review and new perspectives. Journal of the Australian Ceramic Society. 2013;49:1-40.
[23] Lynn AK, Yannas IV, Bonfield W. Antigenicity and immunogenicity of collagen. Journal of Biomedical Materials Research Part B: Applied Biomaterials. 2004;71B:343-54.
[24] Yazdimamaghani M, Vashaee D, Assefa S, Walker KJ, Madihally SV, Köhler GA, et al. Hybrid macroporous gelatin/bioactive-glass/nanosilver scaffolds with controlled degradation behavior and antimicrobial activity for bone tissue engineering. Journal of Biomedical Nanotechnology. 2014;10:911-31.
[25] Sachot N, Engel E, Castaño O. Hybrid Organic-Inorganic Scaffolding Biomaterials for Regenerative Therapies. Curr Org Chem. 2014;18:2299-314.
[26] Ravichandran R, Sundaramurthi D, Gandhi S, Sethuraman S, Krishnan UM. Bioinspired hybrid mesoporous silica–gelatin sandwich construct for

bone tissue engineering. Microporous and Mesoporous Materials. 2014;187:53-62.
[27] Munoz-Pinto DJ, McMahon RE, Kanzelberger MA, Jimenez-Vergara AC, Grunlan MA, Hahn MS. Inorganic-organic hybrid scaffolds for osteochondral regeneration. Journal of Biomedical Materials Research - Part A. 2010;94:112-21.
[28] Yuki Shirosaki, Akiyoshi Osaka, Kanji Tsuru, Hayakawa S. Inorganic-Organic Sol-Gel Hybrids. In: Julian R. Jones, Clare AG, editors. Bio-Glasses: An Introduction. First ed: John Wiely & Sons; 2012. p. 139-58.
[29] Valliant EM, Jones JR. Softening bioactive glass for bone regeneration: Sol-gel hybrid materials. Soft Matter. 2011;7:5083-95.
[30] Lin M, Xu P, Zhong W. Preparation, characterization, and release behavior of aspirin-loaded poly(2-hydroxyethyl acrylate)/silica hydrogels. Journal of Biomedical Materials Research - Part B Applied Biomaterials. 2012;100 B:1114-20.
[31] Survey AH. 4324.0.55.001 - Microdata: Australian Health Survey, National Health Survey, 2011-12. 2014.
[32] Khan SN, Cammisa FP, Sandhu HS, Diwan AD, Girardi FP, Lane JM. The Biology of Bone Grafting. Journal of the American Academy of Orthopaedic Surgeons. 2005;13:77-86.
[33] Laurencin C, Khan Y, El-Amin SF. Bone graft substitutes. Expert Review of Medical Devices. 2006;3:49-57.
[34] Moore WR, Graves SE, Bain GI. Synthetic bone graft substitutes. ANZ Journal of Surgery. 2001;71:354-61.
[35] Dimitriou R, Jones E, McGonagle D, Giannoudis PV. Bone regeneration: Current concepts and future directions. BMC Med. 2011;9.
[36] Siddiqui NA, Owen JM. Clinical advances in bone regeneration. Current Stem Cell Research and Therapy. 2013;8:192-200.
[37] Bates P, Ramachandran M. Bone injury, healing and grafting. In: Ramachandran M, editor. Orthopaedic Sciences The Stanmore Guide. London: Hodder Arnold; 2007. p. 123-34.
[38] Calvi LM, Adams GB, Weibrecht KW, Weber JM, Olson DP, Knight MC, et al. Osteoblastic cells regulate the haematopoietic stem cell niche. Nature. 2003;425:841-6.
[39] Li Z, Kong K, Qi W. Osteoclast and its roles in calcium metabolism and bone development and remodeling. Biochemical and Biophysical Research Communications. 2006;343:345-50.
[40] Alford AI, Hankenson KD. Matricellular proteins: Extracellular modulators of bone development, remodeling, and regeneration. Bone. 2006;38:749-57.
[41] Pittenger MF, Flake AM, Deans RJ. Stem Cell Culture: Meshenchymal Stem Cells from Bone Marrow. In: Atala A, Lanza RP, editors. Methods of Tissue Engineering. San Diego: Academic Press; 2002. p. 461-9.
[42] Caplan AI. Mesenchymal stem cells. Journal of Orthopaedic Research. 1991;9:641-50.
[43] Knothe Tate ML. "Whither flows the fluid in bone?" An osteocyte's perspective. Journal of Biomechanics. 2003;36:1409-24.

[44] Wan C, He Q, Li G. Osteoclastogenesis in the nonadherent cell population of human bone marrow is inhibited by rhBMP-2 alone or together with rhVEGF. Journal of Orthopaedic Research. 2006;24:29-36.
[45] Baroli B. From natural bone grafts to tissue engineering therapeutics: Brainstorming on pharmaceutical formulative requirements and challenges. Journal of Pharmaceutical Sciences. 2009;98:1317-75.
[46] Pina S, Oliveira JM, Reis RL. Natural-based nanocomposites for bone tissue engineering and regenerative medicine: A review. Advanced Materials. 2015;27:1143-69.
[47] Marie PJ, Ammann P, Boivin G, Rey C. Mechanisms of Action and Therapeutic Potential of Strontium in Bone. Calcif Tissue Int. 2001;69:121-9.
[48] O'Dell BL. Zinc Plays Both Structural and Catalytic Roles in Metalloproteins. Nutr Rev. 1992;50:48-50.
[49] Wiesmann H-P, Plate U, Zierold K, Höhling HJ. Potassium is Involved in Apatite Biomineralization. Journal of Dental Research. 1998;77:1654-7.
[50] Ginty F, Flynn A, Cashman KD. The effect of dietary sodium intake on biochemical markers of bone metabolism in young women. Br J Nutr. 1998;79:343-50.
[51] Schlesinger PH, Blair HC, Teitelbaum SL, Edwards JC. Characterization of the Osteoclast Ruffled Border Chloride Channel and Its Role in Bone Resorption. Journal of Biological Chemistry. 1997;272:18636-43.
[52] Burg KJL, Porter S, Kellam JF. Biomaterial developments for bone tissue engineering. Biomaterials. 2000;21:2347-59.
[53] Sen MK, Miclau T. Autologous iliac crest bone graft: Should it still be the gold standard for treating nonunions? Injury. 2007;38:S75-S80.
[54] Amini AR, Laurencin CT, Nukavarapu SP. Bone tissue engineering: Recent advances and challenges. Crit Rev Biomed Eng. 2012;40:363-408.
[55] Faldini C, Traina F, Perna F, Borghi R, Nanni M, Chehrassan M. Surgical treatment of aseptic forearm nonunion with plate and opposite bone graft strut. Autograft or allograft? International Orthopaedics. 2015.
[56] Houdek MT, Wagner ER, Stans AA, Shin AY, Bishop AT, Sim FH, et al. What Is the Outcome of Allograft and Intramedullary Free Fibula (Capanna Technique) in Pediatric and Adolescent Patients With Bone Tumors? Clinical Orthopaedics and Related Research. 2015.
[57] Hernigou P. Bone transplantation and tissue engineering, part III: allografts, bone grafting and bone banking in the twentieth century. International Orthopaedics. 2015.
[58] Shibuya N, Jupiter DC. Bone Graft Substitute: Allograft and Xenograft. Clinics in Podiatric Medicine and Surgery. 2015;32:21-34.
[59] Pederson WC, Person DW. Long Bone Reconstruction with Vascularized Bone Grafts. Orthopedic Clinics of North America. 2007;38:23-35.
[60] Korompilias AV, Beris AE, Lykissas MG, Kostas-Agnantis IP, Soucacos PN. Femoral head osteonecrosis: Why choose free vascularized fibula grafting. Microsurgery. 2011;31:223-8.
[61] Altman GH, Horan RL, Martin I, Farhadi J, Stark PRH, Volloch V, et al. Cell differentiation by mechanical stress. The FASEB Journal. 2001.

[62] Palsson BQ, Bhatia SN. Tissue Engineering. San Diego: Pearson Prentic Hall; 2004.
[63] Vacanti JP. Tissue engineering and the road to whole organs. British Journal of Surgery. 2012;99:451-3.
[64] Shieh SJ, Vacanti JP. State-of-the-art tissue engineering: From tissue engineering to organ building. Surgery. 2005;137:1-7.
[65] Ferreira LS, Gerecht S, Fuller J, Shieh HF, Vunjak-Novakovic G, Langer R. Bioactive hydrogel scaffolds for controllable vascular differentiation of human embryonic stem cells. Biomaterials. 2007;28:2706-17.
[66] Itälä AI, Ylänen HO, Ekholm C, Karlsson KH, Aro HT. Pore diameter of more than 100 μm is not requisite for bone ingrowth in rabbits. Journal of Biomedical Materials Research. 2001;58:679-83.
[67] Nemati Hayati A, Hosseinalipour SM, Rezaie HR, Shokrgozar MA. Characterization of poly(3-hydroxybutyrate)/nano-hydroxyapatite composite scaffolds fabricated without the use of organic solvents for bone tissue engineering applications. Materials Science and Engineering: C. 2012;32:416-22.
[68] Liu C, Han Z, Czernuszka JT. Gradient collagen/nanohydroxyapatite composite scaffold: Development and characterization. Acta Biomaterialia. 2009;5:661-9.
[69] Chatterjea A, Meijer G, van Blitterswijk C, de Boer J. Clinical Application of Human Mesenchymal Stromal Cells for Bone Tissue Engineering. Stem Cells International. 2010;2010:12.
[70] Xiao Y, Qian H, Young WG, Bartold PM. Tissue Engineering for Bone Regeneration Using Differentiated Alveolar Bone Cells in Collagen Scaffolds. Tissue Engineering. 2003;9:1167-77.
[71] Seyednejad H, Gawlitta D, Dhert WJA, Van Nostrum CF, Vermonden T, Hennink WE. Preparation and characterization of a three-dimensional printed scaffold based on a functionalized polyester for bone tissue engineering applications. Acta Biomaterialia. 2011;7:1999-2006.
[72] Smith IO, Liu XH, Smith LA, Ma PX. Nanostructured polymer scaffolds for tissue engineering and regenerative medicine. Wiley Interdiscip Rev: Nanomed Nanobiotechnol FIELD Full Journal Title:Wiley Interdisciplinary Reviews: Nanomedicine and Nanobiotechnology. 2009;1:226-36.
[73] Gentile P, Chiono V, Tonda-Turo C, Mattu C, Baino F, Vitale-Brovarone C, et al. Bioresorbable glass effect on the physico-chemical properties of bilayered scaffolds for osteochondral regeneration. Materials Letters. 2012;89:74-6.
[74] Padmanabhan SK, Carrozzo M, Gervaso F, Scalera F, Sannino A, Licciulli A. Mechanical performance and in vitro studies of hydroxyapatite/wollastonite scaffold for bone tissue engineering. Key Eng Mater. 2012;493-494:855-60.
[75] Martin RA, Yue S, Hanna JV, Lee PD, Newport RJ, Smith ME, et al. Characterizing the hierarchical structures of bioactive sol–gel silicate glass and hybrid scaffolds for bone regeneration. Philosophical Transactions of the Royal Society A: Mathematical, Physical and Engineering Sciences. 2012;370:1422-43.

[76] Shao R, Quan R, Zhang L, Wei X, Yang D, Xie S. Porous hydroxyapatite bioceramics in bone tissue engineering: Current uses and perspectives. Nippon Seramikkusu Kyokai Gakujutsu Ronbunshi/Journal of the Ceramic Society of Japan. 2015;123:17-20.
[77] Venkatesan J, Bhatnagar I, Manivasagan P, Kang KH, Kim SK. Alginate composites for bone tissue engineering: A review. International Journal of Biological Macromolecules. 2015;72:269-81.
[78] Li X, He J, Bian W, Li Z, Li D, Snedeker JG. A novel silk-TCP-PEEK construct for anterior cruciate ligament reconstruction: An off-the shelf alternative to a bone-tendon-bone autograft. Biofabrication. 2014;6.
[79] Slaughter BV, Khurshid SS, Fisher OZ, Khademhosseini A, Peppas NA. Hydrogels in Regenerative Medicine. Adv Mater (Weinheim, Ger). 2009;21:3307-29.
[80] Nicodemus GD, Bryant SJ. Cell encapsulation in biodegradable hydrogels for tissue engineering applications. Tissue Engineering - Part B: Reviews. 2008;14:149-65.
[81] Yang C, Hillas PJ, Baez JA, Nokelainen M, Balan J, Tang J, et al. The application of recombinant human collagen in tissue engineering. BioDrugs. 2004;18:103-19.
[82] Bozec L, Horton MA. Skeletal tissues as nanomaterials. Journal of Materials Science: Materials in Medicine. 2006;17:1043-8.
[83] Shih Y-RV, Chen C-N, Tsai S-W, Wang YJ, Lee OK. Growth of Mesenchymal Stem Cells on Electrospun Type I Collagen Nanofibers. STEM CELLS. 2006;24:2391-7.
[84] Keogh M, O' Brien F, Daly J. A novel collagen scaffold supports human osteogenesis—applications for bone tissue engineering. Cell and Tissue Research. 2010;340:169-77.
[85] Blackwood KA, Bock N, Dargaville TR, Ann Woodruff M. Scaffolds for growth factor delivery as applied to bone tissue engineering. International Journal of Polymer Science. 2012;2012.
[86] O'Brien FJ. Biomaterials & scaffolds for tissue engineering. Materials Today. 2011;14:88-95.
[87] Sarker B, Hum J, Nazhat SN, Boccaccini AR. Combining collagen and bioactive glasses for bone tissue engineering: A review. Advanced Healthcare Materials. 2015;4:176-94.
[88] Lee G-S, Park J-H, Shin US, Kim H-W. Direct deposited porous scaffolds of calcium phosphate cement with alginate for drug delivery and bone tissue engineering. Acta Biomaterialia. 2011;7:3178-86.
[89] Zhao L, Weir MD, Xu HHK. An injectable calcium phosphate-alginate hydrogel-umbilical cord mesenchymal stem cell paste for bone tissue engineering. Biomaterials. 2010;31:6502-10.
[90] Park J-H, Lee E-J, Knowles JC, Kim H-W. Preparation of in situ hardening composite microcarriers: Calcium phosphate cement combined with alginate for bone regeneration. Journal of Biomaterials Applications. 2014;28:1079-84.
[91] Zhang J, Nie J, Zhang Q, Li Y, Wang Z, Hu Q. Preparation and characterization of bionic bone structure chitosan/hydroxyapatite scaffold for bone tissue engineering. Journal of Biomaterials Science, Polymer Edition. 2013;25:61-74.

[92] Hongju P, Zi Y, Huanhuan L, Xiao C, Bei F, Huihua Y, et al. Electrospun biomimetic scaffold of hydroxyapatite/chitosan supports enhanced osteogenic differentiation of mMSCs. Nanotechnology. 2012;23:485102.
[93] Khanna R, Katti KS, Katti DR. Bone nodules on chitosan–polygalacturonic acid–hydroxyapatite nanocomposite films mimic hierarchy of natural bone. Acta Biomaterialia. 2011;7:1173-83.
[94] Barbani N, Guerra G, Cristallini C, Urciuoli P, Avvisati R, Sala A, et al. Hydroxyapatite/gelatin/gellan sponges as nanocomposite scaffolds for bone reconstruction. Journal of Materials Science: Materials in Medicine. 2012;23:51-61.
[95] Bakhtiari L, Rezaie HR, Hosseinalipour SM, Shokrgozar MA. Investigation of biphasic calcium phosphate/gelatin nanocomposite scaffolds as a bone tissue engineering. Ceramics International. 2010;36:2421-6.
[96] Khan MN, Islam JMM, Khan MA. Fabrication and characterization of gelatin-based biocompatible porous composite scaffold for bone tissue engineering. Journal of Biomedical Materials Research Part A. 2012;100A:3020-8.
[97] Azami M, Samadikuchaksaraei A, Poursamar SA. Synthesis and characterization of a laminated hydroxyapatite/gelatin nanocomposite scaffold with controlled pore structure for bone tissue engineering. International Journal of Artificial Organs. 2010;33:86-95.
[98] Pereira DR, Canadas RF, Silva-Correia J, Marques AP, Reis RL, Oliveira JM. Gellan gum-based hydrogel bilayered scaffolds for osteochondral tissue engineering. Key Engineering Materials2014. p. 255-60.
[99] Martínez-Sanz E, Varghese OP, Kisiel M, Engstrand T, Reich KM, Bohner M, et al. Minimally invasive mandibular bone augmentation using injectable hydrogels. Journal of Tissue Engineering and Regenerative Medicine. 2012;6:s15-s23.
[100] Bhumiratana S, Grayson WL, Castaneda A, Rockwood DN, Gil ES, Kaplan DL, et al. Nucleation and growth of mineralized bone matrix on silk-hydroxyapatite composite scaffolds. Biomaterials. 2011;32:2812-20.
[101] Yan L-P, Salgado AJ, Oliveira JM, Oliveira AL, Reis RL. De novo bone formation on macro/microporous silk and silk/nano-sized calcium phosphate scaffolds. Journal of Bioactive and Compatible Polymers. 2013;28:439-52.
[102] Zhang Y, Wu C, Friis T, Xiao Y. The osteogenic properties of CaP/silk composite scaffolds. Biomaterials. 2010;31:2848-56.
[103] Sabir M, Xu X, Li L. A review on biodegradable polymeric materials for bone tissue engineering applications. Journal of Materials Science. 2009;44:5713-24.
[104] Idris SB, Arvidson K, Plikk P, Ibrahim S, Finne-Wistrand A, Albertsson A-C, et al. Polyester copolymer scaffolds enhance expression of bone markers in osteoblast-like cells. Journal of Biomedical Materials Research Part A. 2010;94A:631-9.
[105] Gonçalves F, Bentini R, Burrows M, Carreira A, Kossugue P, Sogayar M, et al. Hybrid Membranes of PLLA/Collagen for Bone Tissue

Engineering: A Comparative Study of Scaffold Production Techniques for Optimal Mechanical Properties and Osteoinduction Ability. Materials. 2015;8:408-23.
[106] Zhang Q, Mochalin VN, Neitzel I, Knoke IY, Han J, Klug CA, et al. Fluorescent PLLA-nanodiamond composites for bone tissue engineering. Biomaterials. 2011;32:87-94.
[107] Ma PX. Scaffolds for tissue fabrication. Materials Today. 2004;7:30-40.
[108] Chen G, Ushida T, Tateishi T. Scaffold design for tissue engineering. Macromolecular Bioscience. 2002;2:67-77.
[109] Williams JM, Adewunmi A, Schek RM, Flanagan CL, Krebsbach PH, Feinberg SE, et al. Bone tissue engineering using polycaprolactone scaffolds fabricated via selective laser sintering. Biomaterials. 2005;26:4817-27.
[110] Salerno A, Guarnieri D, Iannone M, Zeppetelli S, Di Maio E, Iannace S, et al. Engineered μ-bimodal poly(ε-caprolactone) porous scaffold for enhanced hMSC colonization and proliferation. Acta Biomaterialia. 2009;5:1082-93.
[111] Nair PD, Mukundan LM, Nirmal R, Mohan N. A PVA-PCL bioglass composite with potential implications for osteochondral tissue engineering. Mater Res Soc Symp Proc. 2009;1235.
[112] Chuenjitkuntaworn B, Inrung W, Damrongsri D, Mekaapiruk K, Supaphol P, Pavasant P. Polycaprolactone/hydroxyapatite composite scaffolds: Preparation, characterization, and in vitro and in vivo biological responses of human primary bone cells. Journal of Biomedical Materials Research Part A. 2010;94A:241-51.
[113] Shi Q, Zhong S, Chen Y, Whitaker A. Photo-crosslinking copolymers based polyanhydride and 1G polyamidoamine-methacrylamide as bone tissue engineering: Synthesis, characterization, and in vitro degradation. Polymer Degradation and Stability. 2010;95:1961-8.
[114] Nukavarapu SP, Kumbar SG, Brown JL, Krogman NR, Weikel AL, Hindenlang MD, et al. Polyphosphazene/nano-hydroxyapatite composite microsphere scaffolds for bone tissue engineering. Biomacromolecules. 2008;9:1818-25.
[115] Guarino V, Gloria A, Raucci MG, Ambrosio L. Hydrogel-Based Platforms for the Regeneration of Osteochondral Tissue and Intervertebral Disc. Polymers. 2012;4:1590-612.
[116] Moura MJ, Faneca H, Lima MP, Gil MH, Figueiredo MM. In Situ Forming Chitosan Hydrogels Prepared via Ionic/Covalent Co-Cross-Linking. Biomacromolecules. 2011;12:3275-84.
[117] Augst AD, Kong HJ, Mooney DJ. Alginate Hydrogels as Biomaterials. Macromolecular Bioscience. 2006;6:623-33.
[118] Liu H, Gao C. Preparation and properties of ionically cross-linked chitosan nanoparticles. Polymers for Advanced Technologies. 2009;20:613-9.
[119] Oliveira JT, Santos TC, Martins L, Picciochi R, Marques AP, Castro AG, et al. Gellan gum injectable hydrogels for cartilage tissue engineering applications: In vitro studies and preliminary in vivo evaluation. Tissue Engineering - Part A. 2010;16:343-53.

[120] Vorvolakos K, Isayeva IS, Luu H-MD, Patwardhan DV, Pollack SK. Ionically cross-linked hyaluronic acid: wetting, lubrication, and viscoelasticity of a modified adhesion barrier gel. Medical Devices (Auckland, NZ). 2011;4:1-10.
[121] Millon LE, Mohammadi H, Wan WK. Anisotropic polyvinyl alcohol hydrogel for cardiovascular applications. Journal of Biomedical Materials Research Part B: Applied Biomaterials. 2006;79B:305-11.
[122] Lee CW, Manoshiro T, Hsu Y-I, Kimura Y. Gelation Behavior of Bioabsorbable Hydrogels Consisting of Enantiomeric Mixtures of A–B–A Tri-block Copolymers of Polylactides (A) and Poly(ethylene glycol) (B). Macromolecular Chemistry and Physics. 2012;213:2174-80.
[123] van Nostrum CF, Veldhuis TFJ, Bos GW, Hennink WE. Tuning the Degradation Rate of Poly(2-hydroxypropyl methacrylamide)-graft-oligo(lactic acid) Stereocomplex Hydrogels. Macromolecules. 2004;37:2113-8.
[124] Bos GW, Hennink WE, Brouwer LA, den Otter W, Veldhuis TFJ, van Nostrum CF, et al. Tissue reactions of in situ formed dextran hydrogels crosslinked by stereocomplex formation after subcutaneous implantation in rats. Biomaterials. 2005;26:3901-9.
[125] Huynh CT, Nguyen QV, Kang SW, Lee DS. Synthesis and characterization of poly(amino urea urethane)-based block copolymer and its potential application as injectable pH/temperature-sensitive hydrogel for protein carrier. Polymer. 2012;53:4069-75.
[126] Garbern JC, Hoffman AS, Stayton PS. Injectable pH- and Temperature-Responsive Poly(N-isopropylacrylamide-co-propylacrylic acid) Copolymers for Delivery of Angiogenic Growth Factors. Biomacromolecules. 2010;11:1833-9.
[127] Diaz IL, Parra C, Linarez M, Perez LD. Design of Micelle Nanocontainers Based on PDMAEMA-b-PCL-b-PDMAEMA Triblock Copolymers for the Encapsulation of Amphotericin B. AAPS PharmSciTech. 2015.
[128] Petrova S, Venturini CG, Jäger A, Jäger E, Černoch P, Kereïche S, et al. Novel thermo-responsive double-hydrophilic and hydrophobic MPEO-b-PEtOx-b-PCL triblock terpolymers: Synthesis, characterization and self-assembly studies. Polymer (United Kingdom). 2015;59:215-25.
[129] Li Z, Tan BH. Towards the development of polycaprolactone based amphiphilic block copolymers: Molecular design, self-assembly and biomedical applications. Materials Science and Engineering C. 2014;45:620-34.
[130] Chen Z, Greaves TL, Caruso RA, Drummond CJ. Effect of cosolvents on the self-assembly of a non-ionic polyethylene oxide-polypropylene oxide-polyethylene oxide block copolymer in the protic ionic liquid ethylammonium nitrate. Journal of Colloid and Interface Science. 2015;441:46-51.
[131] Fathi A, Mithieux SM, Wei H, Chrzanowski W, Valtchev P, Weiss AS, et al. Elastin based cell-laden injectable hydrogels with tunable gelation, mechanical and biodegradation properties. Biomaterials. 2014;35:5425-35.

[132] Huynh CT, Nguyen MK, Lee DS. Injectable Block Copolymer Hydrogels: Achievements and Future Challenges for Biomedical Applications. Macromolecules. 2011;44:6629-36.
[133] Chen Z, Greaves TL, Caruso RA, Drummond CJ. Long-range ordered lyotropic liquid crystals in intermediate-range ordered protic ionic liquid used as templates for hierarchically porous silica. Journal of Materials Chemistry. 2012;22:10069-76.
[134] Grieshaber SE, Jha AK, Farran AJE, Jia X. Hydrogels in tissue engineering. Biomaterials for Tissue Engineering Applications: A Review of the Past and Future Trends2011. p. 9-46.
[135] Li Y, Rodrigues J, Tomas H. Injectable and biodegradable hydrogels: gelation, biodegradation and biomedical applications. Chemical Society Reviews. 2012;41:2193-221.
[136] Ko DY, Shinde UP, Yeon B, Jeong B. Recent progress of in situ formed gels for biomedical applications. Progress in Polymer Science. 2013;38:672-701.
[137] Hiemstra C, van der Aa LJ, Zhong Z, Dijkstra PJ, Feijen J. Rapidly in situ-forming degradable hydrogels from dextram triols through Michael addition. Biomacromolecules. 2007;8:1548-56.
[138] Shu XZ, Ahmad S, Liu Y, Prestwich GD. Synthesis and evaluation of injectable, in situ crosslinkable synthetic extracellular matrices for tissue engineering. Journal of Biomedical Materials Research Part A. 2006;79A:902-12.
[139] Cohen JM, Southwood LL, Engiles J, Leitch M, Nunamaker DM. Effects of a novel hydrogel on equine bone healing: A pilot study. Veterinary and Comparative Orthopaedics and Traumatology. 2012;25:184-91.
[140] Fu Y, Xu K, Zheng X, Giacomin AJ, Mix AW, Kao WJ. 3D cell entrapment in crosslinked thiolated gelatin-poly(ethylene glycol) diacrylate hydrogels. Biomaterials. 2012;33:48-58.
[141] Shu XZ, Ghosh K, Liu Y, Palumbo FS, Luo Y, Clark RA, et al. Attachment and spreading of fibroblasts on an RGD peptide-modified injectable hyaluronan hydrogel. Journal of Biomedical Materials Research - Part A. 2004;68:365-75.
[142] Censi R, Fieten PJ, Di Martino P, Hennink WE, Vermonden T. In situ forming hydrogels by tandem thermal gelling and Michael addition reaction between thermosensitive triblock copolymers and thiolated hyaluronan. Macromolecules. 2010;43:5771-8.
[143] Skardal A, Zhang J, Prestwich GD. Bioprinting vessel-like constructs using hyaluronan hydrogels crosslinked with tetrahedral polyethylene glycol tetracrylates. Biomaterials. 2010;31:6173-81.
[144] Jeong CG, Francisco AT, Niu Z, Mancino RL, Craig SL, Setton LA. Screening of hyaluronic acid-poly(ethylene glycol) composite hydrogels to support intervertebral disc cell biosynthesis using artificial neural network analysis. Acta Biomaterialia. 2014;10:3421-30.
[145] Liu SQ, Tian Q, Hedrick JL, Po Hui JH, Rachel Ee PL, Yang YY. Biomimetic hydrogels for chondrogenic differentiation of human mesenchymal stem cells to neocartilage. Biomaterials. 2010;31:7298-307.

[146] Metters A, Hubbell J. Network formation and degradation behavior of hydrogels formed by Michael-type addition reactions. Biomacromolecules. 2005;6:290-301.
[147] Lei Y, Segura T. DNA delivery from matrix metalloproteinase degradable poly(ethylene glycol) hydrogels to mouse cloned mesenchymal stem cells. Biomaterials. 2009;30:254-65.
[148] Zustiak SP, Leach JB. Characterization of protein release from hydrolytically degradable poly(ethylene glycol) hydrogels. Biotechnology and Bioengineering. 2011;108:197-206.
[149] Elbert DL, Pratt AB, Lutolf MP, Halstenberg S, Hubbell JA. Protein delivery from materials formed by self-selective conjugate addition reactions. Journal of Controlled Release. 2001;76:11-25.
[150] Elbert DL, Lutolf MP, Pratt AB, Halstenberg S, Hubbell JA. Protein release from PEG hydrogels that are similar to ideal Flory-Rehner networks. Proceedings of 28th International Symposium on Controlled Release of Bioactive Materials San Diego, CA, United States2001. p. 987-8.
[151] Park Y, Lutolf MP, Hubbell JA, Hunziker EB, Wong M. Bovine Primary Chondrocyte Culture in Synthetic Matrix Metalloproteinase-Sensitive Poly(ethylene glycol)-Based Hydrogels as a Scaffold for Cartilage Repair. Tissue Engineering. 2004;10:515-22.
[152] Chen G, Sato T, Ohgushi H, Ushida T, Tateishi T, Tanaka J. Culturing of skin fibroblasts in a thin PLGA–collagen hybrid mesh. Biomaterials. 2005;26:2559-66.
[153] Panda NN, Jonnalagadda S, Pramanik K. Development and evaluation of cross-linked collagen-hydroxyapatite scaffolds for tissue engineering. Journal of Biomaterials Science, Polymer Edition. 2013;24:2031-44.
[154] Hosseini MS, Amjadi I, Haghighipour N. Preparation of poly (vinyl alcohol)/chitosan-blended hydrogels: Properties, in vitro studies and kinetic evaluation. Journal of Biomimetics, Biomaterials, and Tissue Engineering. 2012;15:63-72.
[155] Hsieh C-Y, Tsai S-P, Ho M-H, Wang D-M, Liu C-E, Hsieh C-H, et al. Analysis of freeze-gelation and cross-linking processes for preparing porous chitosan scaffolds. Carbohydr Polym. 2007;67:124-32.
[156] Pulat M, Akalin GO. Preparation and characterization of gelatin hydrogel support for immobilization of Candida Rugosa lipase. Artificial Cells, Nanomedicine and Biotechnology. 2013;41:145-51.
[157] Veríssimo DM, Leitão RFC, Ribeiro RA, Figueiró SD, Sombra ASB, Góes JC, et al. Polyanionic collagen membranes for guided tissue regeneration: Effect of progressive glutaraldehyde cross-linking on biocompatibility and degradation. Acta Biomaterialia. 2010;6:4011-8.
[158] Schacht E, Bogdanov B, Bulcke AVD, De Rooze N. Hydrogels prepared by crosslinking of gelatin with dextran dialdehyde. Reactive and Functional Polymers. 1997;33:109-16.
[159] Ito T, Yeo Y, Highley CB, Bellas E, Kohane DS. Dextran-based in situ cross-linked injectable hydrogels to prevent peritoneal adhesions. Biomaterials. 2007;28:3418-26.
[160] Balakrishnan B, Jayakrishnan A. Self-cross-linking biopolymers as injectable in situ forming biodegradable scaffolds. Biomaterials. 2005;26:3941-51.

[161] Tan H, Chu CR, Payne KA, Marra KG. Injectable in situ forming biodegradable chitosan–hyaluronic acid based hydrogels for cartilage tissue engineering. Biomaterials. 2009;30:2499-506.
[162] Nguyen MK, Alsberg E. Bioactive factor delivery strategies from engineered polymer hydrogels for therapeutic medicine. Progress in Polymer Science. 2014;39:1235-65.
[163] Tan H, Rubin JP, Marra KG. Injectable in situ forming biodegradable chitosan-hyaluronic acid based hydrogels for adipose tissue regeneration. Organogenesis. 2010;6:173-80.
[164] Hudson SP, Langer R, Fink GR, Kohane DS. Injectable in situ cross-linking hydrogels for local antifungal therapy. Biomaterials. 2010;31:1444-52.
[165] Tsai C-C, Huang R-N, Sung H-W, Liang HC. In vitro evaluation of the genotoxicity of a naturally occurring crosslinking agent (genipin) for biologic tissue fixation. Journal of Biomedical Materials Research. 2000;52:58-65.
[166] Rose J, Pacelli S, Haj A, Dua H, Hopkinson A, White L, et al. Gelatin-Based Materials in Ocular Tissue Engineering. Materials. 2014;7:3106-35.
[167] Gorgieva S, Kokol V. Collagen- vs. Gelatine-Based Biomaterials and Their Biocompatibility: Review and Perspectives. In: Pignatello R, editor. Biomaterials Applications for Nanomedicine: InTech; 2011. p. 470.
[168] Mi F-L, Shyu S-S, Peng C-K. Characterization of ring-opening polymerization of genipin and pH-dependent cross-linking reactions between chitosan and genipin. Journal of Polymer Science Part A: Polymer Chemistry. 2005;43:1985-2000.
[169] Pandis C, Madeira S, Matos J, Kyritsis A, Mano JF, Ribelles JLG. Chitosan–silica hybrid porous membranes. Materials Science and Engineering: C. 2014;42:553-61.
[170] Arteche Pujana M, Pérez-Álvarez L, Cesteros Iturbe LC, Katime I. Biodegradable chitosan nanogels crosslinked with genipin. Carbohydrate Polymers. 2013;94:836-42.
[171] Fessel G, Gerber C, Snedeker JG. Potential of collagen cross-linking therapies to mediate tendon mechanical properties. Journal of Shoulder and Elbow Surgery. 2012;21:209-17.
[172] Jeng L, Olsen BR, Spector M. Engineering endostatin-expressing cartilaginous constructs using injectable biopolymer hydrogels. Acta Biomaterialia. 2012.
[173] Ma W, Tang C-H, Yin S-W, Yang X-Q, Qi J-R. Genipin-crosslinked gelatin films as controlled releasing carriers of lysozyme. Food Research International. 2013;51:321-4.
[174] Elzoghby AO. Gelatin-based nanoparticles as drug and gene delivery systems: Reviewing three decades of research. Journal of Controlled Release. 2013;172:1075-91.
[175] Kast CE, Bernkop-Schnürch A. Thiolated polymers — thiomers: development and in vitro evaluation of chitosan–thioglycolic acid conjugates. Biomaterials. 2001;22:2345-52.

[176] Hornof MD, Kast CE, Bernkop-Schnürch A. In vitro evaluation of the viscoelastic properties of chitosan–thioglycolic acid conjugates. European Journal of Pharmaceutics and Biopharmaceutics. 2003;55:185-90.
[177] Shu XZ, Liu Y, Luo Y, Roberts MC, Prestwich GD. Disulfide Cross-Linked Hyaluronan Hydrogels. Biomacromolecules. 2002;3:1304-11.
[178] Choh SY, Cross D, Wang C. Facile synthesis and characterization of disulfide-cross-linked hyaluronic acid hydrogels for protein delivery and cell encapsulation. Biomacromolecules. 2011;12:1126-36.
[179] Shu XZ, Liu Y, Palumbo F, Prestwich GD. Disulfide-crosslinked hyaluronan-gelatin hydrogel films: a covalent mimic of the extracellular matrix for in vitro cell growth. Biomaterials. 2003;24:3825-34.
[180] Sakloetsakun D, Hombach JMR, Bernkop-Schnürch A. In situ gelling properties of chitosan-thioglycolic acid conjugate in the presence of oxidizing agents. Biomaterials. 2009;30:6151-7.
[181] Anumolu SS, Menjoge AR, Deshmukh M, Gerecke D, Stein S, Laskin J, et al. Doxycycline hydrogels with reversible disulfide crosslinks for dermal wound healing of mustard injuries. Biomaterials. 2011;32:1204-17.
[182] van Dijk M, Rijkers DTS, Liskamp RMJ, van Nostrum CF, Hennink WE. Synthesis and Applications of Biomedical and Pharmaceutical Polymers via Click Chemistry Methodologies. Bioconjug Chem. 2009;20:2001-16.
[183] Uliniuc A, Popa M, Hamaide T, Dobromir M. New approaches in hydrogel synthesis - Click chemistry: A review. Cellul Chem Technol. 2012;46:1-11.
[184] Binder WH, Sachsenhofer R. Polymersome/Silica Capsules by 'Click'-Chemistry. Macromolecular Rapid Communications. 2008;29:1097-103.
[185] Ossipov DA, Hilborn J. Poly(vinyl alcohol)-Based Hydrogels Formed by "Click Chemistry". Macromolecules. 2006;39:1709-18.
[186] Altin H, Kosif I, Sanyal R. Fabrication of "Clickable" Hydrogels via Dendron−Polymer Conjugates. Macromolecules. 2010;43:3801-8.
[187] Malkoch M, Vestberg R, Gupta N, Mespouille L, Dubois P, Mason AF, et al. Synthesis of well-defined hydrogel networks using Click chemistry. Chemical Communications. 2006:2774-6.
[188] Tzokova N, Fernyhough CM, Topham PD, Sandon N, Adams DJ, Butler MF, et al. Soft Hydrogels from Nanotubes of Poly(ethylene oxide)−Tetraphenylalanine Conjugates Prepared by Click Chemistry. Langmuir. 2009;25:2479-85.
[189] van Dijk M, van Nostrum CF, Hennink WE, Rijkers DTS, Liskamp RMJ. Synthesis and Characterization of Enzymatically Biodegradable PEG and Peptide-Based Hydrogels Prepared by Click Chemistry. Biomacromolecules. 2010;11:1608-14.
[190] Crescenzi V, Cornelio L, Di Meo C, Nardecchia S, Lamanna R. Novel Hydrogels via Click Chemistry: Synthesis and Potential Biomedical Applications. Biomacromolecules. 2007;8:1844-50.
[191] Hu X, Li D, Zhou F, Gao C. Biological hydrogel synthesized from hyaluronic acid, gelatin and chondroitin sulfate by click chemistry. Acta Biomaterialia. 2011;7:1618-26.

[192] DeForest CA, Sims EA, Anseth KS. Peptide-Functionalized Click Hydrogels with Independently Tunable Mechanics and Chemical Functionality for 3D Cell Culture. Chemistry of Materials. 2010;22:4783-90.
[193] Agard NJ, Prescher JA, Bertozzi CR. A Strain-Promoted [3 + 2] Azide−Alkyne Cycloaddition for Covalent Modification of Biomolecules in Living Systems. Journal of the American Chemical Society. 2004;126:15046-7.
[194] Prescher JA, Bertozzi CR. Chemistry in living systems. Nat Chem Biol. 2005;1:13-21.
[195] Johnson JA, Baskin JM, Bertozzi CR, Koberstein JT, Turro NJ. Copper-free click chemistry for the in situ crosslinking of photodegradable star polymers. Chemical Communications. 2008:3064-6.
[196] Truong VX, Ablett MP, Gilbert HTJ, Bowen J, Richardson SM, Hoyland JA, et al. In situ-forming robust chitosan-poly(ethylene glycol) hydrogels prepared by copper-free azide-alkyne click reaction for tissue engineering. Biomaterials Science. 2014;2:167-75.
[197] Tibbitt MW, Kloxin AM, Sawicki LA, Anseth KS. Mechanical Properties and Degradation of Chain and Step-Polymerized Photodegradable Hydrogels. Macromolecules. 2013;46:2785-92.
[198] Lee SY, Zhong X, Valtchev P, Dehghani F. Synthesis of a biodegradable polymer in gas expanded solution: effect of the process on cytocompatibility. Green Chemistry. 2013;15:1280-91.
[199] Shung AK, Behravesh E, Jo S, Mikos AG. Crosslinking Characteristics of and Cell Adhesion to an Injectable Poly(Propylene Fumarate-co-Ethylene Glycol) Hydrogel Using a Water-Soluble Crosslinking System. Tissue Eng. 2003;9:243-54.
[200] Temenoff JS, Athanasiou KA, LeBaron RG, Mikos AG. Effect of poly(ethylene glycol) molecular weight on tensile and swelling properties of oligo(poly(ethylene glycol) fumarate) hydrogels for cartilage tissue engineering. Journal of Biomedical Materials Research, Part A. 2002;59:429-37.
[201] Xu W, Ma J, Jabbari E. Material properties and osteogenic differentiation of marrow stromal cells on fiber-reinforced laminated hydrogel nanocomposites. Acta Biomaterialia. 2010;6:1992-2002.
[202] Ferreira L, Rafael A, Lamghari M, Barbosa MA, Gil MH, Cabrita AMS, et al. Biocompatibility of chemoenzymatically derived dextran-acrylate hydrogels. Journal of Biomedical Materials Research Part A. 2004;68A:584-96.
[203] Varaprasad K, Reddy NN, Kumar NM, Vimala K, Ravindra S, Raju KM. Poly(acrylamide-chitosan) hydrogels: Interaction with surfactants. International Journal of Polymeric Materials and Polymeric Biomaterials. 2010;59:981-93.
[204] Guo X, Park H, Liu G, Liu W, Cao Y, Tabata Y, et al. In vitro generation of an osteochondral construct using injectable hydrogel composites encapsulating rabbit marrow mesenchymal stem cells. Biomaterials. 2009;30:2741-52.
[205] Bostan MS, Senol M, Cig T, Peker I, Goren AC, Ozturk T, et al. Controlled release of 5-aminosalicylicacid from chitosan based pH and

temperature sensitive hydrogels. International Journal of Biological Macromolecules. 2013;52:177-83.
[206] Hong Y, Song H, Gong Y, Mao Z, Gao C, Shen J. Covalently crosslinked chitosan hydrogel: Properties of in vitro degradation and chondrocyte encapsulation. Acta Biomaterialia. 2007;3:23-31.
[207] Jin R, Moreira Teixeira LS, Dijkstra PJ, van Blitterswijk CA, Karperien M, Feijen J. Enzymatically-crosslinked injectable hydrogels based on biomimetic dextran–hyaluronic acid conjugates for cartilage tissue engineering. Biomaterials. 2010;31:3103-13.
[208] Westhaus E, Messersmith PB. Triggered release of calcium from lipid vesicles: a bioinspired strategy for rapid gelation of polysaccharide and protein hydrogels. Biomaterials. 2001;22:453-62.
[209] Bieniarz C, Young DF, Cornwell MJ. Thermally Stabilized Immunoconjugates: Conjugation of Antibodies to Alkaline Phosphatase Stabilized with Polymeric Cross-Linkers. Bioconjug Chem. 1998;9:399-402.
[210] Chen T, Embree HD, Brown EM, Taylor MM, Payne GF. Enzyme-catalyzed gel formation of gelatin and chitosan: potential for in situ applications. Biomaterials. 2003;24:2831-41.
[211] Toledano S, Williams RJ, Jayawarna V, Ulijn RV. Enzyme-Triggered Self-Assembly of Peptide Hydrogels via Reversed Hydrolysis. J Am Chem Soc. 2006;128:1070-1.
[212] Burke MD, Park JO, Srinivasarao M, Khan SA. A novel enzymatic technique for limiting drug mobility in a hydrogel matrix. Journal of Controlled Release. 2005;104:141-53.
[213] Hughes M, Xu H, Frederix PWJM, Smith AM, Hunt NT, Tuttle T, et al. Biocatalytic self-assembly of 2D peptide-based nanostructures. Soft Matter. 2011;7:10032-8.
[214] Lee BP, Dalsin JL, Messersmith PB. Synthesis and Gelation of DOPA-Modified Poly(ethylene glycol) Hydrogels. Biomacromolecules. 2002;3:1038-47.
[215] Jin R, Moreira Teixeira LS, Dijkstra PJ, Karperien M, van Blitterswijk CA, Zhong ZY, et al. Injectable chitosan-based hydrogels for cartilage tissue engineering. Biomaterials. 2009;30:2544-51.
[216] Park KM, Ko KS, Joung YK, Shin H, Park KD. In situ cross-linkable gelatin-poly(ethylene glycol)-tyramine hydrogel viaenzyme-mediated reaction for tissue regenerative medicine. Journal of Materials Chemistry. 2011;21:13180-7.
[217] Jin R, Moreira TLS, Dijkstra PJ, van BCA, Karperien M, Feijen J. Chondrogenesis in injectable enzymatically crosslinked heparin/dextran hydrogels. Journal of Controlled Release. 2011;152:186-95.
[218] Lee F, Chung JE, Kurisawa M. An injectable enzymatically crosslinked hyaluronic acid-tyramine hydrogel system with independent tuning of mechanical strength and gelation rate. Soft Matter. 2008;4:880-7.
[219] Kurisawa M, Chung JE, Yang YY, Gao SJ, Uyama H. Injectable biodegradable hydrogels composed of hyaluronic acid-tyramine conjugates for drug delivery and tissue engineering. Chemical Communications. 2005:4312-4.

[220] Tran NQ, Joung YK, Lih E, Park KM, Park KD. Supramolecular Hydrogels Exhibiting Fast In Situ Gel Forming and Adjustable Degradation Properties. Biomacromolecules. 2010;11:617-25.
[221] Lorand L, Conrad SM. Transglutaminases. Mol Cell Biochem. 1984;58:9-35.
[222] Sperinde JJ, Griffith LG. Synthesis and Characterization of Enzymically-Cross-Linked Poly(ethylene glycol) Hydrogels. Macromolecules. 1997;30:5255-64.
[223] Chen T, Small DA, McDermott MK, Bentley WE, Payne GF. Enzymatic Methods for in Situ Cell Entrapment and Cell Release. Biomacromolecules. 2003;4:1558-63.
[224] Ferreira P, Coelho JFJ, Almeida JF, Gil MH. Photocrosslinkable Polymers for Biomedical Applications2011.
[225] Park H, Choi B, Hu J, Lee M. Injectable chitosan hyaluronic acid hydrogels for cartilage tissue engineering. Acta Biomaterialia. 2013;9:4779-86.
[226] Hashemi Doulabi AS, Mirzadeh H, Imani M, Sharifi S, Atai M, Mehdipour-Ataei S. Synthesis and preparation of biodegradable and visible light crosslinkable unsaturated fumarate-based networks for biomedical applications. Polymers for Advanced Technologies. 2008;19:1199-208.
[227] Duan B, Hockaday LA, Kapetanovic E, Kang KH, Butcher JT. Stiffness and adhesivity control aortic valve interstitial cell behavior within hyaluronic acid based hydrogels. Acta Biomaterialia. 2013;9:7640-50.
[228] Fertier L, Koleilat H, Stemmelen M, Giani O, Joly-Duhamel C, Lapinte V, et al. The use of renewable feedstock in UV-curable materials – A new age for polymers and green chemistry. Progress in Polymer Science. 2013;38:932-62.
[229] Nettles DL, Vail TP, Morgan MT, Grinstaff MW, Setton LA. Photocrosslinkable hyaluronan as a scaffold for articular cartilage repair. Annals of Biomedical Engineering. 2004;32:391-7.
[230] Erickson IE, Huang AH, Sengupta S, Kestle S, Burdick JA, Mauck RL. Macromer density influences mesenchymal stem cell chondrogenesis and maturation in photocrosslinked hyaluronic acid hydrogels. Osteoarthritis and Cartilage. 2009;17:1639-48.
[231] Allen NS, Marin MC, Edge M, Davies DW, Garrett J, Jones F, et al. Photochemistry and photoinduced chemical crosslinking activity of type I & II co-reactive photoinitiators in acrylated prepolymers. Journal of Photochemistry and Photobiology A: Chemistry. 1999;126:135-49.
[232] Jeon O, Bouhadir KH, Mansour JM, Alsberg E. Photocrosslinked alginate hydrogels with tunable biodegradation rates and mechanical properties. Biomaterials. 2009;30:2724-34.
[233] Amsden BG, Sukarto A, Knight DK, Shapka SN. Methacrylated Glycol Chitosan as a Photopolymerizable Biomaterial. Biomacromolecules. 2007;8:3758-66.
[234] Li Q, Williams CG, Sun DDN, Wang J, Leong K, Elisseeff JH. Photocrosslinkable polysaccharides based on chondroitin sulfate. Journal of Biomedical Materials Research - Part A. 2004;68:28-33.
[235] Daniele MA, Adams AA, Naciri J, North SH, Ligler FS. Interpenetrating networks based on gelatin methacrylamide and PEG

formed using concurrent thiol click chemistries for hydrogel tissue engineering scaffolds. Biomaterials. 2014;35:1845-56.
[236] Ding H, Zhong M, Kim YJ, Pholpabu P, Balasubramanian A, Hui CM, et al. Biologically derived soft conducting hydrogels using heparin-doped polymer networks. ACS Nano. 2014;8:4348-57.
[237] Skardal A, Zhang J, McCoard L, Xu X, Oottamasathien S, Prestwich GD. Photocrosslinkable Hyaluronan-Gelatin Hydrogels for Two-Step Bioprinting. Tissue Engineering Part A. 2010;16:2675-85.
[238] Hedin J, Östlund Å, Nydén M. UV induced cross-linking of starch modified with glycidyl methacrylate. Carbohydrate Polymers. 2010;79:606-13.
[239] Annabi N, Mithieux SM, Zorlutuna P, Camci-Unal G, Weiss AS, Khademhosseini A. Engineered cell-laden human protein-based elastomer. Biomaterials. 2013;34:5496-505.
[240] Annabi N, Tsang K, Mithieux SM, Nikkhah M, Ameri A, Khademhosseini A, et al. Highly Elastic Micropatterned Hydrogel for Engineering Functional Cardiac Tissue. Advanced Functional Materials. 2013;23:4950-9.
[241] Nichol JW, Koshy ST, Bae H, Hwang CM, Yamanlar S, Khademhosseini A. Cell-laden microengineered gelatin methacrylate hydrogels. Biomaterials. 2010;31:5536-44.
[242] Cha C, Shin SR, Gao X, Annabi N, Dokmeci MR, Tang X, et al. Controlling mechanical properties of cell-laden hydrogels by covalent incorporation of graphene oxide. Small. 2014;10:514-23.
[243] Duan B, Kapetanovic E, Hockaday LA, Butcher JT. Three-dimensional printed trileaflet valve conduits using biological hydrogels and human valve interstitial cells. Acta Biomaterialia. 2014.
[244] Pedron S, Harley BAC. Impact of the biophysical features of a 3D gelatin microenvironment on glioblastoma malignancy. Journal of Biomedical Materials Research - Part A. 2013;101:3404-15.
[245] Hoch E, Hirth T, Tovar GEM, Borchers K. Chemical tailoring of gelatin to adjust its chemical and physical properties for functional bioprinting. Journal of Materials Chemistry B. 2013;1:5675-85.
[246] Hosseini V, Ahadian S, Ostrovidov S, Camci-Unal G, Chen S, Kaji H, et al. Engineered Contractile Skeletal Muscle Tissue on a Microgrooved Methacrylated Gelatin Substrate. Tissue Engineering Part A. 2012;18:2453-65.
[247] Bae H, Ahari AF, Shin H, Nichol JW, Hutson CB, Masaeli M, et al. Cell-laden microengineered pullulan methacrylate hydrogels promote cell proliferation and 3D cluster formation. Soft Matter. 2011;7:1903-11.
[248] Cha C, Soman P, Zhu W, Nikkhah M, Camci-Unal G, Chen S, et al. Structural reinforcement of cell-laden hydrogels with microfabricated three dimensional scaffolds. Biomaterials Science. 2014;2:703-9.
[249] Jiang X, Luo S, Armes SP, Shi W, Liu S. UV irradiation-induced shell cross-linked micelles with pH-responsive cores using ABC triblock copolymers. Macromolecules. 2006;39:5987-94.
[250] Nicodemus GD, Skaalure SC, Bryant SJ. Gel structure has an impact on pericellular and extracellular matrix deposition, which subsequently

alters metabolic activities in chondrocyte-laden PEG hydrogels. Acta Biomater. 2011;7:492-504.
[251] Hou Y, Schoener CA, Regan KR, Munoz-Pinto D, Hahn MS, Grunlan MA. Photo-Cross-Linked PDMSstar-PEG Hydrogels: Synthesis, Characterization, and Potential Application for Tissue Engineering Scaffolds. Biomacromolecules. 2010;11:648-56.
[252] Doroski DM, Levenston ME, Temenoff JS. Cyclic Tensile Culture Promotes Fibroblastic Differentiation of Marrow Stromal Cells Encapsulated in Poly(Ethylene Glycol)-Based Hydrogels. Tissue Engineering Part A. 2010;16:3457-66.
[253] Sharma B, Williams CG, Khan M, Manson P, Elisseeff JH. In Vivo Chondrogenesis of Mesenchymal Stem Cells in a Photopolymerized Hydrogel. Plastic and Reconstructive Surgery. 2007;119:112-20.
[254] Fathi A, Lee S, Breen A, Negahi Shirazi A, Valtchev P, Dehghani F. Enhancing the Mechanical Properties and Physical Stability of Biomimetic Polymer Hydrogels for Micro-patterning and Tissue Engineering Applications. European Polymer Journal. 2014;59:161-70.
[255] Serafim A, Dragusin DM, Zecheru T, Dubruel P, Petre D, Ciocan LT, et al. Gelatin hydrogels: Effect of ethylene oxide based synthetic crosslinking agents on the physico-chemical properties. Digest Journal of Nanomaterials and Biostructures. 2012;8:101-10.
[256] Hutson CB, Nichol JW, Aubin H, Bae H, Yamanlar S, Al-Haque S, et al. Synthesis and characterization of tunable poly(ethylene glycol): Gelatin methacrylate composite hydrogels. Tissue Engineering - Part A. 2011;17:1713-23.
[257] Hutson CB, Nichol JW, Koshy S, Bae H, Aubin H, Khademhosseini A. PEG-methacrylated gelatin composite hydrogels with tunable mechanical and cell responsive properties. 239th ACS National Meeting. 2010:BIOT-367.
[258] Fedorovich NE, Oudshoorn MH, van Geemen D, Hennink WE, Alblas J, Dhert WJA. The effect of photopolymerization on stem cells embedded in hydrogels. Biomaterials. 2009;30:344-53.
[259] Habraken WJEM, Wolke JGC, Jansen JA. Ceramic composites as matrices and scaffolds for drug delivery in tissue engineering. Advanced Drug Delivery Reviews. 2007;59:234-48.
[260] Hench LL. The future of bioactive ceramics. Journal of Materials Science: Materials in Medicine. 2015;26.
[261] Roohani-Esfahani S-I, Wong KY, Lu Z, Juan Chen Y, Li JJ, Gronthos S, et al. Fabrication of a novel triphasic and bioactive ceramic and evaluation of its in vitro and in vivo cytocompatibility and osteogenesis. Journal of Materials Chemistry B. 2014;2:1866-78.
[262] Shikinami Y, Matsusue Y, Nakamura T. The complete process of bioresorption and bone replacement using devices made of forged composites of raw hydroxyapatite particles/poly l-lactide (F-u-HA/PLLA). Biomaterials. 2005;26:5542-51.
[263] Rangavittal N, Landa-Cánovas AR, González-Calbet JM, Vallet-Regí M. Structural study and stability of hydroxyapatite and β-tricalcium phosphate: Two important bioceramics. Journal of Biomedical Materials Research. 2000;51:660-8.

[264] Ducheyne P, Qiu Q. Bioactive ceramics: the effect of surface reactivity on bone formation and bone cell function. Biomaterials. 1999;20:2287-303.
[265] EGGLI PS, MOLLER W, SCHENK RK. Porous Hydroxyapatite and Tricalcium Phosphate Cylinders with Two Different Pore Size Ranges Implanted in the Cancellous Bone of Rabbits: A Comparative Histomorphometric and Histologic Study of Bony Ingrowth and Implant Substitution. Clinical Orthopaedics and Related Research. 1988;232:127-38.
[266] El-Ghannam A. Bone reconstruction: From bioceramics to tissue engineering. Expert Review of Medical Devices. 2005;2:87-101.
[267] Dorozhkin SV. Calcium Orthophosphates as Bioceramics: State of the Art. Journal of Functional Biomaterials. 2010;1:22-107.
[268] Kannan S, Ferreira JMF. Synthesis and Thermal Stability of Hydroxyapatite−β-Tricalcium Phosphate Composites with Cosubstituted Sodium, Magnesium, and Fluorine. Chemistry of Materials. 2006;18:198-203.
[269] Yan L-P, Silva-Correia J, Correia C, Caridade SG, Fernandes EM, Sousa RA, et al. Bioactive macro/micro porous silk fibroin/nano-sized calcium phosphate scaffolds with potential for bone-tissue-engineering applications. Nanomedicine. 2012;8:359-78.
[270] Yazaki Y, Oyane A, Sogo Y, Ito A, Yamazaki A, Tsurushima H. Control of gene transfer on a DNA–fibronectin–apatite composite layer by the incorporation of carbonate and fluoride ions. Biomaterials. 2011;32:4896-902.
[271] Joanna L-Ł, Sylwia F, Łucja R, Marcin K, Maria N. Bioactive hydrogel-nanosilica hybrid materials: a potential injectable scaffold for bone tissue engineering. Biomedical Materials. 2015;10:015020.
[272] Suchanek WL, Byrappa K, Shuk P, Riman RE, Janas VF, TenHuisen KS. Preparation of magnesium-substituted hydroxyapatite powders by the mechanochemical–hydrothermal method. Biomaterials. 2004;25:4647-57.
[273] Fadeev IV, Shvorneva LI, Barinov SM, Orlovskii VP. Synthesis and Structure of Magnesium-Substituted Hydroxyapatite. Inorganic Materials. 2003;39:947-50.
[274] Kannan S, Ventura JM, Ferreira JMF. In Situ Formation and Characterization of Flourine-Substituted Biphasic Calcium Phosphate Ceramics of Varied F-HAP/β-TCP Ratios. Chemistry of Materials. 2005;17:3065-8.
[275] Kannan S, Rocha JHG, Ferreira JMF. Synthesis and thermal stability of sodium, magnesium co-substituted hydroxyapatites. Journal of Materials Chemistry. 2006;16:286-91.
[276] Torres PMC, Vieira SI, Cerqueira AR, Pina S, da Cruz Silva OAB, Abrantes JCC, et al. Effects of Mn-doping on the structure and biological properties of β-tricalcium phosphate. J Inorg Biochem. 2014;136:57-66.
[277] Kose N, Otuzbir A, Pekşen C, Kiremitçi A, Doğan A. A Silver Ion-doped Calcium Phosphate-based Ceramic Nanopowder-coated Prosthesis Increased Infection Resistance. Clinical Orthopaedics and Related Research®. 2013;471:2532-9.

[278] Kannan S, Pina S, Ferreira JMF. Formation of Strontium-Stabilized β-Tricalcium Phosphate from Calcium-Deficient Apatite. J Am Ceram Soc. 2006;89:3277-80.
[279] Bandyopadhyay A, Petersen J, Fielding G, Banerjee S, Bose S. ZnO, SiO2, and SrO doping in resorbable tricalcium phosphates: Influence on strength degradation, mechanical properties, and in vitro bone–cell material interactions. Journal of Biomedical Materials Research Part B: Applied Biomaterials. 2012;100B:2203-12.
[280] Tomoaia G, Mocanu A, Vida-Simiti I, Jumate N, Bobos L-D, Soritau O, et al. Silicon effect on the composition and structure of nanocalcium phosphates: In vitro biocompatibility to human osteoblasts. Materials Science and Engineering: C. 2014;37:37-47.
[281] Valerio P, Pereira MM, Goes AM, Leite MF. The effect of ionic products from bioactive glass dissolution on osteoblast proliferation and collagen production. Biomaterials. 2004;25:2941-8.
[282] Hoppe A, Mouriño V, Boccaccini AR. Therapeutic inorganic ions in bioactive glasses to enhance bone formation and beyond. Biomaterials Science. 2013;1:254-6.
[283] Lin S, Ionescu C, Pike KJ, Smith ME, Jones JR. Nanostructure evolution and calcium distribution in sol-gel derived bioactive glass. Journal of Materials Chemistry. 2009;19:1276-82.
[284] Yousefi A-M, Oudadesse H, Akbarzadeh R, Wers E, Lucas-Girot A. Physical and biological characteristics of nanohydroxyapatite and bioactive glasses used for bone tissue engineering. Nanotechnology Reviews2014. p. 527.
[285] Jones JR. Review of bioactive glass: From Hench to hybrids. Acta Biomaterialia. 2013;9:4457-86.
[286] Bonhomme C, Gervais C, Folliet N, Pourpoint F, Coelho Diogo C, Lao J, et al. 87Sr Solid-State NMR as a Structurally Sensitive Tool for the Investigation of Materials: Antiosteoporotic Pharmaceuticals and Bioactive Glasses. Journal of the American Chemical Society. 2012;134:12611-28.
[287] Isaac J, Nohra J, Lao J, Jallot E, Nedelec JM, Berdal A, et al. Effects of strontium-doped bioactive glass on the differentiation of cultured osteogenic cells. European Cells and Materials. 2011;21:130-43.
[288] Chen Q, Zhu C, Thouas G. Progress and challenges in biomaterials used for bone tissue engineering: bioactive glasses and elastomeric composites. Prog Biomater. 2012;1:1-22.
[289] Kaur G, Pandey OP, Singh K, Homa D, Scott B, Pickrell G. A review of bioactive glasses: Their structure, properties, fabrication and apatite formation. Journal of Biomedical Materials Research Part A. 2014;102:254-74.
[290] Hoppe A, Güldal NS, Boccaccini AR. A review of the biological response to ionic dissolution products from bioactive glasses and glass-ceramics. Biomaterials. 2011;32:2757-74.
[291] Bassett DC, Meszaros R, Orzol D, Woy M, Ling Zhang Y, Tiedemann K, et al. A new class of bioactive glasses: Calcium-magnesium sulfophosphates. Journal of Biomedical Materials Research - Part A. 2014;102:2842-8.

[292] Lakhkar NJ, Park J-H, Mordan NJ, Salih V, Wall IB, Kim H-W, et al. Titanium phosphate glass microspheres for bone tissue engineering. Acta Biomaterialia. 2012;8:4181-90.
[293] Saravanapavan P, Hench LL. Mesoporous calcium silicate glasses. I. Synthesis. Journal of Non-Crystalline Solids. 2003;318:1-13.
[294] Jain H, Moawad HMM. Nano/macroporous bioactive glasses made by melt-quench methods. Lehigh University, USA . 2008. p. 31pp.
[295] Fardad MA. Catalysts and the structure of SiO2 sol-gel films. Journal of Materials Science. 2000;35:1835-41.
[296] Gerhardt L-C, Boccaccini AR. Bioactive Glass and Glass-Ceramic Scaffolds for Bone Tissue Engineering. Materials. 2010;3:3867-910.
[297] Lukowiak A, Lao J, Lacroix J, Nedelec JM. Bioactive glass nanoparticles obtained through sol-gel chemistry. Chemical Communications. 2013;49:6620-2.
[298] Shu C, Zhang W, Xu G, Wei Z, Wei J, Wang D. Dissolution behavior and bioactivity study of glass ceramic scaffolds in the system of CaO-P2O5-Na2O-ZnO prepared by sol-gel technique. Materials Science & Engineering, C: Biomimetic and Supramolecular Systems. 2010;30:105-11.
[299] Brauer DS, Anjum MN, Mneimne M, Wilson RM, Doweidar H, Hill RG. Fluoride-containing bioactive glass-ceramics. Journal of Non-Crystalline Solids. 2012;358:1438-42.
[300] Kose DA, Aydogmus N, Zumreoglu-Karan B. Bioactive glasses prepared from organic-mediated BOP bonded materials. Journal of Non-Crystalline Solids. 2014;402:187-93.
[301] Studart AR, Gonzenbach UT, Tervoort E, Gauckler LJ. Processing Routes to Macroporous Ceramics: A Review. J Am Ceram Soc. 2006;89:1771-89.
[302] Hoppe A, Jokic B, Janackovic D, Fey T, Greil P, Romeis S, et al. Cobalt-releasing 1393 bioactive glass-derived scaffolds for bone tissue engineering applications. ACS Applied Materials and Interfaces. 2014;6:2865-77.
[303] Shahini A, Yazdimamaghani M, Walker KJ, Eastman MA, Hatami-Marbini H, Smith BJ, et al. 3D conductive nanocomposite scaffold for bone tissue engineering. International Journal of Nanomedicine. 2014;9:167-81.
[304] Hickey DJ, Ercan B, Sun L, Webster TJ. Adding MgO nanoparticles to hydroxyapatite–PLLA nanocomposites for improved bone tissue engineering applications. Acta Biomaterialia. 2015;14:175-84.
[305] Poologasundarampillai G, Wang D, Li S, Nakamura J, Bradley R, Lee PD, et al. Cotton-wool-like bioactive glasses for bone regeneration. Acta Biomaterialia. 2014;10:3733-46.
[306] Oliveira JM, Silva SS, Malafaya PB, Rodrigues MT, Kotobuki N, Hirose M, et al. Macroporous hydroxyapatite scaffolds for bone tissue engineering applications: Physicochemical characterization and assessment of rat bone marrow stromal cell viability. Journal of Biomedical Materials Research Part A. 2009;91A:175-86.
[307] Lu Z, Roohani-Esfahani S-I, Li J, Zreiqat H. Synergistic effect of nanomaterials and BMP-2 signalling in inducing osteogenic differentiation of adipose tissue-derived mesenchymal stem cells. Nanomedicine: Nanotechnology, Biology and Medicine. 2015;11:219-28.

[308] Lu Z, Wang G, Roohani-Esfahani I, Dunstan CR, Zreiqat H. Baghdadite Ceramics Modulate the Cross Talk Between Human Adipose Stem Cells and Osteoblasts for Bone Regeneration. Tissue Engineering Part A. 2013;20:992-1002.
[309] Roohani-Esfahani SI, Dunstan CR, Li JJ, Lu Z, Davies B, Pearce S, et al. Unique microstructural design of ceramic scaffolds for bone regeneration under load. Acta Biomaterialia. 2013;9:7014-24.
[310] Schexnailder P, Schmidt G. Nanocomposite polymer hydrogels. Colloid Polym Sci. 2009;287:1-11.
[311] Gaharwar AK, Peppas NA, Khademhosseini A. Nanocomposite hydrogels for biomedical applications. Biotechnology and Bioengineering. 2014;111:441-53.
[312] Xiao G, Su H, Tan T. Synthesis of core-shell bioaffinity chitosan-TiO2 composite and its environmental applications. J Hazard Mater. 2015;283:888-96.
[313] Klemenčič D, Tomšič B, Kovač F, Žerjav M, Simončič A, Simončič B. Preparation of novel fibre-silica-Ag composites: The influence of fibre structure on sorption capacity and antimicrobial activity. Journal of Materials Science. 2014;49:3785-94.
[314] Milovac D, Gallego Ferrer G, Ivankovic M, Ivankovic H. PCL-coated hydroxyapatite scaffold derived from cuttlefish bone: Morphology, mechanical properties and bioactivity. Materials Science and Engineering C. 2014;34:437-45.
[315] Wang Q, Mynar JL, Yoshida M, Lee E, Lee M, Okuro K, et al. High-water-content mouldable hydrogels by mixing clay and a dendritic molecular binder. Nature. 2010;463:339-43.
[316] Gaharwar AK, Dammu SA, Canter JM, Wu CJ, Schmidt G. Highly extensible, tough, and elastomeric nanocomposite hydrogels from poly(ethylene glycol) and hydroxyapatite nanoparticles. Biomacromolecules. 2011;12:1641-50.
[317] Novak BM. Hybrid nanocomposite materials - Between inorganic glasses and organic polymers. Advanced Materials. 1993;5:422-33.
[318] Schmidt H, Scholze H, Kaiser A. Principles of hydrolysis and condensation reaction of alkoxysilanes. Journal of Non-Crystalline Solids. 1984;63:1-11.
[319] Schmidt H. Organic modification of glass structure new glasses or new polymers? Journal of Non-Crystalline Solids. 1989;112:419-23.
[320] Tripathi VS, Kandimalla VB, Ju H. Preparation of ormosil and its applications in the immobilizing biomolecules. Sensors and Actuators B: Chemical. 2006;114:1071-82.
[321] Ellsworth MW, Novak BM. Mutually interpenetrating inorganic-organic networks. New routes into nonshrinking sol-gel composite materials. Journal of the American Chemical Society. 1991;113:2756-8.
[322] Hay JN, Raval HM. Synthesis of organic-inorganic hybrids via the non-hydrolytic sol-gel process. Chemistry of Materials. 2001;13:3396-403.
[323] Novak BM, Grubbs RH. Catalytic organometallic chemistry in water: the aqueous ring-opening metathesis polymerization of 7-oxanorbornene derivatives. Journal of the American Chemical Society. 1988;110:7542-3.

[324] Oki A, Qiu X, Alawode O, Foley B. Synthesis of organic-inorganic hybrid composite and its thermal conversion to porous bioactive glass monolith. Materials Letters. 2006;60:2751-5.
[325] Novak BM, Ellsworth MW. “Inverse” organic-inorganic composite materials: high glass content non-shrinking sol-gel composites. Materials Science and Engineering: A. 1993;162:257-64.
[326] Novak BM, Davies C. 'Inverse' organic-inorganic composite materials. 2. Free-radical routes into nonshrinking sol-gel composites. Macromolecules. 1991;24:5481-3.
[327] Baino F, Vitale-Brovarone C. Three-dimensional glass-derived scaffolds for bone tissue engineering: Current trends and forecasts for the future. Journal of Biomedical Materials Research - Part A. 2011;97 A:514-35.
[328] Sato M, Slamovich EB, Webster TJ. Enhanced osteoblast adhesion on hydrothermally treated hydroxyapatite/titania/poly(lactide-co-glycolide) sol–gel titanium coatings. Biomaterials. 2005;26:1349-57.
[329] Podbielska H, Ulatowska-Jarza A. Sol-gel technology for biomedical engineering. Bulletin of the Polish Academy of Sciences: Technical Sciences. 2005;53:261-71.
[330] Gupta R, Kumar A. Bioactive materials for biomedical applications using sol-gel technology. Biomedical Materials. 2008;3.
[331] Gerritsen M, Kros A, Sprakel V, Lutterman JA, Nolte RJM, Jansen JA. Biocompatibility evaluation of sol–gel coatings for subcutaneously implantable glucose sensors. Biomaterials. 2000;21:71-8.
[332] Li C-I, Lin Y-H, Shih C-L, Tsaur J-P, Chau L-K. Sol–gel encapsulation of lactate dehydrogenase for optical sensing of l-lactate. Biosensors and Bioelectronics. 2002;17:323-30.
[333] Avnir D, Lev O, Livage J. Recent bio-applications of sol-gel materials. Journal of Materials Chemistry. 2006;16:1013-30.
[334] Barbé C, Kong L, Finnie K, Calleja S, Hanna J, Drabarek E, et al. Sol–gel matrices for controlled release: from macro to nano using emulsion polymerisation. Journal of Sol-Gel Science and Technology. 2008;46:393-409.
[335] Wang N, Wu C, Cheng Y, Xu T. Organic-inorganic hybrid anion exchange hollow fiber membranes: A novel device for drug delivery. International Journal of Pharmaceutics. 2011;408:39-49.
[336] Desimone MF, Alvarez GS, Foglia ML, Diaz LE. Development of Sol-Gel Hybrid Materials for Whole Cell Immobilization. Recent Patents on Biotechnology. 2009;3:55-60.
[337] Gill I, Ballesteros A. Bioencapsulation within synthetic polymers (Part 1): Sol-gel encapsulated biologicals. Trends in Biotechnology. 2000;18:282-96.
[338] Gill I, Ballesteros A. Bioencapsulation within synthetic polymers (Part 2): Non-sol-gel protein-polymer biocomposites. Trends in Biotechnology. 2000;18:469-79.
[339] Kickelbick G. Concepts for the incorporation of inorganic building blocks into organic polymers on a nanoscale. Progress in Polymer Science. 2003;28:83-114.

[340] Ogoshi T, Chujo Y. Synthesis of Organic-Inorganic Polymer Hybrids Utilizing Amphiphilic Solvent as a Compatibilizer. Bull Chem Soc Jpn. 2003;76:1865-71.
[341] Huang KS, Lee EC, Chang YS. Synthesis and characterization of soluble hybrids of poly(vinyl pyrrolidone) or its copolymer. Journal of Applied Polymer Science. 2006;100:2164-70.
[342] Novak BM, Ellsworth M, Wallow T, Davies C. Simultaneous interpenetrating networks of inorganic glasses and organic polymers. New routes into nonshrinking sol-gel derived composites. Polymer Preprints (American Chemical Society, Division of Polymer Chemistry) 1990;31:698-9.
[343] Yano S, Iwata K, Kurita K. Physical properties and structure of organic-inorganic hybrid materials produced by sol-gel process. Materials Science and Engineering: C. 1998;6:75-90.
[344] Mizushima Y. Preparation of alkoxide-derived chitosan-silica complex membrane. Journal of Non-Crystalline Solids. 1992;144:305-7.
[345] Suzuki T, Mizushima Y. Characteristics of silica-chitosan complex membrane and their relationships to the characteristics of growth and adhesiveness of L-929 cells cultured on the biomembrane. J Ferment Bioeng. 1997;84:128-32.
[346] Heinemann S, Heinemann C, Ehrlich H, Meyer M, Baltzer H, Worch H, et al. A Novel Biomimetic Hybrid Material Made of Silicified Collagen: Perspectives for Bone Replacement. Advanced Engineering Materials. 2007;9:1061-8.
[347] Ehrlich H, Heinemann S, Heinemann C, Simon P, Bazhenov VV, Shapkin NP, et al. Nanostructural Organization of Naturally Occurring Composites-Part I: Silica-Collagen-Based Biocomposites. Journal of Nanomaterials. 2008;2008:8.
[348] Heinemann S, Ehrlich H, Knieb C, Hanke T. Biomimetically inspired hybrid materials based on silicified collagen. International Journal of Materials Research. 2007;98:603-8.
[349] Cha C, Oh J, Kim K, Qiu Y, Joh M, Shin SR, et al. Microfluidics-assisted fabrication of gelatin-silica core-shell microgels for injectable tissue constructs. Biomacromolecules. 2014;15:283-90.
[350] Brahatheeswaran D, Yoshida Y, Maekawa T, Kumar DS. Polymeric Scaffolds in Tissue Engineering Application: A Review. International Journal of Polymer Science. 2011;2011.
[351] Tsuru K, Ohtsuki C, Osaka A, Iwamoto T, Mackenzie JD. Bioactivity of sol–gel derived organically modified silicates: Part I: In vitro examination. Journal of Materials Science: Materials in Medicine. 1997;8:157-61.
[352] Tsuru K, Aburatani Y, Yabuta T, Hayakawa S, Ohtsuki C, Osaka A. Synthesis and In Vitro Behavior of Organically Modified Silicate Containing Ca Ions. Journal of Sol-Gel Science and Technology. 2001;21:89-96.
[353] Yabuta T, Bescher EP, Mackenzie JD, Tsuru K, Hayakawa S, Osaka A. Synthesis of PDMS-based porous materials for biomedical applications. Journal of Sol-Gel Science and Technology. 2003;26:1219-22.

[354] Sánchez-Téllez DA, Téllez-Jurado L, Chávez-Alcalá JF. Bioactivity and degradability of hybrids nano-composites materials with great application as bone tissue substitutes. J Alloys Compd. 2014;615:S670-S5.
[355] Tamayo A, Téllez L, Rodríguez-Reyes M, Mazo MA, Rubio F, Rubio J. Surface properties of bioactive TEOS–PDMS–TiO2–CaO ormosils. Journal of Materials Science. 2014;49:4656-69.
[356] Chen J, Que W, Xing Y, Lei B. Molecular level-based bioactive glass-poly (caprolactone) hybrids monoliths with porous structure for bone tissue repair. Ceramics International. 2015;41:3330-4.
[357] Columbus S, Krishnan LK, Kalliyana Krishnan V. Relating pore size variation of poly (ε-caprolactone) scaffolds to molecular weight of porogen and evaluation of scaffold properties after degradation. Journal of Biomedical Materials Research Part B: Applied Biomaterials. 2014;102:789-96.
[358] Mirmohammadi SA, Imani M, Uyama H, Atai M. Hybrid organic-inorganic nanocomposites based on poly(ε-Caprolactone)/ polyhedral oligomeric silsesquioxane: Synthesis and in vitro evaluations. International Journal of Polymeric Materials and Polymeric Biomaterials. 2014;63:624-31.
[359] Choy DKS, Nga VDW, Lim J, Lu J, Chou N, Yeo TT, et al. Brain Tissue Interaction with Three-Dimensional, Honeycomb Polycaprolactone-Based Scaffolds Designed for Cranial Reconstruction Following Traumatic Brain Injury. Tissue Engineering Part A. 2013.
[360] Annabi N, Fathi A, Mithieux SM, Martens P, Weiss AS, Dehghani F. The effect of elastin on chondrocyte adhesion and proliferation on poly (ε-caprolactone)/elastin composites. Biomaterials. 2011;32:1517-25.
[361] Dessì M, Raucci MG, Zeppetelli S, Ambrosio L. Design of injectable organic-inorganic hybrid for bone tissue repair. Journal of Biomedical Materials Research - Part A. 2012;100 A:2063-70.
[362] Allo BA, Lin S, Mequanint K, Rizkalla AS. Role of bioactive 3D hybrid fibrous scaffolds on mechanical behavior and spatiotemporal osteoblast gene expression. ACS Applied Materials and Interfaces. 2013;5:7574-83.
[363] Catauro M, Raucci MG, de Marco D, Ambrosio L. Release kinetics of ampicillin, characterization and bioactivity of TiO2/PCL hybrid materials synthesized by sol–gel processing. Journal of Biomedical Materials Research Part A. 2006;77A:340-50.
[364] Catauro M, Raucci M, Ausanio G. Sol–gel processing of drug delivery zirconia/polycaprolactone hybrid materials. Journal of Materials Science: Materials in Medicine. 2008;19:531-40.
[365] Catauro M, Raucci MG, De Gaetano F, Marotta A. Sol-gel synthesis, characterization and bioactivity of polycaprolactone/SiO2 hybrid material. Journal of Materials Science. 2003;38:3097-102.
[366] Russo T, Gloria A, D'Antò V, D'Amora U, Ametrano G, Bollino F, et al. Poly(ε-caprolactone) reinforced with sol-gel synthesized organic-inorganic hybrid fillers as composite substrates for tissue engineering. Journal of Applied Biomaterials and Biomechanics. 2010;8:146-52.

[367] Catauro M, Verardi D, Melisi D, Belotti F, Mustarelli P. Novel sol-gel organic-inorganic hybrid materials for drug delivery. Journal of Applied Biomaterials and Biomechanics. 2010;8:42-51.
[368] De Santis R, Gloria A, Russo T, D'Amora U, D'Antò V, Bollino F, et al. Advanced composites for hard-tissue engineering based on PCL/organic-inorganic hybrid fillers: From the design of 2D substrates to 3D rapid prototyped scaffolds. Polym Compos. 2013;34:1413-7.
[369] Castaño O, Sachot N, Xuriguera E, Engel E, Planell JA, Park JH, et al. Angiogenesis in bone regeneration: Tailored calcium release in hybrid fibrous scaffolds. ACS Applied Materials and Interfaces. 2014;6:7512-22.
[370] Allo BA, Rizkalla AS, Mequanint K. Hydroxyapatite formation on sol-gel derived poly(ε-caprolactone)/ bioactive glass hybrid biomaterials. ACS Applied Materials and Interfaces. 2012;4:3148-56.
[371] Chiellini E, Corti A, D'Antone S, Solaro R. Biodegradation of poly (vinyl alcohol) based materials. Progress in Polymer Science. 2003;28:963-1014.
[372] Corti A, Solaro R, Chiellini E. Biodegradation of poly(vinyl alcohol) in selected mixed microbial culture and relevant culture filtrate. Polymer Degradation and Stability. 2002;75:447-58.
[373] Eubeler JP, Bernhard M, Knepper TP. Environmental biodegradation of synthetic polymers II. Biodegradation of different polymer groups. TrAC Trends in Analytical Chemistry. 2010;29:84-100.
[374] Pereira APV, Vasconcelos WL, Oréfice RL. Novel multicomponent silicate–poly(vinyl alcohol) hybrids with controlled reactivity. Journal of Non-Crystalline Solids. 2000;273:180-5.
[375] Costa H, Rocha M, Andrade G, Barbosa-Stancioli E, Pereira M, Orefice R, et al. Sol–gel derived composite from bioactive glass–polyvinyl alcohol. Journal of Materials Science. 2008;43:494-502.
[376] Costa H, Stancioli EB, Pereira M, Oréfice R, Mansur H. Synthesis, neutralization and blocking procedures of organic/inorganic hybrid scaffolds for bone tissue engineering applications. Journal of Materials Science: Materials in Medicine. 2009;20:529-35.
[377] Costa HS, Mansur AAP, Pereira MM, Mansur HS. Engineered hybrid scaffolds of poly(vinyl alcohol)/bioactive glass for potential bone engineering applications: Synthesis, characterization, cytocompatibility, and degradation. Journal of Nanomaterials. 2012;2012.
[378] Mansur HS, Costa HS, Mansur AAP, Pereira M. 3D-macroporous hybrid scaffolds for tissue engineering: Network design and mathematical modeling of the degradation kinetics. Materials Science and Engineering: C. 2012;32:404-15.
[379] Interrante LV, Rushkin I, Shen Q. Linear and Hyperbranched Polycarbosilanes with Si-CH2-Si Bridging Groups: A Synthetic Platform for the Construction of Novel Functional Polymeric Materials. Appl Organomet Chem. 1998;12:695-705.
[380] Sangermano M, Marchi S, Ligorio D, Meier P, Kornmann X. UV-induced frontal polymerization of a pt-catalyzed hydrosilation reaction. Macromolecular Chemistry and Physics. 2013;214:943-7.
[381] Ogoshi T, Chujo Y. Organic–inorganic polymer hybrids prepared by the sol-gel method. Composite Interfaces. 2005;11:539-66.

[382] Hermanson GT. Chapter 13 - Silane Coupling Agents. In: Hermanson GT, editor. Bioconjugate Techniques (Third edition). Boston: Academic Press; 2013. p. 535-48.
[383] Shojaie SS, Rials TG, Kelley SS. Preparation and characterization of cellulose acetate organic/inorganic hybrid films. Journal of Applied Polymer Science. 1995;58:1263-74.
[384] Wojciechowska P, Foltynowicz Z, Nowicki M. Cellulose acetate butyrate nanocomposites synthesized via sol-gel method. Polimery/Polymers. 2013;58:543-9.
[385] Wojciechowska P, Foltynowicz Z, Nowicki M. Synthesis and Characterization of Modified Cellulose Acetate Propionate Nanocomposites via Sol-Gel Process. Journal of Spectroscopy. 2013;2013:8.
[386] Sakai S, Ono T, Ijima H, Kawakami K. Synthesis and transport characterization of alginate/aminopropyl-silicate/alginate microcapsule: application to bioartificial pancreas. Biomaterials. 2001;22:2827-34.
[387] Sakai S, Ono T, Ijima H, Kawakami K. In vitro and in vivo evaluation of alginate/sol–gel synthesized aminopropyl-silicate/alginate membrane for bioartificial pancreas. Biomaterials. 2002;23:4177-83.
[388] Shirosaki Y, Tsuru K, Hayakawa S, Osaka A, Lopes MA, Santos JD, et al. In vitro cytocompatibility of MG63 cells on chitosan-organosiloxane hybrid membranes. Biomaterials. 2005;26:485-93.
[389] Shirosaki Y, Okayama T, Tsuru K, Hayakawa S, Osaka A. Synthesis and cytocompatibility of porous chitosan-silicate hybrids for tissue engineering scaffold application. Chemical Engineering Journal. 2008;137:122-8.
[390] Shirosaki Y, Tsuru K, Hayakawa S, Osaka A, Lopes MA, Santos JD, et al. Physical, chemical and in vitro biological profile of chitosan hybrid membrane as a function of organosiloxane concentration. Acta Biomaterialia. 2009;5:346-55.
[391] Chen S, Hanagata N. Directing osteoblast alignment and elongation on the micro-grooved silica-based hybrid membrane. Advanced Materials Research. 2013;647:165-9.
[392] Foglia ML, Camporotondi DE, Alvarez GS, Heinemann S, Hanke T, Perez CJ, et al. A new method for the preparation of biocompatible silica coated-collagen hydrogels. Journal of Materials Chemistry B. 2013;1:6283-90.
[393] Chen S, Chinnathambi S, Shi X, Osaka A, Zhu Y, Hanagata N. Fabrication of novel collagen-silica hybrid membranes with tailored biodegradation and strong cell contact guidance ability. Journal of Materials Chemistry. 2012;22:21885-92.
[394] Tonda-Turo C, Gentile P, Saracino S, Chiono V, Nandagiri VK, Muzio G, et al. Comparative analysis of gelatin scaffolds crosslinked by genipin and silane coupling agent. International Journal of Biological Macromolecules. 2011;49:700-6.
[395] Tonda-Turo C, Cipriani E, Gnavi S, Chiono V, Mattu C, Gentile P, et al. Crosslinked gelatin nanofibres: Preparation, characterisation and in vitro studies using glial-like cells. Materials Science and Engineering C. 2013;33:2723-35.

[396] Lei B, Shin KH, Koh YH, Kim HE. Porous gelatin-siloxane hybrid scaffolds with biomimetic structure and properties for bone tissue regeneration. Journal of Biomedical Materials Research - Part B Applied Biomaterials. 2014;102:1528-36.
[397] Tsuru K, Robertson Z, Annaz B, Gibson IR, Best SM, Shirosaki Y, et al. Sol-gel synthesis and in vitro cell compatibility analysis of silicate-containing biodegradable hybrid gels. Key Engineering Materials. 2008;361-363 I:447-50.
[398] Ren L, Tsuru K, Hayakawa S, Osaka A. Novel approach to fabricate porous gelatin–siloxane hybrids for bone tissue engineering. Biomaterials. 2002;23:4765-73.
[399] Song J-H, Yoon B-H, Kim H-E, Kim H-W. Bioactive and degradable hybridized nanofibers of gelatin–siloxane for bone regeneration. Journal of Biomedical Materials Research Part A. 2008;84A:875-84.
[400] Mahony O, Tsigkou O, Ionescu C, Minelli C, Ling L, Hanly R, et al. Silica-Gelatin Hybrids with Tailorable Degradation and Mechanical Properties for Tissue Regeneration. Advanced Functional Materials. 2010;20:3835-45.
[401] Mahony O, Yue S, Turdean-Ionescu C, Hanna J, Smith M, Lee P, et al. Silica–gelatin hybrids for tissue regeneration: inter-relationships between the process variables. Journal of Sol-Gel Science and Technology. 2014;69:288-98.
[402] Gao C, Gao Q, Li Y, Rahaman MN, Teramoto A, Abe K. In vitro evaluation of electrospun gelatin-bioactive glass hybrid scaffolds for bone regeneration. Journal of Applied Polymer Science. 2013;127:2588-99.
[403] Dashnyam K, Perez RA, Singh RK, Lee E-J, Kim H-W. Hybrid magnetic scaffolds of gelatin-siloxane incorporated with magnetite nanoparticles effective for bone tissue engineering. RSC Advances. 2014;4:40841-51.
[404] Yoo JJ, Lee JE, Kim HJ, Kim S-J, Lim JH, Lee SJ, et al. Comparative in vitro and in vivo studies using a bioactive poly(ε-caprolactone)-organosiloxane nanohybrid containing calcium salt. Journal of Biomedical Materials Research Part B: Applied Biomaterials. 2007;83B:189-98.
[405] Skarmoutsou A, Lolas G, Charitidis CA, Chatzinikolaidou M, Vamvakaki M, Farsari M. Nanomechanical properties of hybrid coatings for bone tissue engineering. Journal of the Mechanical Behavior of Biomedical Materials. 2013;25:48-62.
[406] Terzaki K, Kissamitaki M, Skarmoutsou A, Fotakis C, Charitidis CA, Farsari M, et al. Pre-osteoblastic cell response on three-dimensional, organic-inorganic hybrid material scaffolds for bone tissue engineering. Journal of Biomedical Materials Research - Part A. 2013;101 A:2283-94.
[407] Chatzinikolaidou M, Rekstyte S, Danilevicius P, Pontikoglou C, Papadaki H, Farsari M, et al. Adhesion and growth of human bone marrow mesenchymal stem cells on precise-geometry 3D organic-inorganic composite scaffolds for bone repair. Materials Science and Engineering C. 2015;48:301-9.
[408] Poologasundarampillai G, Ionescu C, Tsigkou O, Murugesan M, Hill RG, Stevens MM, et al. Synthesis of bioactive class II poly([gamma]-

glutamic acid)/silica hybrids for bone regeneration. Journal of Materials Chemistry. 2010;20:8952-61.
[409] Poologasundarampillai G, Yu B, Tsigkou O, Valliant E, Yue S, Lee PD, et al. Bioactive silica-poly([gamma]-glutamic acid) hybrids for bone regeneration: effect of covalent coupling on dissolution and mechanical properties and fabrication of porous scaffolds. Soft Matter. 2012;8:4822-32.
[410] Poologasundarampillai G, Yu B, Tsigkou O, Wang D, Romer F, Bhakhri V, et al. Poly(γ-glutamic acid)/Silica Hybrids with Calcium Incorporated in the Silica Network by Use of a Calcium Alkoxide Precursor. Chemistry – A European Journal. 2014;20:8149-60.
[411] Wang D, Nakamura J, Poologasundarampillai G, Kasuga T, Jones JR, McPhail DS. ToF-SIMS evaluation of calcium-containing silica/γ-PGA hybrid systems for bone regeneration. Applied Surface Science. 2014;309:231-9.
[412] Maeda H, Kasuga T, Hench LL. Preparation of poly(l-lactic acid)-polysiloxane-calcium carbonate hybrid membranes for guided bone regeneration. Biomaterials. 2006;27:1216-22.
[413] Sachot N, Castaño O, Mateos-Timoneda MA, Engel E, Planell JA. Hierarchically engineered fibrous scaffolds for bone regeneration. Journal of The Royal Society Interface. 2013;10:1-5.
[414] Ravarian R, Zhong X, Barbeck M, Ghanaati S, Kirkpatrick CJ, Murphy CM, et al. Nanoscale chemical interaction enhances the physical properties of bioglass composites. ACS Nano. 2013;7:8469-83.
[415] Rey C, Combes C, Drouet C, Glimcher MJ. Bone mineral: Update on chemical composition and structure. Osteoporos Int. 2009;20:1013-21.
[416] Wang Y, Azaïs T, Robin M, Vallée A, Catania C, Legriel P, et al. The predominant role of collagen in the nucleation, growth, structure and orientation of bone apatite. Nat Mater. 2012;11:724-33.
[417] Heinemann S, Coradin T, Desimone MF. Bio-inspired silica-collagen materials: applications and perspectives in the medical field. Biomaterials Science. 2013;1:688-702.
[418] Lausch AJ, Quan BD, Miklas JW, Sone ED. Extracellular Matrix Control of Collagen Mineralization In Vitro. Advanced Functional Materials. 2013;23:4906-12.
[419] Marelli B, Ghezzi CE, Mohn D, Stark WJ, Barralet JE, Boccaccini AR, et al. Accelerated mineralization of dense collagen-nano bioactive glass hybrid gels increases scaffold stiffness and regulates osteoblastic function. Biomaterials. 2011;32:8915-26.
[420] Bi L, Li D, Liu J, Hu Y, Yang P, Yang B, et al. Fabrication and characterization of a biphasic scaffold for osteochondral tissue engineering. Materials Letters. 2011;65:2079-82.
[421] Swetha M, Sahithi K, Moorthi A, Srinivasan N, Ramasamy K, Selvamurugan N. Biocomposites containing natural polymers and hydroxyapatite for bone tissue engineering. International Journal of Biological Macromolecules. 2010;47:1-4.
[422] Ren L, Tsuru K, Hayakawa S, Osaka A. Synthesis and Characterization of Gelatin-Siloxane Hybrids Derived through Sol-Gel Procedure. Journal of Sol-Gel Science and Technology. 2001;21:115-21.

[423] Ren L, Tsuru K, Hayakawa S, Osaka A. Sol–gel preparation and in vitro deposition of apatite on porous gelatin–siloxane hybrids. Journal of Non-Crystalline Solids. 2001;285:116-22.
[424] unter GK, Goldberg HA. Modulation of crystal formation by bone phosphoproteins: Role of glutamic acid-rich sequences in the nucleation of hydroxyapatite by bone sialoprotein. Biochemical Journal. 1994;302:175-9.
[425] Tian D, Dubois P, Jerome R. A new poly(ε-caprolactone) containing hybrid ceramer prepared by the sol-gel process. Polymer. 1996;37:3983-7.
[426] Tian D, Dubois P, Grandfils C, Jérôme R, Viville P, Lazzaroni R, et al. A Novel Biodegradable and Biocompatible Ceramer Prepared by the Sol−Gel Process. Chemistry of Materials. 1997;9:871-4.
[427] Tian D, Dubois P, Jérôme R. Biodegradable and biocompatible inorganic–organic hybrid materials. I. Synthesis and characterization. Journal of Polymer Science Part A: Polymer Chemistry. 1997;35:2295-309.
[428] Tian D, Blacher S, Dubois P, Jérôme R. Biodegradable and biocompatible inorganic-organic hybrid materials: 2. Dynamic mechanical properties, structure and morphology. Polymer. 1998;39:855-64.
[429] Tian D, Blacher S, Pirard J-P, Jérôme R. Biodegradable and Biocompatible Inorganic−Organic Hybrid Materials. 3. A Valuable Route to the Control of the Silica Porosity. Langmuir. 1998;14:1905-10.
[430] Tian D, Blacher S, Jerome R. Biodegradable and biocompatible inorganic–organic hybrid materials: 4. Effect of acid content and water content on the incorporation of aliphatic polyesters into silica by the sol-gel process. Polymer. 1999;40:951-7.
[431] Ravarian R, Wei H, Rawal A, Hook J, Chrzanowski W, Dehghani F. Molecular interactions in coupled PMMA-bioglass hybrid networks. Journal of Materials Chemistry B. 2013;1:1835-45.
[432] Nagarale RK, Shin W, Singh PK. Progress in ionic organic-inorganic composite membranes for fuel cell applications. Polymer Chemistry. 2010;1:388-408.
[433] Nagarale RK, Gohil GS, Shahi VK, Rangarajan R. Organic−Inorganic Hybrid Membrane: Thermally Stable Cation-Exchange Membrane Prepared by the Sol−Gel Method. Macromolecules. 2004;37:10023-30.
[434] Nagarale RK, Shahi VK, Rangarajan R. Preparation of polyvinyl alcohol–silica hybrid heterogeneous anion-exchange membranes by sol–gel method and their characterization. Journal of Membrane Science. 2005;248:37-44.
[435] Kickelbick G. The search of a homogeneously dispersed material—the art of handling the organic polymer/metal oxide interface. Journal of Sol-Gel Science and Technology. 2008;46:281-90.
[436] Scherer GW. Recent progress in drying of gels. Journal of Non-Crystalline Solids. 1992;147–148:363-74.
[437] Wang B, Zhang W, Mujumdar AS, Huang L. Progress in drying technology for nanomaterials. Drying Technol. 2005;23:7-32.
[438] Zarzycki J, Prassas M, Phalippou J. Synthesis of glasses from gels: the problem of monolithic gels. Journal of Materials Science. 1982;17:3371-9.
[439] Phalippou J, Woignier T, Prassas M. Glasses from aerogels. Journal of Materials Science. 1990;25:3111-7.

[440] Ruiz-Hitzky E, Casal B, Aranda P, Galván JC. Inorganic-organic nanocomposite materials based on macrocyclic compounds. Rev Inorg Chem. 2001;21:125-59.
[441] Hamidi M, Azadi A, Rafiei P. Hydrogel nanoparticles in drug delivery. Advanced Drug Delivery Reviews. 2008;60:1638-49.
[442] Kokubo T, Takadama H. How useful is SBF in predicting in vivo bone bioactivity? Biomaterials. 2006;27:2907-15.
[443] Van Den Bulcke AI, Bogdanov B, De Rooze N, Schacht EH, Cornelissen M, Berghmans H. Structural and Rheological Properties of Methacrylamide Modified Gelatin Hydrogels. Biomacromolecules. 2000;1:31-8.
[444] Caldwell CG, Wurzburg OB. Unsaturated starch compounds and insoluble derivatives thereof. Google Patents; 1954.
[445] Coradin T, Eglin D, Livage J. The silicomolybdic acid spectrophotometric method and its application to silicate/biopolymer interaction studies. Spectroscopy. 2004;18:567-76.
[446] Xu K, Fu Y, Chung W, Zheng X, Cui Y, Hsu IC, et al. Thiol-ene-based biological/synthetic hybrid biomatrix for 3-D living cell culture. Acta Biomaterialia. 2012;8:2504-16.
[447] Taddei P, Chiono V, Anghileri A, Vozzi G, Freddi G, Ciardelli G. Silk Fibroin/Gelatin Blend Films Crosslinked with Enzymes for Biomedical Applications. Macromolecular Bioscience. 2013;13:1492-510.
[448] Lim KS, Alves MH, Poole-Warren LA, Martens PJ. Covalent incorporation of non-chemically modified gelatin into degradable PVA-tyramine hydrogels. Biomaterials. 2013;34:7097-105.
[449] Chatterjee S, Bohidar HB. Effect of cationic size on gelation temperature and properties of gelatin hydrogels. International Journal of Biological Macromolecules. 2005;35:81-8.
[450] Pavan FA, Hoffmann HS, Gushikem Y, Costa TMH, Benvenutti EV. The gelation temperature effects in the anilinepropylsilica xerogel properties. Materials Letters. 2002;55:378-82.
[451] Musgo J, Echeverría JC, Estella J, Laguna M, Garrido JJ. Ammonia-catalyzed silica xerogels: Simultaneous effects of pH, synthesis temperature, and ethanol:TEOS and water:TEOS molar ratios on textural and structural properties. Microporous and Mesoporous Materials. 2009;118:280-7.
[452] Iler RK. The Chemisrty of Silica. New York: John Wiley & Sons; 1979.
[453] Tosh SM, Marangoni AG. Determination of the maximum gelation temperature in gelatin gels. Applied Physics Letters. 2004;84:4242-4.
[454] Giraudier S, Hellio D, Djabourov M, Larreta-Garde V. Influence of weak and covalent bonds on formation and hydrolysis of gelatin networks. Biomacromolecules. 2004;5:1662-6.
[455] Benton JA, Deforest CA, Vivekanandan V, Anseth KS. Photocrosslinking of gelatin macromers to synthesize porous hydrogels that promote valvular interstitial cell function. Tissue Engineering - Part A. 2009;15:3221-30.
[456] Jung J, Oh J. Influence of photo-initiator concentration on the viability of cells encapsulated in photo-crosslinked microgels fabricated by

microfluidics. Digest Journal of Nanomaterials and Biostructures. 2014;9:503-9.
[457] Sabnis A, Rahimi M, Chapman C, Nguyen KT. Cytocompatibility studies of an in situ photopolymerized thermoresponsive hydrogel nanoparticle system using human aortic smooth muscle cells. Journal of Biomedical Materials Research - Part A. 2009;91:52-9.
[458] Kosmulski M. Chemical Properties of Material Surfaces. New York-Basel: Marcel Dekker; 2001.
[459] Solorio L, Zwolinski C, Lund AW, Farrell MJ, Stegemann JP. Gelatin microspheres crosslinked with genipin for local delivery of growth factors. Journal of tissue engineering and regenerative medicine. 2010;4:514-23.
[460] Smitha S, Shajesh P, Mukundan P, Warrier KGK. Sol-gel synthesis of biocompatible silica-chitosan hybrids and hydrophobic coatings. Journal of Materials Research. 2008;23:2053-60.
[461] Chernev G, Rangelova N, Djambazki P, Nenkova S, Salvado I, Fernandes M, et al. Sol-gel silica hybrid biomaterials for application in biodegradation of toxic compounds. Journal of Sol-Gel Science and Technology. 2011;58:619-24.
[462] Russo L, Gabrielli L, Valliant EM, Nicotra F, Jiménez-Barbero J, Cipolla L, et al. Novel silica/bis(3-aminopropyl) polyethylene glycol inorganic/organic hybrids by sol–gel chemistry. Materials Chemistry and Physics. 2013;140:168-75.
[463] Arkles B, Steinmetz JR, Zazyczny J, Mehta P. Factors contributing to the stability of alkoxysilanes in aqueous solution. Journal of Adhesion Science and Technology. 1992;6:193-206.
[464] Gabrielli L, Russo L, Poveda A, Jones JR, Nicotra F, Jiménez-Barbero J, et al. Epoxide Opening versus Silica Condensation during Sol–Gel Hybrid Biomaterial Synthesis. Chemistry – A European Journal. 2013;19:7856-64.
[465] Tsuru K, Hayakawa S, Osaka A. Cell proliferation and tissue compatibility of organic-inorganic hybrid materials. Key Engineering Materials. 2008;377:167-80.
[466] Gabrielli L, Connell L, Russo L, Jimenez-Barbero J, Nicotra F, Cipolla L, et al. Exploring GPTMS reactivity against simple nucleophiles: chemistry beyond hybrid materials fabrication. RSC Advances. 2014;4:1841-8.
[467] Lei B, Shin K-H, Noh D-Y, Jo I-H, Koh Y-H, Choi W-Y, et al. Nanofibrous gelatin-silica hybrid scaffolds mimicking the native extracellular matrix (ECM) using thermally induced phase separation. Journal of Materials Chemistry. 2012;22:14133-40.
[468] Ball DWH, John W., Scott RJ. Amino Acids, Proteins, and Enzymes. Introduction to Chemistry: General, Organic, and Biological2011. p. 1009-83.
[469] Coates J. Interpretation of Infrared Spectra, A Practical Approach. In: Meyers RA, editor. Encyclopedia of Analytical Chemistry. Chichester: John Wiley & Sons Ltd; 2000. p. 10815–37.
[470] Yoon BH, Kim HE, Kim HW. Bioactive microspheres produced from gelatin-siloxane hybrids for bone regeneration. Journal of Materials Science: Materials in Medicine. 2008;19:2287-92.

[471] Hillel AS, P, J.H. E. Hydrogels in cell encapsulation and tissue engineering. In: Jenkins M, editor. Biomedical Polymers Cambrdige: Woodhead Publishing; 2007. p. 57-82.
[472] Allo BA, Costa DO, Dixon SJ, Mequanint K, Rizkalla AS. Bioactive and Biodegradable Nanocomposites and Hybrid Biomaterials for Bone Regeneration. Journal of Functional Biomaterials. 2012;3:432-63.
[473] Zhang R, Ma PX. Biomimetic Polymer/Apatite Composite Scaffolds for Mineralized Tissue Engineering. Macromolecular Bioscience. 2004;4:100-11.
[474] Marques MRC, Loebenberg R, Almukainzi M. Simulated Biological Fluids with Possible Application in Dissolution Testing. Dissolution Technologies. 2011;18:15-28.
[475] Oyane A, Kim H-M, Furuya T, Kokubo T, Miyazaki T, Nakamura T. Preparation and assessment of revised simulated body fluids. Journal of Biomedical Materials Research Part A. 2003;65A:188-95.
[476] Noémie L, Rune SF, Thor CM, Nathalie IR, Shivendra U, Luca De V, et al. Effects of buffer composition and dilution on nanowire field-effect biosensors. Nanotechnology. 2013;24:035501.
[477] Nelson MT, Johnson J, Lannutti J. Media-based effects on the hydrolytic degradation and crystallization of electrospun synthetic-biologic blends. Journal of Materials Science: Materials in Medicine. 2014;25:297-309.
[478] Patterson J, Siew R, Herring SW, Lin ASP, Guldberg R, Stayton PS. Hyaluronic acid hydrogels with controlled degradation properties for oriented bone regeneration. Biomaterials. 2010;31:6772-81.
[479] Chatterjee K, Lin-Gibson S, Wallace WE, Parekh SH, Lee YJ, Cicerone MT, et al. The effect of 3D hydrogel scaffold modulus on osteoblast differentiation and mineralization revealed by combinatorial screening. Biomaterials. 2010;31:5051-62.
[480] Killion JA, Kehoe S, Geever LM, Devine DM, Sheehan E, Boyd D, et al. Hydrogel/bioactive glass composites for bone regeneration applications: Synthesis and characterisation. Materials Science and Engineering C. 2013;33:4203-12.
[481] Ahadian S, Ramón-Azcón J, Estili M, Liang X, Ostrovidov S, Shiku H, et al. Hybrid hydrogels containing vertically aligned carbon nanotubes with anisotropic electrical conductivity for muscle myofiber fabrication. Sci Rep. 2014;4.
[482] Ramón-Azcón J, Ahadian S, Estili M, Liang X, Ostrovidov S, Kaji H, et al. Dielectrophoretically Aligned Carbon Nanotubes to Control Electrical and Mechanical Properties of Hydrogels to Fabricate Contractile Muscle Myofibers. Advanced Materials. 2013;25:4028-34.
[483] Kishi R, Kubota K, Miura T, Yamaguchi T, Okuzaki H, Osada Y. Mechanically tough double-network hydrogels with high electronic conductivity. Journal of Materials Chemistry C. 2014;2:736-43.
[484] Shin H, Olsen BD, Khademhosseini A. The mechanical properties and cytotoxicity of cell-laden double-network hydrogels based on photocrosslinkable gelatin and gellan gum biomacromolecules. Biomaterials. 2012;33:3143-52.

[485] Hagiwara Y, Putra A, Kakugo A, Furukawa H, Gong J. Ligament-like tough double-network hydrogel based on bacterial cellulose. Cellulose. 2010;17:93-101.
[486] Bakarich SE, Gorkin R, in het Panhuis M, Spinks GM. Three-Dimensional Printing Fiber Reinforced Hydrogel Composites. ACS Applied Materials & Interfaces. 2014;6:15998-6006.
[487] Agrawal A, Rahbar N, Calvert PD. Strong fiber-reinforced hydrogel. Acta Biomaterialia. 2013;9:5313-8.
[488] Masuelli MA. Introduction of Fibre-Reinforced Polymers − Polymers and Composites: Concepts, Properties and Processes2013.
[489] Zhou Y, Ma G, Shi S, Yang D, Nie J. Photopolymerized water-soluble chitosan-based hydrogel as potential use in tissue engineering. International Journal of Biological Macromolecules. 2011;48:408-13.
[490] Coutinho DF, Sant SV, Shin H, Oliveira JT, Gomes ME, Neves NM, et al. Modified Gellan Gum hydrogels with tunable physical and mechanical properties. Biomaterials. 2010;31:7494-502.
[491] Tahir MN, Adnan A, Cho E, Jung S. Controlled ondansetron release based on hydroxyethyl starch hydroxyethyl methacrylate. Bulletin of the Korean Chemical Society. 2012;33:4035-40.
[492] Mendes A, Boesel L, Reis R. Degradation studies of hydrophilic, partially degradable and bioactive cements (HDBCs) incorporating chemically modified starch. Journal of Materials Science: Materials in Medicine. 2012;23:667-76.
[493] Heydari M, Rahman M, Gupta R. Kinetic Study and Thermal Decomposition Behavior of Lignite Coal. International Journal of Chemical Engineering. 2015;2015:9.
[494] Tester RF, Morrison WR. Swelling and gelatinization of cereal starches. I. Effects of amylopectin, amylose, and lipids. Cereal Chemistry. 1990;67:551-7.
[495] Caves JM, Cui W, Wen J, Kumar VA, Haller CA, Chaikof EL. Elastin-like protein matrix reinforced with collagen microfibers for soft tissue repair. Biomaterials. 2011;32:5371-9.
[496] Grover GN, Rao N, Christman KL. Myocardial matrix-polyethylene glycol hybrid hydrogels for tissue engineering. Nanotechnology. 2014;25.
[497] Lee CY, Teymour F, Camastral H, Tirelli N, Hubbell JA, Elbert DL, et al. Characterization of the Network Structure of PEG Diacrylate Hydrogels Formed in the Presence of N-Vinyl Pyrrolidone. Macromolecular Reaction Engineering. 2014;8:314-28.
[498] Zuo Y, Xiao W, Chen X, Tang Y, Luo H, Fan H. Bottom-up approach to build osteon-like structure by cell-laden photocrosslinkable hydrogel. Chemical Communications. 2012;48:3170-2.
[499] Liu Z, Wang L, Bao C, Li X, Cao L, Dai K, et al. Cross-linked PEG via degradable phosphate ester bond: Synthesis, water-swelling, and application as drug carrier. Biomacromolecules. 2011;12:2389-95.
[500] Cuchiara MP, Allen ACB, Chen TM, Miller JS, West JL. Multilayer microfluidic PEGDA hydrogels. Biomaterials. 2010;31:5491-7.
[501] Negahi Shirazi A, Tajabadi M, Imani M, Sharifi S. Grafting and characterization of poly(ethylene glycol) mono methyl ether on poly(methacrylic acid-co-methyl methacrylate) via direct condensation.

Industrial Electronics & Applications, 2009 ISIEA 2009 IEEE Symposium on2009. p. 842-5.
[502] Lin C-C, Anseth K. PEG Hydrogels for the Controlled Release of Biomolecules in Regenerative Medicine. Pharmaceutical research. 2009;26:631-43.
[503] Paxton JZ, Donnelly K, Keatch RP, Baar K. Engineering the bone-ligament interface using polyethylene glycol diacrylate incorporated with hydroxyapatite. Tissue Engineering - Part A. 2009;15:1201-9.
[504] Shirosaki Y. Preparation of organic-inorganic hybrids with silicate network for the medical applications. Nippon Seramikkusu Kyokai Gakujutsu Ronbunshi/Journal of the Ceramic Society of Japan. 2012;120:555-9.
[505] Albee FH. Studies in Bone Growth Triple Calcium Phosphate as a Stimulus to Osteogenesis. Annals of Surgery. 1920;71:32-9.
[506] Seidi A, Ramalingam M, Elloumi-Hannachi I, Ostrovidov S, Khademhosseini A. Gradient biomaterials for soft-to-hard interface tissue engineering. Acta Biomaterialia. 2011;7:1441-51.
[507] Peppas NA, Hilt JZ, Khademhosseini A, Langer R. Hydrogels in biology and medicine: from molecular principles to bionanotechnology. Adv Mat. 2006;18:1345-60.
[508] Caggioni M, Bayles AV, Lenis J, Furst EM, Spicer PT. Interfacial stability and shape change of anisotropic endoskeleton droplets. Soft Matter. 2014;10:7647-52.
[509] van de Wetering P, Metters AT, Schoenmakers RG, Hubbell JA. Poly(ethylene glycol) hydrogels formed by conjugate addition with controllable swelling, degradation, and release of pharmaceutically active proteins. Journal of Controlled Release. 2005;102:619-27.
[510] Kim J, Kim IS, Cho TH, Kim HC, Yoon SJ, Choi J, et al. In vivo evaluation of MMP sensitive high-molecular weight HA-based hydrogels for bone tissue engineering. Journal of Biomedical Materials Research Part A. 2010;95A:673-81.
[511] Ross AE, Tang MY, Gemeinhart RA. Effects of Molecular Weight and Loading on Matrix Metalloproteinase-2 Mediated Release from Poly(Ethylene Glycol) Diacrylate Hydrogels. The AAPS Journal. 2012;14:482-90.
[512] Browning MB, Cereceres SN, Luong PT, Cosgriff-Hernandez EM. Determination of the in vivo degradation mechanism of PEGDA hydrogels. Journal of Biomedical Materials Research Part A. 2014;102:4244-51.
[513] Parlato M, Reichert S, Barney N, Murphy WL. Poly(ethylene glycol) Hydrogels with Adaptable Mechanical and Degradation Properties for Use in Biomedical Applications. Macromolecular bioscience. 2014;14:687-98.
[514] Xin AX, Gaydos C, Mao JJ. In vitro Degradation Behavior of Photopolymerized PEG Hydrogels as Tissue Engineering Scaffold. Engineering in Medicine and Biology Society, 2006 EMBS '06 28th Annual International Conference of the IEEE2006. p. 2091-3.
[515] Tzaphlidou M. Bone Architecture: Collagen Structure and Calcium/Phosphorus Maps. J Biol Phys. 2008;34:39-49.
[516] Lin R-Z, Chen Y-C, Moreno-Luna R, Khademhosseini A, Melero-Martin JM. Transdermal regulation of vascular network bioengineering

using a photopolymerizable methacrylated gelatin hydrogel. Biomaterials. 2013;34:6785-96.
[517] Chen Y-C, Lin R-Z, Qi H, Yang Y, Bae H, Melero-Martin JM, et al. Functional Human Vascular Network Generated in Photocrosslinkable Gelatin Methacrylate Hydrogels. Advanced Functional Materials. 2012;22:2027-39.
[518] Berdichevski A, Shachaf Y, Wechsler R, Seliktar D. Protein composition alters in vivo resorption of PEG-based hydrogels as monitored by contrast-enhanced MRI. Biomaterials. 2015;42:1-10.
[519] Miyawaki O, Norimatsu Y, Kumagai H, Irimoto Y, Kumagai H, Sakurai H. Effect of water potential on sol–gel transition and intermolecular interaction of gelatin near the transition temperature. Biopolymers. 2003;70:482-91.
[520] Chen X, Jia Y, Feng L, Sun S, An L. Numerical simulation of coil-helix transition processes of gelatin. Polymer. 2009;50:2181-9.
[521] Herrera A, Martínez F, Iglesias D, Cegõino J, Ibarz E, Gracia L. Fixation strength of biocomposite wedge interference screw in ACL reconstruction: Effect of screw length and tunnel/screw ratio. A controlled laboratory study. BMC Musculoskeletal Disorders. 2010;11.
[522] Harvey A, Thomas NP, Amis AA. Fixation of the graft in reconstruction of the anterior cruciate ligament. Journal of Bone & Joint Surgery, British Volume. 2005;87-B:593-603.

# Appendix A

## *Appendix A the precise amount of materials for synthesising of photocrosslinkable polymers and fabrication of various hydrogels*

**Table 1 The accurate amount of materials for synthesis of GelMA***

| Material | Polymeric solution | | Temperature (C) | MA* solution | | Final Volume (ml) |
|---|---|---|---|---|---|---|
| | Mass (g) | PBS* (ml) | | Mass (g) | PBS (ml) | |
| Gelatin (Porcine) | 10.625 | 87.5 | 50 | 1.51 | 20 | 600 (100+500) |

*__GelMA__: Gelatin-methacrylate; **MA**: Methacrylic anhydride; **PBS**: Phosphate Buffer Saline

**Table 2 The accurate amount of materials for synthesis of StaMA***

| Material | Polymeric solution | | Temperature (C) | MA* solution | | NaOH solution | | Final Volume (ml) |
|---|---|---|---|---|---|---|---|---|
| | Mass (g) | PBS* (ml) | | Mass (g) | PBS (ml) | Mass (g) | PBS (mL) | |
| Starch | 40 | 80 | 50 | 1.51 | 20 | 3 | 100 | 100 |

*__StaMA__: Starch-Methacrylate; **MA**: Methacrylic anhydride; **PBS**: Phosphate Buffer Saline.

**Table 3 The accurate amount of materials for synthesis of BG***

| Material | Bioactive glass precursor (ml) | Distilled Water (ml) | Hydrochloric acid (µl) |
|---|---|---|---|
| Tetraethyl orthosilicate (TEOS) | 5.54 | 3.625 | 50 |
| Tetramethyl orthosilicate (TMOS) | 2 | 18 | - |

*__BG__: Bioactive Glass

**Table 4 The precise amount of materials for fabrication of interpenetrated gelatin-BG hybrid hydrogels**

| Hydrogel | Gelatin (GelMA*) | | Genipin | | Irgacure | | BG* | | Final Volume (ml) |
|---|---|---|---|---|---|---|---|---|---|
| | Mass (mg) | PBS* (ml) | Mass (mg) | PBS (ml) | Mass (mg) | PBS (ml) | Ratio (µl/mg) | Volume (ml) | |
| Gel_GP1 | 200 | 1.25 | 2.67 | 0.75 | - | - | 0 | 0 | 2 |
| Gel_GP2.5 | 200 | 1.25 | 6.67 | 0.75 | - | - | 0 | 0 | 2 |
| Gel_GP5 | 200 | 1.25 | 13.3 | 0.75 | - | - | 0 | 0 | 2 |
| Gel_GP7.5 | 200 | 1.25 | 20 | 0.75 | - | - | 0 | 0 | 2 |
| Hybrid_B1 | 200 | 1.0 | 6.25 | 0.8 | - | - | 1 | 0.2 | 2 |
| Hybrid_B1.5 | 200 | 1.0 | 7.14 | 0.7 | - | - | 1.5 | 0.3 | 2 |
| Hybrid_B2 | 200 | 1.0 | 8.3 | 0.6 | - | - | 2 | 0.4 | 2 |
| Hybrid_B4 | 200 | 0.8 | 12.5 | 0.4 | - | - | 4 | 0.8 | 2 |
| Hybrid_B6 | 200 | 0.5 | 16.7 | 0.3 | - | - | 6 | 1.2 | 2 |
| GelMA | 200 | 2 | - | - | 6.67 | 0.3 | 0 | 0 | 2 |
| Gel-B0.5 | 200 | 1.6 | - | - | 6.67 | 0.3 | 0.5 | 0.1 | 2 |
| Gel-B1 | 200 | 1.5 | - | - | 6.67 | 0.3 | 1 | 0.2 | 2 |
| Gel-B2 | 200 | 1.3 | - | - | 6.67 | 0.3 | 2 | 0.4 | 2 |

*__GelMA__: Gelatin-Methacrylate; **BG**: Bioactive Glass (from Tetraethyl orthosilicate); **PBS**: Phosphate Buffer Saline.

**Table 5 The precise amount of materials for fabrication of covalently-bonded Fn-GelMA-BG hybrid hydrogels**

| Hydrogel | GelMA* | | Irgacure | | GPTMS* (ml) | BG* | | Final Volume (ml) |
|---|---|---|---|---|---|---|---|---|
| | Mass (mg) | PBS* (ml) | Mass (mg) | PBS (ml) | | Ratio (µl/mg) | Volume (ml) | |
| Gel_75 | 150 | 1.7 | 6.67 | 0.3 | 0 | 0 | 0 | 2 |
| Fn-Gel_75 | 150 | 1.686 | 6.67 | 0.3 | 0.014 | 0 | 0 | 2 |
| Fn-G75-B0.25 | 150 | 1.648 | 6.67 | 0.3 | 0.014 | 0.25 | 0.038 | 2 |
| Fn-G75-B0.5 | 150 | 1.611 | 6.67 | 0.3 | 0.014 | 0.5 | 0.075 | 2 |
| Fn-G75-B1 | 150 | 1.536 | 6.67 | 0.3 | 0.014 | 1 | 0.15 | 2 |
| Gel_100 | 200 | 1.7 | 6.67 | 0.3 | 0 | 0 | 0 | 2 |
| Fn-Gel_100 | 200 | 1.682 | 6.67 | 0.3 | 0.018 | 0 | 0 | 2 |
| Fn-G100-B0.25 | 200 | 1.632 | 6.67 | 0.3 | 0.018 | 0.25 | 0.05 | 2 |
| Fn-G100-B0.5 | 200 | 1.582 | 6.67 | 0.3 | 0.018 | 0.5 | 0.1 | 2 |
| Fn-G100-B1 | 200 | 1.482 | 6.67 | 0.3 | 0.018 | 1 | 0.2 | 2 |
| Gel_150 | 300 | 1.7 | 6.67 | 0.3 | 0 | 0 | 0 | 2 |
| Fn-Gel_150 | 300 | 1.672 | 6.67 | 0.3 | 0.028 | 0 | 0 | 2 |
| Fn-G150-B0.25 | 300 | 1.597 | 6.67 | 0.3 | 0.028 | 0.25 | 0.075 | 2 |
| Fn-G150-B0.5 | 300 | 1.522 | 6.67 | 0.3 | 0.028 | 0.5 | 0.15 | 2 |
| Fn-G150-B1 | 300 | 1.372 | 6.67 | 0.3 | 0.028 | 1 | 0.3 | 2 |

*__GelMA__: Gelatin-Methacrylate; **GPTMS**: Glycidoxypropylene trimethoxysilane; **BG**: Bioactive Glass (from Tetraethyl orthosilicate); **PBS**: Phosphate Buffer Saline.

**Table 6 The precise amount of materials for fabrication of conjugated Fn-GelMA-StaMA-BG hybrid hydrogels**

| Hydrogel | Organic Content | | | Irgacure | | GPTMS* (ml) | BG* | | Final Volume (ml) |
|---|---|---|---|---|---|---|---|---|---|
| | GelMA* (mg) | StaMA* (mg) | PBS* (ml) | Mass (mg) | PBS (ml) | | Ratio (µl/mg) | Volume (ml) | |
| Gel | 200 | 0 | 1.7 | 6.67 | 0.3 | 0 | 0 | 0 | 2 |
| Fn-Gel-BG | 200 | 0 | 1.582 | 6.67 | 0.3 | 0.018 | 0.5 | 0.1 | 2 |
| Gel-Sta | 200 | 40 | 1.7 | 6.67 | 0.3 | 0 | 0 | 0 | 2 |
| Fn-Gel-Sta-BG | 200 | 40 | 1.562 | 6.67 | 0.3 | 0.018 | 0.5 | 0.12 | 2 |

*__GelMA__: Gelatin-Methacrylate; **StaMA**: Starch-Methacrylate; **GPTMS**: Glycidoxypropylene trimethoxysilane; **BG**: Bioactive Glass (from Tetraethyl orthosilicate); **PBS**: Phosphate Buffer Saline.

**Table 7 The precise amount of materials for fabrication of conjugated Fn-GelMA-PEGDA-BG hybrid**

| Hydrogel | Organic Content | | | Irgacure | | GPTMS* (ml) | BG* | | Final Volume (ml) |
|---|---|---|---|---|---|---|---|---|---|
| | GelMA* (mg) | PEGDA* (mg) | PBS* (ml) | Mass (mg) | PBS (ml) | | Ratio (µl/mg) | Volume (ml) | |
| Gel | 200 | 0 | 1.7 | 6.67 | 0.3 | 0 | 0 | 0 | 2 |
| Gel-P50 | 200 | 100 | 1.7 | 6.67 | 0.3 | 0 | 0 | 0 | 2 |
| Gel-P100 | 200 | 200 | 1.7 | 6.67 | 0.3 | 0 | 0 | 0 | 2 |
| Gel-P150 | 200 | 300 | 1.7 | 6.67 | 0.3 | 0 | 0 | 0 | 2 |
| Gel-P200 | 200 | 400 | 1.7 | 6.67 | 0.3 | 0 | 0 | 0 | 2 |
| Fn-Gel-BG | 200 | 0 | 1.582 | 6.67 | 0.3 | 0.018 | 0.5 | 0.1 | 2 |
| Fn-Gel-P50-BG | 200 | 100 | 1.532 | 6.67 | 0.3 | 0.018 | 0.5 | 0.15 | 2 |
| Fn-Gel-P100-BG | 200 | 200 | 1.482 | 6.67 | 0.3 | 0.018 | 0.5 | 0.2 | 2 |

*__GelMA__: Gelatin-Methacrylate; **PEGDA**: Poly(ethylene glycol diacrylate); **GPTMS**: Glycidoxypropylene trimethoxysilane; **BG**: Bioactive Glass (from Tetraethyl orthosilicate); **PBS**: Phosphate Buffer Saline.